REGULATION OF SPECIALIZED METABOLISM IN *STREPTOMYCES*

REGULATION OF SPECIALIZED METABOLISM IN *STREPTOMYCES*

By XIAFEI ZHANG, B.Sc

A Thesis Submitted to the School of Graduate Studies in Partial Fulfilment of the Requirements

for the Degree of Doctor of Philosophy

McMaster University
Hamilton, Ontario

Doctor of Philosophy
Biology

TITLE: Regulation of specialized metabolism in *Streptomyces*

AUTHOR: Xiafei Zhang, B.Sc. (Sichuan Normal University)

SUPERVISOR: Dr. Marie A. Elliot

Number of pages: xvi; 129

LAY ABSTRACT

Streptomyces bacteria produce the majority of naturally-derived antibiotics, and they have the genetic potential to produce many more antibiotics and antibiotic-like compounds ('specialized metabolites'). Specialized metabolism is controlled by multiple regulatory systems. In *Streptomyces venezuelae*, we have discovered that the nucleoid-associated protein, Lsr2, represses the expression of most specialized metabolic clusters, and manipulating Lsr2 activity can stimulate antibiotic production. To better understand how Lsr2 exerts its repressive effect, we explored how Lsr2 controlled the production of a known antibiotic. We ultimately identified multiple regulators that could impact the expression and/or activity of Lsr2. Building on the regulatory foundation provided by Lsr2, we then set out to establish a comprehensive regulatory network that governs biosynthetic gene cluster expression. Collectively, this work improves our understanding of antibiotic gene regulation in *Streptomyces* bacteria, and has the potential to guide novel strategies aimed at stimulating the production of new antibiotics in *Streptomyces.*

ABSTRACT

In *Streptomyces* bacteria, the expression of many antibiotic biosynthetic clusters is controlled by both cluster-specific regulators and more globally-acting regulators; however, much remains unknown about the factors that govern antibiotic production. In *Streptomyces venezuelae*, we have discovered that the broadly-conserved nucleoid-associated protein Lsr2, plays a major role in repressing specialized metabolic cluster gene expression.

To understand how Lsr2 exerts its gene silencing effects, we focused our attention on the well-studied, but transcriptionally silent, chloramphenicol cluster in *S. venezuelae*. We established that Lsr2 represses transcription of the chloramphenicol cluster by binding DNA both within the cluster and at distal positions. CmlR is a known activator of the chloramphenicol cluster, but expression of its associated gene is not under Lsr2 control. We discovered that CmlR functions to 'counter-silence' Lsr2 activity, alleviating Lsr2 repression and permitting chloramphenicol production, by recruiting RNA polymerase.

Lsr2 plays a central role in controlling antibiotic production in *Streptomyces*; however, beyond this counter-silencing activity, little is known about how Lsr2 is regulated. We identified regulators that could control the expression of *lsr2*, and found that Lsr2 and LsrL, an Lsr2 homologue that is encoded by all streptomycetes, interact directly with each other, and that their respective DNA-binding activities are altered by the presence of the other protein. These data suggest that LsrL may impact Lsr2 activity in regulating antibiotic production in *Streptomyces.*

Beyond Lsr2, we wanted to develop a comprehensive understanding of the regulatory proteins that impact biosynthetic gene cluster expression. To define the regulatory protein occupancy of antibiotic clusters, we developed '*in vivo* protein occupancy display-high resolution' (IPOD-HR) technology for use in *Streptomyces*. This work will lay the foundation for establishing a comprehensive regulatory network map for biosynthetic clusters in *Streptomyces*, and guide future work aimed at stimulating the expression of metabolic clusters in any *Streptomyces* species.

ACKNOWLEDGEMENTS

First and foremost, thank you to my supervisor, Dr. Marie Elliot, for your support, patience, and endless encouragement during the past six years. Thank you for teaching me how to be a scientist, for providing helps even when not related to academic matters, and for giving guidance related to my career goal. I feel extremely fortunate to have been accepted into your lab, and I could not have imagined having a better supervisor for my PhD study. Thank you to my committee members, Dr. Turlough Finan and Dr. Gerry Wright, for your guidance and insightful suggestions throughout this process.

To all the past and present members of the Elliot lab, it's been a great pleasure to work with you all. Savannah – I want to thank you for many things, for being extremely patient with me when I could only understand 10% of conversations and you needed to explain everything to me, for going over my transfer exam presentation many times until I felt comfortable with it, and for being caring and encouraging when I was upset. I have said many times that I'll visit you in Ottawa, hopefully I can finally do it this summer! David – Thank you for making the first two years of grad school enjoyable for me, and for so many great memories, studying in the library together, making a four-layer cake, and accidently wearing the exact same outfit to work… It still makes me laugh when I see the picture of the most tree-like broccoli drawn on my negative ligation plate. Matt – you say you make the worst decision when you have multiple options, but you (almost?) always give me great advice. Grad school is hard, and I had some difficult times during the last two years, but I'm so lucky to have a caring and knowledgeable friend like you who can relate to my struggles and is always willing to provide help. Thank you also for all the laughs, I will never forget the time when I was alone in the lab and saw a scary clown you put in the cassette, and I will forever be proud of myself for tricking you into going to the lab at 11:30pm. Christine – Thank you for being on my side as the only witness when we talk about the bird story. I think we make a great team for many things, arguing with Matt, judging spikeball and playing spikball (just for fun though, still can't believe we lost 0 – 11…). You're brilliant and hard working, and I'm sure you'll be awesome no matter what you decide to do next. Meghan – You're a great scientist and the sweetest person I know. Playing squash with you is the best way of relieving stress from work and TA, and I think our squash skills have really improved a lot over the past few years! The parties we had in your backyard were the best things during the pandemic, and they will forever be my favorite memories about grad school. Evan – I keep getting amazed by how much knowledge you have and how good you are at trivia questions, there were a lot of times I thought 'how could you possibly know this?'. Going to the conference at Queen's University with you was one of my favorite experiences of grad school. Dr. Hindra – Thank you for always having answers to my scientific questions, and for giving insightful advice on my project during our weekly group meeting.

To my parents, thank you for your unconditional support and love throughout my life, and I can't thank you enough for everything you've given me. I know it wasn't easy for you to let me move to the other side of the world, but you still supported me to pursue my dream. Thank you to Peter for being caring, understanding, and supportive throughout my grad school experience. We both had some tough times during the past few years, but I'm glad we went through everything together, and I'm so excited to start our next journey!

TABLE OF CONTENTS

LIST OF TABLES

LIST OF FIGURES

LIST OF ABBREVIATIONS AND SYMBOLS

A	Adenine
ACN	Acetonitrile
AFM	Atomic force microscopy
Ala or A	Alanine
Arg or R	Arginine
Asp or D	Aspartic acid
asRNA	Antisense ribonucleic acid
ATP	Adenosine triphosphate
bp	Base-pair
C	Cytosine
cAMP	3′-5′-cyclic adenosine monophosphate
c-di-GMP	Cyclic-di-GMP
ChIP	Chromatin immunoprecipitation
ChIP-seq	ChIP sequencing
Co-IP	Co-immunoprecipitation
C-terminus	Carboxyl terminus
DMSO	Dimethyl sulfoxide
DNA	Deoxyribonucleic acid
DNase	Deoxyribonuclease
DTT	Dithiothreitol
E	Glutamic acid
EMSA	Electrophoretic mobility shift assay
F	Phenylalanine
FA	Formic acid
G	Guanine
g	Gram
g	Gravity
GFP	Green fluorescent protein
Gly or G	Glycine

Glc*N*Ac	*N*-acetylglucosamine
Gus	β-glucuronidase
h	Hour
H	Histone
His or H	Histidine
HCl	Hydrochloric acid
IP	Immunoprecipitation
IPTG	Isopropyl-β-D-thiogalactopyranoside
kb	Kilo bp
KCl	Potassium chloride
kDa	Kilo Daltons
L	Litre
LB	Lysogeny broth
LC-MS	Liquid chromatography-mass spectrometry
Leu or L	Leucine
Lys or K	Lysine
M	Molar
Mb	Mega base pairs
Met	Methionine
mg	Milligram
$MgCl_2$	Magnesium chloride
$MgSO_4$	Magnesium sulphate
min	Minutes
mL	Millilitre
mM	Millimolar
MOPS	3-(N-morpholino)propanesulfonic acid
mRNA	Messenger ribonucleic acid
MYM	Maltose-yeast extract-malt extract
m/z	mass/charge
n	Any nucleotide

N	Asparagine
NaCl	Sodium chloride
NaH_2PO_4	Monosodium phosphate
Na_2HPO_4	Disodium phosphate
$NaHSO_3$	Sodium bisulfite
ncRNA	Non-coding ribonucleic acid
ng	Nanogram
Ni-NTA	Nickel-nitrilotriacetic acid
nL	Nanolitre
nm	Nanometre
nt	Nucleotide
N-terminus	Amino terminus
OD	Optical density
ONPG	Ortho-Nitrophenyl-β-galactoside
ori	Origin of replication
oriT	Origin of transfer
P	Proline
PAGE	Polyacrylamide gel electrophoresis
PCR	Polymerase chain reaction
pH	Potential hydrogen
PNPG	p-nitrophenyl β–D-glucuronide
PVDF	polyvinylidene fluoride
Q	Glutamine
qPCR	Quantitative polymerase chain reaction
RNA	Ribonucleic acid
RNAP	RNA polymerase
RNA-seq	RNA sequencing
RNase	Ribonuclease
SDS	Sodium dodecyl sulfate
Ser or S	Serine

SVEN	*Streptomyces venezuelae*
T	Thymine
Thr or T	Threonine
Try or Y	Tyrosine
U	Enzyme unit
UTR	Untranslated region
V	Valine
W	Tryptophan
YP	Yeast extract-peptone
YPD	Yeast extract-peptone-glucose (dextrose)
$ZnCl_2$	Zinc chloride
µg	Microgram
µL	Microlitre
α	Alpha
β	Beta
γ	Gamma
σ	Sigma
°C	Degrees Celsius
Δ	Delta or mutant
^{32}P	Phosphorus-32 isotope
5′ UTR	5′ untranslated region

CHAPTER1: GENERAL INTRODUCTION

1.1 Actinomycetes and *Streptomyces*

The actinomycetes are a group of free-living, ubiquitous Gram-positive bacteria with a high genomic G+C (guanine and cytosine) content. They were first observed in the 1870s, and were given the name *Actinomyces,* meaning "ray fungus" in Greek. Due to their ability to produce elongated cells and form branched hyphae, the actinomycetes were originally considered as transitional forms between bacteria and fungi, but they were eventually characterized as bacteria based on morphology (cell wall) analysis and cellular chemical composition (Waksman, 1967; Barka et al., 2016). Actinomycetes can use a wide range of nutrients, and therefore can grow in diverse natural habitats, including soil, and fresh and salt water. It has been estimated that over one million actinomycetes are found per gram of soil, with 95% of them being *Streptomyces.* (Dilip et al., 2013).

Streptomyces are the largest genus within the phylum Actinobacteria. These bacteria play a key role in establishing soil ecology, and it is estimated they make up 1-20% of the culturable soil microbes (Olanrewaju and Babalola, 2019). *Streptomyces* are best known for their complex life cycle and their remarkable ability to produce a wide variety of bioactive compounds, including antibiotics, antifungal agents, immunosuppressant, and pesticides.

1.1.1 Two model species: *Streptomyces coelicolor* and *Streptomyces venezuelae*

Streptomyces coelicolor is the most well-studied species in the *Streptomyces* genus and is the model species for most of the fundamental work conducted on *Streptomyces* development and specialized metabolism. *S. coelicolor* encodes 27 biosynthetic clusters (annotated by antiSMASH (Blin et al., 2021)), including two that produce the pigmented antibiotics actinorhodin and undecylprodigiosin (Bentley et al., 2002; Rudd and Hopwood, 1979; Hopwood et al., 1995; Chong et al., 1998). Production of these pigmented specialized metabolites greatly facilitated the genetic study of metabolic pathways in *S. coelicolor.* However, the study of development and differentiation in *S. coelicolor* has been challenging because it only completes its development lifecycle on solid medium but not in liquid culture, making it more difficult to both synchronize development and separate/identify different developmental cell types (Flardh and Buttner, 2009). In contrast, *Streptomyces venezuelae* is an excellent model organism for development studies. On solid medium, *S. venezuelae* grows considerably faster than *S. coelicolor.* Unlike *S. coelicolor, S. venezuelae* fully differentiates both on solid medium and in liquid culture, facilitating the study of gene regulation at each growth stage (Glazebrook et al., 1990). *S. venezuelae* also has great specialized metabolic potential, encoding 30 biosynthetic clusters, including those that

direct the production of two well-characterized antibiotics – chloramphenicol and jadomycin (Carter et al., 1948; Kim et al., 2020; Ehrlich et al., 1947; Ayer et al., 1991).

1.2 *Streptomyces* life cycle and development

1.2.1 Classical life cycle overview

Amongst the Actinobacteria, the streptomycetes are the only bacteria whose development has been studied in detail (Barka et al., 2016). *Streptomyces* have a uniquely complex life cycle that encompasses both multicellular differentiation and specialized metabolite production. On solid media when nutrients are abundant, their life cycle begins with the germination of a dormant spore and the emergence of germ tubes. Germ tubes grow into their growth substrate through hyphal tip extension and branching from lateral walls, leading to the formation of a dense network of hyphae termed the vegetative mycelium. When essential nutrients become limited, non-branching and hydrophobic aerial hyphae emerge from the vegetative mycelium and extend into the air (Zambri et al., 2022; Swiercz and Elliot, 2012). The production of specialized metabolites generally coincides with the formation of these aerial hyphae, although these processes are typically spatially segregated (Bibb, 1996). Pre-spore compartments are then formed within the aerial hyphae, and these pre-spores are then subject to a series of maturation steps to produce polyketide pigment-coated mature spores. The life cycle starts anew when a mature dormant spore is released and is dispersed to a new location (Flardh and Buttner, 2009; Swiercz and Elliot, 2012) (**Figure 1.1**).

1.2.2 Spore germination and vegetative growth

Spores are dormant cells, and germination requires both initiation of metabolic activity and morphological changes (Bobek et al., 2017). How germination proceeds, including the associated signal transduction cascades, is still not fully understood. During germination, spores go through three distinctive stages: darkening, swelling, and germ tube emergence (Hardisson et al., 1978; Bobek et al., 2017). An essential next step involves the emergence of germ tubes through a process mediated by the essential protein DivIVA. DivIVA localizes to the spore poles and subsequent cell tips (specifically, areas of negative membrane curvature), where it recruits proteins required for cell wall synthesis, ultimately forming a complex termed the “polarisome” (Flardh, 2003). DivIVA activity is regualted by post-translational modification in the form of phosphorylation. When DivIVA is unphosphorylated, it localizes to the hyphal cell tips to form the polarisome and drive tip growth, and along the side wall to facilitate branches formation; when phosphorylated by the serine/threonine kinase AfsK, DivIVA de-localizes from the tip, leading to growth arrest (Zambri et al., 2022; Hempel et al., 2012).

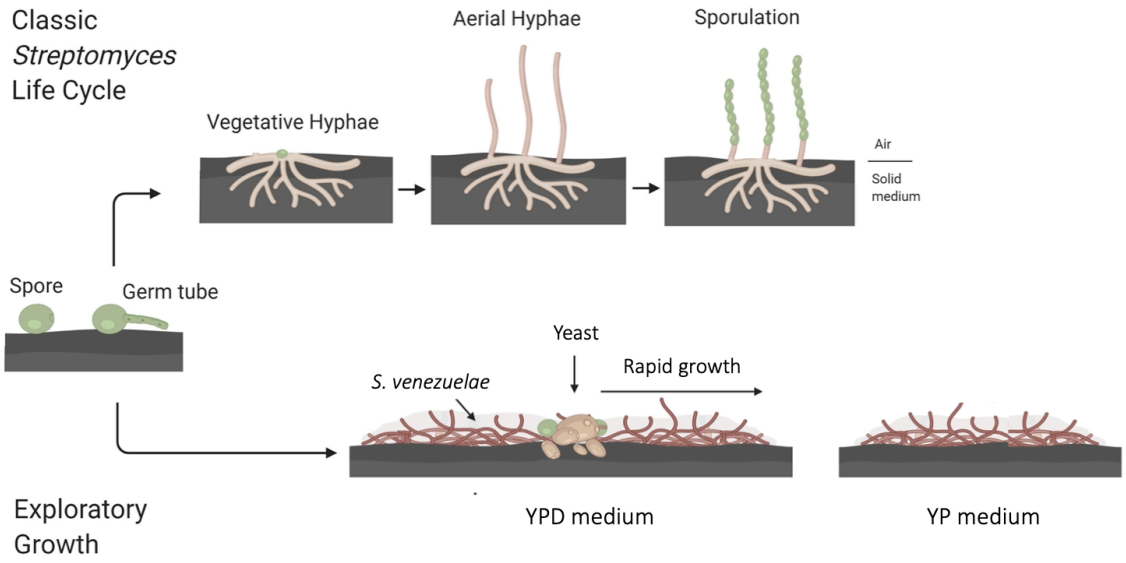

Figure 1.1: Classical life cycle and exploratory growth of *S. venezuelae*. Top panel: During classical development, the *S. venezuelae* life cycle begins with spore germination. Germ tubes then grow into the substrate by tip extension and branching to form a network of branching vegetative hyphae. Upon nutrient depletion, non-branching aerial hyphae grow away from the vegetative mycelium, where they are then subdivided to form chains of pre-spore compartments. These ultimately develop into mature dormant spores, which are dispersed into the environment where they can restart the life cycle. **Bottom panel:** In response to specific conditions, including interacting with yeast on glucose-rich medium (YPD-yeast extract, peptone, dextrose) and growing alone on glucose depleted medium (YP), *S. venezuelae* transits into exploratory growth, where it grows as generally unbranched hydrophilic hyphae that rapidly extend across the growth surface.

1.2.3 Aerial hyphae growth

Upon nutrient depletion, *Streptomyces* enter into their reproductive growth phase, where non-branching aerial hyphae emerge from the vegetative mycelium and grow into the air. The growth of aerial hyphae is controlled by the Bld regulators (encoded by the *bld* genes), and like the vegetative hyphae, is driven by DivIVA. The *bld* genes were first identified in mutants that were unable to produce fuzzy colonies, characteristic of those undergoing reproductive growth, and instead have a “bald” appearance (Merrick, 1976). BldD is a master regulator of *Streptomyces* development (Elliot et al., 2001; Elliot and Leskiw, 1999; Elliot et al., 2003b). Studies have revealed

that BldD binds to the promoters of ~170 genes, including most of developmental regulatory genes (den Hengst et al., 2010; Schumacher et al., 2017). Aerial hyphae are coated in a hydrophobic sheath made of three proteins: the rodlins, SapB, and the chaplins (encoded by the *chp* genes). The rodlins exert their function by organizing the chaplins on the aerial hyphae and spore surface (Claessen et al., 2003). In contrast, SapB and the chaplins share similar surfactant properties where they reduce surface tension to facilitate aerial hyphae up-growth (Elliot et al., 2003a; Claessen et al., 2003; Capstick et al., 2007). However, SapB is only expressed during growth on rich medium, whereas the chaplins play a role in aerial hyphae formation on both minimal and rich media (Capstick et al., 2007). The expression of *chp* genes is regulated by two Bld regulators, BldD and BldN (σ^{BldN}) (Zambri et al., 2022; den Hengst et al., 2010). These two regulators also control the expression of *bldM*, where BldM is an orphaned response regulator lacking an associated histidine kinase, and it is essential for *Streptomyces* aerial hyphae development (Molle and Buttner, 2000). BldD functions to repress *bldM* expression, while BldN activates its expression (den Hengst et al., 2010). BldM functions as an unusual response regulator, in that it regulates the expression of two sets of target genes by forming either a BldM-BldM homodimer or a BldM-WhiI heterodimer (where WhiI is an orphaned response regulator required for sporulation); these different BldM oligomers bind different consensus sequences (Al-Bassam et al., 2014).

1.2.4 Sporulation and chromosome segregation

Following aerial growth, the classical *Streptomyces* life cycle enters its final stage: sporulation. This process can be divided into two steps: formation of pre-spore compartments, and maturation of these unicellular compartments (Bush et al., 2022). The *whi* (white) genes are indispensable for *Streptomyces* sporulation. The products of the *whi* genes play important roles in both spore formation and maturation processes. Mutations in the *whi* genes block sporulation and result in “white” colonies rather than wild type pigmented colonies (Flardh and Buttner, 2009). The products of *whi* genes have significant effects on the initiation of sporulation, spore maturation and expression of genes involved in chromosome segregation and cell division, including *ftsZ, ssgAB* and *parAB* (McCormick and Flardh, 2012; Chater, 2001; Jakimowicz and van Wezel, 2012). During sporulation, FtsZ polymerizes to form filaments which then are assembled into Z-rings that recruit the cell division machinery and direct septation (Willemse et al., 2011; Adams and Errington, 2009). Localization of FtsZ requires SsgA and SsgB, two SsgA-like proteins (‘Ssg’ for ‘sporulation of *Streptomyces griseus*’). SsgA foci form first at the sites of future cross-wall formation, and are thought to recruit SsgB, which in turn recruits FtsZ by interacting with both FtsZ and the cell membrane (Zambri et al., 2022; Willemse et al., 2011) (**Figure 1.2**). The resulting Z-rings are tethered to the membrane by SepF family proteins, and stabilized by the dynamin-like proteins DynA and DynB during sporulation (Schlimpert et al., 2017). A recent study found that SepH, a conserved cell

division protein in Actinobacteria, positively regulates Z-ring formation by interacting directly with FtsZ and promoting FtsZ polymerization (Ramos-Leon et al., 2021). This synchronous round of cell division is coupled to efficient chromosome segregation, which in *Streptomyces* is mediated by the ParA and ParB family proteins. ParB homologues bind chromosome at partitioning sites (*parS*) and segregate chromosomes to ensure that each pre-spore compartment contains only one copy of the chromosome; ParA polymerizes along the chromosome at the hyphal tip and provides energy for ParB movement through its ATPase activity (Leonard et al., 2005; Pioro and Jakimowicz, 2020; Kim et al., 2000; Jakimowicz et al., 2005; Jakimowicz et al., 2007) (**Figure 1.2**).

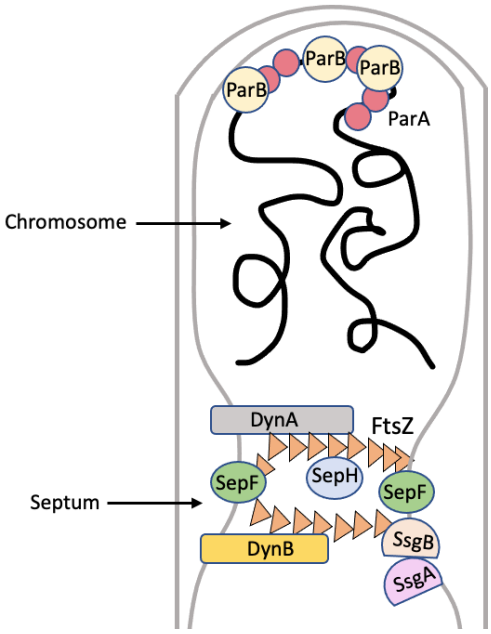

Figure 1.2: *Streptomyces* chromosome segregation and cell division machinery. Top: During chromosome segregation, ParA polymerizes along the chromosome to provide energy for chromosome segregation driven by ParB movement. **Bottom**: SsgA recruits SsgB, which subsequently recruits FtsZ to the sites of future cross-wall formation, where FtsZ polymerizes to form filaments which are then assembled into the Z-ring. The Z-ring formation is regulated by SepH and SepF, and stabilized by the dynamins DynA and DynB.

1.2.5 Exploration growth

It was recently discovered that a number of *Streptomyces* species, including *S. venezuelae,* are capable of undergoing another mode of development termed "exploration" (Jones et al., 2017; Jones and Elliot, 2017). Like classical growth, exploration begins with spore germination. However, instead of progressing through the vegetative-aerial hyphae-sporulation development cycle, exploring cells grow as hydrophilic, vegetative-like hyphae, and rapidly extend over biotic and abiotic surface at a rate that is ~12.5× faster than classically growing colonies (Jones et al., 2017) (**Figure 1.1**). Exploration can be promoted by diverse growth conditions. On YPD (yeast extract, peptone, and D-glucose) medium, exploration can be induced through an interaction with the yeast *Saccharomyces cerevisiae*, where *S. cerevisiae* consumes glucose in the growth medium; exploration is inhibited in the absence of *S. cerevisiae* on YPD. Exploration can also be induced on YP (yeast extract and peptone) medium in the

absence of both glucose and *S. cerevisiae*, and colonies appear to grow more rapidly on YP than on YPD with yeast. Recent work has shown that the addition of glycerol further accelerates *Streptomyces* exploratory growth on YP (Shepherdson et al., 2022).

1.3 Specialized metabolism of *Streptomyces*

1.3.1 Chromosome organization and biosynthetic capacities in *Streptomyces*

Streptomyces have large and linear chromosomes, ranging from 8 – 12 Mb. Given their large genome size, streptomycetes have an enormous coding potential, typically in the range of ~8000 protein-coding genes (Bentley et al., 2002; Ikeda et al., 2003). Genome sequencing and microarray data suggested that under non-limiting or standard laboratory conditions, genes corresponding to the core region of *Streptomyces* linear chromosome are more highly expressed than genes located in the arms of the chromosome, and that most of the specialized metabolic genes are present in the chromosomal arms rather than in the core region (Karoonuthaisiri et al., 2005; Choulet et al., 2006; Bentley et al., 2002; Ikeda et al., 2003; Aigle et al., 2014; Lioy et al., 2021). Now that many *Streptomyces* genomes have been sequenced, it has become apparent that the internal (core) regions are highly conserved, while the more auxiliary (arm-located) genes show large variation (Thibessard and Leblond, 2014; Kirby, 2011; Ohnishi et al., 2008).

Streptomyces are the largest natural source of antibiotics, producing over two thirds of the antibiotics in clinical use today (Procopio et al., 2012; Manteca and Yagüe, 2019). Antibiotic synthesis is largely limited to the vegetative mycelium, and their production typically coincides with the onset of aerial hyphae formation (Bibb, 1996). Antibiotics produced by *Streptomyces* could kill or inhibit the growth of other competing microorganisms. It is possible that organisms killed by these antibiotics could then be used as a nutrient source by the *Streptomyces* mycelium (Davies, 2013; Challis and Hopwood, 2003). Antibiotics also serve as small molecules modulating gene expression and facilitating cell-cell communication under natural conditions (Romero et al., 2011; Yim et al., 2007; Davies, 2006). Whole genome sequencing results have revealed that most streptomycetes encode 20 – 50 specialized metabolites clusters; however, in most cases, fewer than 10% of their associated molecules have been identified. Many of these clusters are poorly transcribed and consequently their products have never been detected under the laboratory conditions. These ‘cryptic clusters’ have the potential to produce an impressive array of novel antibiotics (Nguyen et al., 2020).

1.3.2 Regulation of antibiotic production

In *Streptomyces*, antibiotic production is regulated at multiple levels, including sigma (σ) factors, pathway-specific regulators, and other transcriptional factors.

Initiation of transcription in bacteria requires the addition of a σ factor to RNA polymerase (RNAP), to facilitate the recognition and binding of the promoter by the resulting RNAP holoenzyme. Most, but not all, specialized metabolic clusters in *Streptomyces* contain pathway-specific regulators (Bibb, 2005). Pathway-specific regulators are located within gene clusters and affect metabolite biosynthesis by directly binding at promoter regions within clusters. Consequently, overexpressing pathway-specific activators or deleting pathway-specific repressors generally increases the production of their corresponding antibiotics. In addition to pathway-specific regulators, pleiotropic regulators are also involved in regulating metabolite biosynthesis. Instead of being encoded within a cluster and affecting expression of a specific biosynthetic cluster, pleiotropic regulators are usually encoded elsewhere in the chromosome, and impact the production of multiple metabolic pathways (Martin and Liras, 2010). In bacteria, nucleoid- associated proteins also play important roles as global regulators in controlling specialized metabolite biosynthesis.

1.4 Transcription regulation in *Streptomyces*

Transcription in bacteria is tightly controlled by a wide range of factors: *cis*-acting elements, including promoters and operator sequences; and *trans*-acting proteins, including σ factors and transcriptional regulators (Browning and Busby, 2004).

1.4.1 σ factors

σ factors are divided into two main families: σ^{70} - 'housekeeping (and housekeeping-like) σ factors' – are involved in the transcription of essential genes, and σ^{54}, which recognize promoters that are not associated with members from the σ^{70} family (Wade et al., 2006; Weber et al., 2005). The σ^{70} family can be subdivided into 4 groups based on functions and possession of distinct σ domains: σ_1 (region 1.1), σ_2 (region 1.2, 2.1–2.4), σ_3 (region 3.0–3.2), and σ_4 (region 4.1–4.2) (Sun et al., 2017; Paget, 2015) (**Figure 1.3**). Group 1 σ factors, also known as 'housekeeping σ factors', contain all four σ domains and a non-conserved region within σ_2 between regions 1.2 and 2.1. In *Streptomyces*, σ^{HrdB} belongs to the group 1 σ factors, and is involved in morphological differentiation and specialized metabolism (Sun et al., 2017). Group 2 σ factors are structurally similar to group 1 but lack region 1.1. *Streptomyces* genomes usually possess three group 2 σ factors: σ^{HrdC}, σ^{HrdA} and σ^{HrdD} (Sun et al., 2017). The σ^{HrdD}-RNAP holoenzyme promotes the transcription of genes that are involved in specialized metabolite biosynthesis (*e.g. redD* in *S. coelicolor*) and morphological differentiation (*e.g. whiB* throughout *Streptomyces*) (Sun et al., 2017; Paget, 2015). Group 3 σ factors contain σ_2, σ_3 and σ_4 domains but lack the non-conserved region. In *Streptomyces*, in response to a wide range of intracellular and extracellular signals, group 3 σ factors modulate the transcription of genes involved in morphological differentiation (*e.g.* σ^{WhiG}

modulates differentiation by activating the expression of the *whiH* and *whiI* genes essential for spore maturation (Gallagher et al., 2020)) and environmental stress responses (*e.g.* σ^B in *S. coelicolor* controls the expression of genes involved in responses of osmotic stress, oxidative stress and cold shock (Sun et al., 2017; Lee et al., 2005; Martínez et al., 2009)). Group 4 σ factors, also known as extracytoplasmic function σ factors, possess σ_2 and σ_4 domains. These σ factors sense extracytoplasmic signals and play important roles in stress responses. In *Streptomyces,* σ^{BldN} is a widely distributed extracytoplasmic function σ factor, and is responsible for promoting aerial hyphae formation (Sun et al., 2017; Bibb and Buttner, 2003).

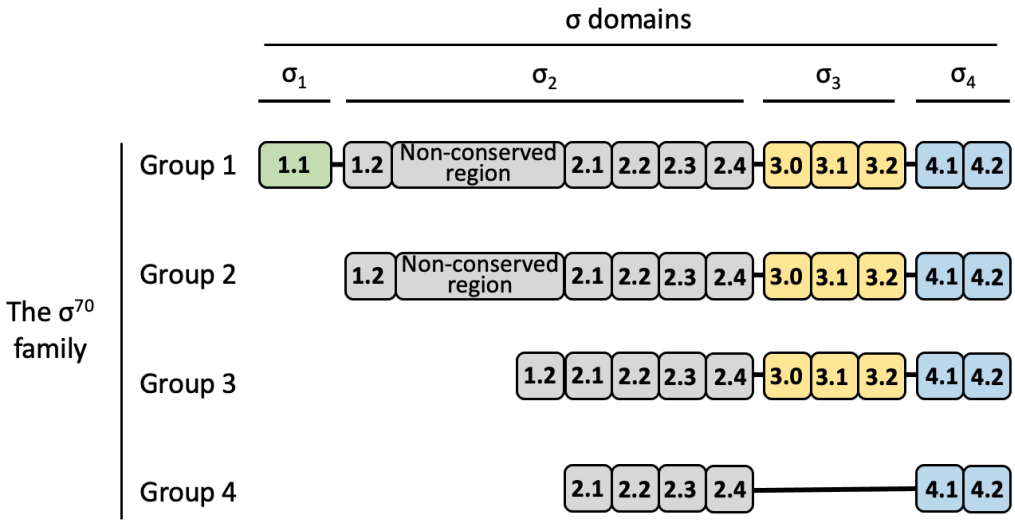

Figure 1.3: Domain organization of the σ^{70} family. The σ^{70} family can be divided into four groups based on domain organization. Group 1 and group 2 are structurally similar except that group 1 contains σ_1 domain (green) which is absent in group 2 (grey). Group 3 contains σ_2 (lacking the non-conserved region), σ_3 (yellow) and σ_4 (blue) domains, and group 4 possess σ_2 (lacking region 1.2 and the non-conserved region) and σ_4 domains.

1.4.2 Two-component system and one-component system regulators

Transcriptional regulators are proteins that bind *cis*-acting elements to repress or activate the transcription of the downstream genes (Browning and Busby, 2004). Transcriptional regulators can be broadly classified into two main categories: two-component system regulators and one-component system regulators. In typical bacterial two-component systems, a membrane-bound histidine kinase senses an exogenous environmental signal. It responds to this signal by first auto-phosphorylating on a conserved histidine residue, then transferring the phosphoryl group to a cognate response regulator (Romero-Rodriguez et al., 2015). In response to stimuli detected by the histidine kinase, the phosphorylated response regulator then either activates or represses the transcription of its downstream target genes (Podgornaia and Laub, 2013).

Most histidine kinases are bifunctional where they phosphorylate their cognate response regulator in the presence of environmental signal but act as phosphatase in the absence of stimuli (Hutchings et al., 2006; Gao and Stock, 2013). Additionally, some kinases function mainly as phosphatase and exogenous environmental signals promote dephosphorylation, other than dephosphorylation, of their cognate response regulator (Raivio and Silhavy, 1997; Som et al., 2017b). The number of two-component systems encoded by an organism roughly correlates with the complexity of its surrounding environment, with *Streptomyces* encoding an average of 90 histidine kinases and 80 response regulators (Romero-Rodriguez et al., 2015; Rodriguez et al., 2013). AfsQ1/Q2 and MtrAB are well-studied examples of two-component systems that are broadly conserved in the Actinobacteria. In response to an illusive signal, AfsQ1 is phosphorylated by AfsQ2 and then is able to bind the promoter regions of genes encoding pathway-specific regulators of actinorhodin (*actII-ORF4*), undecylprodigiosin (*redZ*) and calcium dependent antibiotic (*cdaR*), and further induce the production of their corresponding antibiotics (Wang et al., 2013). The MtrAB two-component system also significantly impacts specialized metabolism in *Streptomyces* In *S. coelicolor,* MtrA functions as an activator and binds upstream of *actII-ORF4* and *redZ*, which encode pathway-specific regulators of the actinorhodin and undecylprodigiosin clusters, respectively; and deleting *mtrB,* the coding gene of sensor kinase, induces production of actinorhodin and undecylprodigiosin (Som et al., 2017a).

In bacterial transcriptional regulatory networks, one-component systems dominate. These are systems in which a protein contains a DNA-binding domain and a ligand-binding or protein-protein interaction domain (Chubukov et al., 2014). In bacterial transcriptional regulators, a helix-turn-helix is the most common DNA-binding domain structure, and the ligands bound by transcription regulator are usually metabolites (Perez-Rueda et al., 2004). Transcriptional regulators can affect transcription in both positive and negative manners. In general, negative regulators repress transcription by: i) binding promoter regions to prevent RNAP binding and transcription initiation, ii) competing with activators for binding sites, and iii) inhibiting transcription elongation by blocking RNAP progression. In contrast, positive regulators activate transcription by: i) stabilizing RNAP-promoter complexes during transcription initiation, or ii) promoting dissociation of repressors and facilitating RNAP promoter binding (Lee et al., 2012).

1.4.3 Transcriptional regulators

Bacterial transcriptional regulators can be divided into specific and pleiotropic regulators, based on their target genes. Specific regulators are frequently encoded within clusters and directly regulate the expression of genes located in the same cluster. In contrast, pleiotropic regulators exert their effects by controlling the transcription of multiple target genes (Romero-Rodriguez et al., 2015; Bibb, 2005). In *S. coelicolor,* ActII-ORF4 is a pathway-specific regulator that controls the production of actinorhodin

(Malpartida et al., 1990), while Crp is a pleiotropic regulator of antibiotic production, with 393 associated binding sites identified in the *S. coelicolor* chromosome (Gao et al., 2012). Transcriptional regulators can also be subdivided into groups base on their regulatory roles in cellular processes. Regulators involved in primary metabolism are typically responsible for the transcriptional control of genes involved in cell growth, nutrient utilization, and reproduction. This group includes GntR, AraC, AsnC, LuxR, IclR, LacI, DeoR and ROK regulator families. A second group includes the TetR, MarR, LysR, MerR, ArsR, Xre and PadR families, and these are regulators that typically control the expression of genes involved in stress responses and specialized metabolism (Romero-Rodriguez et al., 2015; Santos et al., 2009).

In *Streptomyces* genomes, ~12% of genes encode transcriptional regulators, σ factors and other DNA binding proteins, illustrating how important regulatory control is for *Streptomyces* growth, development, metabolism, and stress responses (Bentley et al., 2002). In *Streptomyces,* some of the best characterized transcriptional regulators play roles in primary and specialized metabolism. GntR family regulators are often involved in central carbon utilization, where they directly repress transcription of adjacent/nearby target genes, while indirectly activating target genes located elsewhere on the chromosome (Hoskisson and Rigali, 2009; Kotowska et al., 2019; Finn et al., 2008). DasR and WhiH are GntR- like regulators that are broadly conserved in the streptomycetes, and they play roles in *N*-acetylglucosamine (Glc*N*Ac) utilization and sporulation, respectively (Rigali et al., 2006; Swiatek-Polatynska et al., 2015; Persson et al., 2013). DasR represses the expression of genes involved in Glc*N*Ac uptake and metabolism, and its DNA binding ability can be relieved by binding GlcN-6-phosphate, an intermediate of Glc*N*Ac metabolism, within its C-terminal domain (Engel et al., 2019; Fillenberg et al., 2016; Xia et al., 2020). In contrast, WhiH is essential for sporulation in *S. coelicolor* and *S. venezuelae*, and *whiH* gene expression is confined to the aerial hyphae and depends on the activity of the σ^{WhiG}-RNAP complex and the concentration of c-di-GMP. Nothing is currently known about WhiH direct gene targets, except that WhiH is autoregulatory and it represses its own expression by directly binding to the promoter region (Ryding et al., 1998).

Unlike many of the GntR-like regulators, the majority of AraC family members positively regulate the expression of their target genes and are often autoregulatory (Romero-Rodriguez et al., 2015; Brautaset et al., 2009; Ibarra et al., 2008). AdpA (BldH) is an AraC-like global transcription regulator that controls the expression of hundreds of genes involved in development and primary and specialized metabolism (Guyet et al., 2014; Plachetka et al., 2021; Huang et al., 2022; Kang et al., 2019; Ohnishi et al., 2005).

The TetR family regulators are also often autoregulatory, but are best known for their control of specialized metabolism (Gou et al., 2017; Zhang et al., 2020; Jiang et al., 2017). These regulators repress transcription of their target genes, and like DasR, their repression can be relieved by binding of a ligand to their C-terminal domain

(Cuthbertson and Nodwell, 2013; Ramos et al., 2005; Yu et al., 2010; Ray et al., 2017). A classic example is ActR, a TetR-like regulator from *S. coelicolor.* ActR is encoded within the actinorhodin biosynthetic cluster, where it represses the expression of the adjacent efflux pump-encoding gene *actA*, whose product is proposed to function in exporting actinorhodin. ActR binding activity can be modulated by not only actinorhodin but also by an intermediate product. Ligand binding to the C- terminal domain of ActR changes the conformation of its DNA-binding domain such that it is no longer able to bind DNA, and this in turn relieves repression (Xu et al., 2012; Willems et al., 2008).

While the TetR-like regulators are primarily associated with specialized metabolism, other regulators impact both development and specialized metabolism. BldD, a Xre (xenobiotic response element) family regulator, is a global regulator having ~160 direct regulatory targets in *S. coelicolor*, including genes that are involved in development and antibiotic production (den Hengst et al., 2010; Elliot et al., 2001). Structural studies revealed that the assembly of an unusual $BldD_2$-$(c\text{-}di\text{-}GMP)_4$ complex is required for BldD to exert its function in controlling development, where dimeric BldD directly binds promoters, often repressing the expression of its target genes, including itself (Schumacher et al., 2017; Tschowri et al., 2014; Elliot et al., 1999; Kim et al., 2006).

1.5 Nucleoid-associated proteins

Beyond these traditional transcription factors, there also exist classes of DNA binding proteins that function to both organize the chromosome and regulate gene expression. In both eukaryotes and prokaryotes, genomic DNA is wrapped and compacted by proteins, resulting in the DNA adopting a highly structured configuration. Unlike in eukaryotes where genomic DNA is wrapped around histone proteins, bacteria lack histones but have other factors that influence both chromosome organization and cellular processes such as replication, transcription and chromosome segregation. These factors include DNA supercoiling and nucleoid-associated proteins. Nucleoid-associated proteins are typically low molecular weight proteins that not only constrain and maintain chromosome structure but also regulate gene expression in both positive and negative manners through bending, bridging, polymerizing and wrapping DNA. Most nucleoid-associated proteins bind DNA in a sequence-independent way, but with a preference for AT-rich sequences or specific DNA structures (e.g. curved DNA or single-stranded DNA) (Holowka and Zakrzewska-Czerwinska, 2020; Flores-Rios et al., 2019; Badrinarayanan et al., 2015; Song and Loparo, 2015; Dorman, 2014; Browning et al., 2010).

To date, nucleoid-associated proteins in Gram-negative bacteria have been better characterized than in Gram-positive bacteria. Some nucleoid-associated proteins are broadly conserved in both Gram-negative and Gram-positive bacteria (e.g. HU), while others are unique to one group (e.g. H-NS in the Enterobacteriaceae and Lsr2 in

actinomycetes) (Dillon and Dorman, 2010). In *E. coli,* the HU protein has two subunits, HUα and HUβ, and functions as either a homodimer or a heterodimer *in vivo* (Stojkova et al., 2019; Claret and Rouviere-Yaniv, 1996; Oberto et al., 2009). HU preferentially bends and wraps AT-rich and curved DNA in a concentration-dependent manner: at low concentrations, HU bends DNA and decreases DNA stiffness (by displacing H-NS and other nucleoid-associated proteins), while at high concentrations, HU binds DNA and forms rigid filaments (Claret and Rouviere-Yaniv, 1996; Skoko et al., 2004). HupS is a *Streptomyces*-specific HU homolog that plays an important role in sporulation maturation (Salerno et al., 2009). It contains an N-terminal HU-like domain and a C-terminal histone H1-like domain; both domains are able to bind DNA independently (Salerno et al., 2009; Pandey et al., 2014).

1.5.1 H-NS in *E. coli*

The histone-like nucleoid-structuring protein (H-NS) is a well-studied nucleoid-associated protein, but it is only found in Gram-negative bacteria. Early studies of H-NS in *E. coli* demonstrated that mutations in *hns* lead to increased gene transcription, while *hns* overexpression causes chromosome condensation and even cell death (Song and Loparo, 2015). H-NS is a xenogeneic silencer and global regulator that preferentially binds and spreads along high AT-content DNA to compact the chromosome and/or silence gene expression (Navarre et al., 2006). Studies have shown that although H-NS generally recognizes AT-rich sequences, a high affinity binding motif that is rich in AT content and contains a centrally-located T-A step has been identified (5′ - tCGtTAaATt - 3′) (Lang et al., 2007; Bouffartigues et al., 2007; Fang and Rimsky, 2008). H-NS is a small (~15 kDa) protein with an N-terminal oligomerization domain, a central dimer-dimer interaction domain, and a C-terminal DNA-binding domain, with the dimerization domain and dimer-dimer interaction domain connected by a long α-helix (Shindo et al., 1995; Bloch et al., 2003; Arold et al., 2010). Inter-domain interactions of H-NS are facilitated by the conformation of the α-helix connecting the dimerization domain and dimer-dimer interaction domain (van der Valk et al., 2017). A recent study revealed that the dimerization domain of H-NS contains negatively charged regions, whereas the dimer-dimer interaction domain and DNA-binding domain contain positively charged patches, with the electrostatic interaction between different domains being subject to regulation by ionic environments (Qin et al., 2020). H-NS binds DNA through a QGR motif (residues 112 – 114), and its binding effects of polymerizing and bridging DNA are determined by the structure of H-NS dimer, which is heavily influenced by Mg^{2+} (Dillon and Dorman, 2010; Liu et al., 2010; Winardhi et al., 2015; van der Valk et al., 2017). In the absence of Mg^{2+}, H-NS dimers adopt a ‘closed’ conformation where the DNA-binding domain interacts with the dimerization domain, making one of the QGR motifs inaccessible. Therefore, H-NS can only bind DNA *in cis* through one DNA-binding domain of the H-NS dimer, resulting in H-NS polymerization and formation of a rigid filament

(van der Valk et al., 2017). In the presence of Mg^{2+}, the 'closed' conformation transitions to an 'open' configuration, as Mg^{2+} alters the H-NS structure by binding to glutamate residues in the dimerization domain and preventing an interaction between the dimerization domain and DNA-binding domain. Furthermore, Mg^{2+} stabilizes the α-helix between the dimerization domain and dimer-dimer interaction domain by interacting with three glutamate residues and one serine residue, resulting in a bridging-capable H-NS conformation, allowing H- NS to bind DNA *in trans* and form a bridge structure (van der Valk et al., 2017).

The DNA-binding activity of H-NS is also affected by temperature, but the two binding effects, polymerizing and bridging, respond to temperature changes with different sensitivities. Polymerization of H-NS on DNA (forming rigid filaments) is disrupted by increasing temperatures from 24°C to 37°C, whereas DNA bridging caused by H-NS is insensitive to temperature changes (Amit et al., 2003; Liu et al., 2010). DNA structures formed by H-NS oligomers have the potential to affect gene expression by trapping RNA polymerase and repressing transcription, excluding RNA polymerase at promoter regions, or interfering with transcription elongation, thereby repressing transcription (Shahul Hameed et al., 2019; Amit et al., 2003; Lim et al., 2012; Kotlajich et al., 2015; Dame et al., 2002).

Although H-NS has been identified as a DNA-binding protein and is best studied for its ability to repress transcription, studies have shown H-NS can also bind RNA to regulate RNA stability and facilitate translation (Brescia et al., 2004; Park et al., 2010). In *E. coli,* H-NS binds directly to DsrA, a non-coding RNA, and *rpoS* mRNA, and inhibits their expression by inducing RNA cleavage by RNase I, a single-strand specific ribonuclease. It was hypothesized that in the absence of H-NS, DsrA forms tertiary structures, making it resistant to RNase I cleavage; in the presence of H-NS, DsrA structure is altered by H-NS binding, thus causing exposure of single-strand RNA to RNase I (Brescia et al., 2004). H-NS has also been shown to positively regulate the translation of *malT* mRNA by facilitating translation initiation. The *malT* mRNA contains a suboptimal Shine-Dalgarno sequence which interacts weakly with ribosome, resulting low translation level; binding of H-NS to *malT* mRNA repositions ribosome binding to a more favourable site downstream of Shine-Dalgarno sequence, leading to enhanced translation (Park et al., 2010).

H-NS activity can be modulated by interacting with other proteins. StpA, a H-NS paralogue, has a similar oligomerization domain as H-NS and can interact with H-NS, forming heterodimers (Amit et al., 2003; Muller et al., 2006). H-NS can also interact with the haemolysin expression-modulating (Hha)/YdgT family proteins. Hha lacks a DNA-binding domain and can only exert its regulatory role by interacting with H-NS or StpA through their dimerization domain (Ali et al., 2013; Boudreau et al., 2018; Solorzano et al., 2015; Madrid et al., 2007). In *Salmonella,* Hha interacts with H-NS and the resulting

heterodimer preferentially silences horizontally-transferred genes other than core genome (Banos et al., 2009).

Gene silencing caused by H-NS is weak and can be relieved through a process known as 'counter-silencing'. Several studies have described three mechanisms by which counter-silencing of H-NS can be achieved. In the first, regulatory proteins remodel the DNA and disrupt the H-NS-DNA complex, facilitating transcription by RNA polymerase (*e.g.* HU proteins bend H-NS-coated DNA, effectively displacing H-NS from its binding sites (Stoebel et al., 2008)). By way of example, VirB alleviates H-NS repression at the promoters of virulence genes in *Shigella flexneri*, by inducing DNA bending and promoting DNA wrapping around VirB oligomers, leading to disruption of the DNA-H-NS-DNA complex (Gao et al., 2013). Another classic example involves LuxR, an activator of quorum sensing genes in *Vibrio harveyi*, which counter-silences H-NS by displacing/remodeling the H-NS nucleoprotein at promoter regions (Chaparian et al., 2020). A second mechanism involves DNA binding proteins competing with H-NS for binding to the DNA, and in doing so, relieving H-NS repression. For example, in *Vibrio cholera*, the virulence activator ToxT relieves transcription repression of the toxin encoding operon *ctxAB* by displacing H-NS at the *ctxAB* promoter) (Stone and Withey, 2021). The final mechanism involves transcribing RNA polymerase de-repressing H-NS by remodelling or disrupting the H-NS complex, ultimately enhancing transcription (Rangarajan and Schnetz, 2018). H-NS repression can also be alleviated by proteins encoded by bacteriophages (Patterson-West et al., 2021; Ali et al., 2011; Zhu et al., 2012; Ho et al., 2014). A recent study showed that MotB, an early protein encoded by phage T4, antagonizes H-NS repression by interrupting H-NS-DNA interaction, and overexpressing *motB* up-regulates one-third of genes repressed by H-NS (Patterson-West et al., 2021).

In other bacterial systems, H-NS functional analogues, including MvaT in *Pseudomonas* and Lsr2 in actinomycetes*,* play similar roles to H-NS in organizing chromosome structure and regulating gene expression (Qin et al., 2019).

1.5.2 MvaT in *Pseudomonas*

MvaT is the first H-NS-related protein identified in *Pseudomonas* (Tendeng et al., 2003). In *Pseudomonas aeruginosa,* MvaT binds over 100 regions throughout the chromosome and directly or indirectly impacts the expression of ~150 genes, including genes involved in virulence and biofilm formation (Castang et al., 2008; Vallet et al., 2004; Westfall et al., 2006). Like H-NS, MvaT contains a N-terminal dimerization domain and a C-terminal DNA-binding domain connected by a disordered linker (Castang and Dove, 2010). MvaT preferentially binds AT-rich sequences in a cooperative manner and represses transcription by forming high-order oligomers (Castang and Dove, 2010; Qin et al., 2020). Although MvaT belongs to the H-NS family, the two proteins share very low

sequence similarity, especially in their C-terminal domains (Tendeng et al., 2003). Specifically, H-NS binds DNA through interaction between a 'QGR' AT-hook-like motif and the DNA minor groove, whereas MvaT lacks a 'QGR' motif, and instead binds DNA by forming hydrogen bonds between an 'AT-pincer' motif (R80, G99 and N100) in the C-terminus and DNA bases in the minor groove of double-stranded DNA (Duan et al., 2021). Additionally, the C-terminal domain of MvaT contains six highly conserved lysine residues that form a network that facilitates DNA binding by interacting with DNA phosphate groups (Ding et al., 2015). This DNA-protein interaction mode provides MvaT with higher tolerance towards GC-base pair insertions in its binding site (Ding et al., 2015; Duan et al., 2021). Like H-NS, MvaT contains oppositely charged domains that can interact with each other, and this electrostatic interaction is sensitive to salt concentrations, leading to conformation changes of the MvaT dimer (Qin et al., 2020). Under low salt conditions, one of the DNA-binding domain interacts with the N-terminal domain, forming a 'half-open' structure that polymerizes and forms filaments along the DNA; the interaction between the N- and C-terminal domains is prevented with increasing concentrations of salt, transitioning the protein conformation from the 'half-open' to a 'fully-open' state, which allows MvaT to bridge DNA (Qin et al., 2020). A recent study found that bacteriophage proteins can also mediates MvaT protein conformation changes. The *Pseudomonas* phage LUZ24 encodes a protein (gp4) that inhibits MvaT binding to DNA and prevents its repression of LUZ24 genome expression (Wagemans et al., 2015). Structural studies revealed that gp4 contains a coiled-coil structure that prevents the formation of a 'fully-open' structure by binding the MvaT dimerization domain and linker region, resulting in inhibition of the DNA-bridging activity of MvaT (Bdira et al., 2021).

Like H-NS, transcription repression caused by MvaT can be alleviated via counter-silencing. The *P. aeruginosa* pathogenicity island 1 (PAPI-1) is an integrative and conjugative element that can be transferred to a recipient through conjugation (Bellanger et al., 2014). The conjugative pilus required in horizontal transfer of PAPI-1 is encoded by the *pil2* operon, whose expression is repressed by MvaT binding at a promoter region (Carter et al., 2010; Dangla-Pelissier et al., 2021). Two positive regulators of the *pil2* operon were identified from transposon mutagenesis: TprA, an Arc-like protein, and NdpA2, a nucleoid-associated protein. Overexpressing TprA activates *pil2* operon, while NdpA2 functions in synergy with TprA but has no significant effect when expressed alone (Dangla-Pelissier et al., 2021). Further evidence suggested that NdpA2 may promote a conformation change of MvaT, which induces reorganization of the DNA structure and allows TprA binding to the promoter (Dangla-Pelissier et al., 2021).

1.5.3 Lsr2 in actinomycetes

Lsr2 is a small (~12 kDa) nucleoid-associated protein found in actinomycetes (Gordon et al., 2010). Lsr2 is functionally equivalent to H-NS, and it was the first H-NS-like protein to be identified in Gram-positive bacteria. Lsr2 is a global transcriptional repressor that is organized into two functional domains – an N-terminal dimerization/oligomerization domain and a C-terminal DNA binding domain (Gordon et al., 2011; Kriel et al., 2018; Qin et al., 2019; Gehrke et al., 2019; Gordon et al., 2008). Structural study on Lsr2 in *Mycobacterium tuberculosis* revealed that the N-terminal domain of Lsr2 consists of one β-strand followed by an anti-parallel β-sheet formed by two β-strands and one α-helix (Gordon et al., 2008; Summers et al., 2012). Two residues, D28 and R45, are essential for dimerization, where they function to anchor the anti-parallel β-sheet of one Lsr2 monomer to the α-helix of another monomer, resulting in a 4-stranded anti-parallel β-sheet in the Lsr2 dimer (Summers et al., 2012). Furthermore, ten conserved residues (D11, D12, F25, Y32, I34, D35, L36, L44, L48 and W51) are important for dimerization by connecting the β-sheet and α-helix via tertiary hydrophobic and H-bonding interactions (Summers et al., 2012). The N-terminal domain is also responsible for oligomerization. Each Lsr2 dimer has two single β-strands that can pair with β-strands of adjacent dimers to form oligomer. The formation and stabilization of oligomers are mediated by polar interaction between Lys4, and the interactions are prevented when the three N-terminus residues (Met1, Ala2 and Leu3) are present (Summers et al., 2012). Further work showed that removing the three N-terminus residues by proteolysis induces the formation of Lsr2 oligomerization and condensation of DNA, suggesting the regulation of Lsr2 activity by post-translational modifications (Summers et al., 2012; Kriel et al., 2018). Like H-NS, Lsr2 preferentially binds high AT-content DNA through an AT-hook-like motif at the C-terminus, and silences gene expression by bridging DNA or polymerizing along DNA, forming a rigid filament (Chen et al., 2008; Gordon et al., 2008). The C-terminal domain of Lsr2 has two α-helices connected by a loop, which contains a group of positively charged residues flanking a highly conserved RGR motif (AT-hook-like). The RGR motif is responsible for the electrostatic interaction between Lsr2 and the minor groove of double stranded DNA, and mutating 'RGR' to 'AGA' completely abolished Lsr2 binding to DNA (Gordon et al., 2010; Gordon et al., 2011).

In *Mycobacterium,* Lsr2 is a global repressor and binds to 21% and 13% of the genome in *M. tuberculosis* and *Mycobacterium smegmatis,* respectively (Gordon et al., 2010). It was initially believed that *lsr2* was an essential gene because it could not be deleted in *M. tuberculosis* (Summers et al., 2012). However, *lsr2* was later deleted in *M. tuberculosis,* suggesting it is only required under certain conditions (Bartek et al., 2014). Specifically, Lsr2 is critical for adaptation to both high-oxygen and anerobic conditions, and Lsr2 exerts its function by directly controlling a multitude of genes associated with growth and survival in fluctuant oxygen environments (Bartek et al., 2014; Galagan et al., 2013). Studies in *M. tuberculosis* and other *Mycobacterium* species revealed that Lsr2 has pleiotropic effects on cellular processes, including colony morphology, biofilm

formation, virulence and infection (Le Moigne et al., 2019; Kolodziej et al., 2021a; Kolodziej et al., 2021b; Bartek et al., 2014; Gordon et al., 2010).

Given the central role of Lsr2 in controlling gene expression, it is important to understand the regulation of Lsr2 activity. A recent study reported that cholesterol metabolism in *M. tuberculosis* is controlled by Lsr2 and Rv0081, a transcriptional regulator (Lata et al., 2022). Lsr2 inhibits transcription of the genes involved in cholesterol degradation and transport by directly binding to their intragenic regions; Rv0081 is required for cholesterol utilization when growing on media with cholesterol as sole carbon source, and Rv0081 facilitates cholesterol metabolism by binding to the promoter of *lsr2* and repressing *lsr2* expression (Lata et al., 2022). Like H-NS, Lsr2 repression can be alleviated through counter-silencing, and this has been reported in *M. tuberculosis* with respect to regulation of iron metabolism (Kurthkoti et al., 2015). *bfrB* encodes a ferritin in *M. tuberculosis*, and its promoter activity is regulated by Lsr2 and the Fe-dependent transcriptional regulator IdeR. Lsr2 binds directly to the promoter of *bfrB* thereby preventing its transcription. In Fe-rich conditions, IdeR is activated upon iron binding and alleviates Lsr2 repression by binding directly at the promoter of *bfrB*. However, whether this counter-silencing process happens via direct binding competition or enhancing RNA polymerase activity remains unclear (Kurthkoti et al., 2015).

In *Corynebacterium glutamicum*, CgpS is a prophage-encoded Lsr2-like protein which primarily binds horizontally-acquired DNA and plays an essential role in silencing cryptic prophage elements and repressing prophage activity (Pfeifer et al., 2016). Consistent with other H-NS-like proteins, CgpS preferentially binds AT-rich sequences (Pfeifer et al., 2016). Repression caused by CgpS can be alleviated by the GntR regulator through counter-silencing, where GntR disrupts CgpS binding at promoter regions through binding to engineered operator sites (Wiechert et al., 2020a; Wiechert et al., 2020b).

In *Streptomyces,* Lsr2 is a global repressor controlling the production of antibiotics and other specialized metabolites (Gehrke et al., 2019). Previous work from our lab has shown that *lsr2* is essential to *S. coelicolor*, but it can be deleted in *S. venezuelae* (Gehrke et al., 2019). Deletion of *lsr2* does not have a dramatic effect on growth in *S. venezuelae*. RNA-seq data from the *lsr2* deletion strain has revealed that in the absence of *lsr2*, there are significant increases in the expression of six biosynthetic clusters (>80% of the cluster), where five of these clusters were not expressed in the wild type. Notably, half of the genes whose expression is affected by Lsr2 are associated with specialized metabolism (Gehrke et al., 2019). Additionally, antibiotic bioassays performed with extracts from *S. venezuelae* wild type and *lsr2* deletion strains showed that deleting *lsr2* enhances the production of antibiotics (Gehrke et al., 2019).

1.6 Post-translational modifications of histone proteins and nucleoid-associated proteins

1.6.1 Post-translational modifications of histone proteins in eukaryotes

In eukaryotes, DNA is wrapped around histone proteins and is condensed into chromatin in the nucleus. Nucleosomes are the basic subunit of chromatin, and they consist of 146-147 bp of DNA wrapped around a histone octamer, which itself is composed of two copies of each of the core histones H2A, H2B, H3 and H4 (Luger et al., 1997; Alva et al., 2007). Nucleosomes are separated by 10 – 60 bp of linker DNA, and ultimately adopt a 'beads-on-a-string' arrangement. All four core histones have a highly conserved 'helix-turn-helix-turn-helix' motif that recognizes specific DNA sequences, as well as a long amino-terminal 'tail' domain that promotes histone-histone interaction and the formation of higher-level structures (Alva et al., 2007). In addition to organizing DNA, histones play role in cellular processes including gene regulation, DNA repair, chromosome condensation and spermatogenesis, in response to diverse post-translational modifications. Post-translational modifications happen predominantly but not exclusively, within the histone N-terminal domain (Peterson and Laniel, 2004; Bannister and Kouzarides, 2011).

Histone acetylation occurs on lysine residues, and this is controlled by the opposing activities of two families of enzymes: histone acetyltransferases and histone deacetylases (Dawson et al., 2012; Allfrey et al., 1964). Acetylation by histone acetyltransferases neutralizes the positive charge of lysine and weakens the interaction between histones and DNA (Bowman et al., 2016; Bannister and Kouzarides, 2011; Parthun, 2007). Histone deacetylases have the opposite effects, in that they stabilize DNA binding by histones, and repress transcription by restoring the positive charge to lysine (Yang and Seto, 2007). In addition to acetylation, histones are also subject to phosphorylation. Histone phosphorylation on serine, threonine and tyrosine residues is modulated by dedicated kinases and phosphatases (Bannister and Kouzarides, 2011; Ito, 2007). Histone kinases add negative charges to target residues specifically within the N-terminal tail of histones. This action has the potential to decrease the binding affinity of histones for DNA and in doing so, to change chromatin architecture (Bowman et al., 2016). Histones can also be methylated by methyltransferases and demethylases. These enzymes target the side chains of lysine and arginine (Bannister and Kouzarides, 2011), and their methylation is associated with transcriptional regulation and chromosome condensation (Miller and Grant, 2013).

1.6.2 Post-translational modifications of nucleoid-associated proteins in bacteria

Post-translational modifications of histones have been well-studied for more than 30 years. In bacteria, however, equivalent processes have only recently started to be the focus of serious investigation, with the vast majority of studies to date focussing

on nucleoid-associated proteins from Gram-negative bacteria (H-NS, HU and Fis) (Dilweg and Dame, 2018). Post-translational modifications of nucleoid-associated proteins can affect both DNA-protein and protein-protein interactions, depending on the modification site (Dilweg and Dame, 2018). While post-translational modification of proteins is common in bacteria, the environmental triggers and the protein-modifying enzymes remains to be characterized in most cases. Phosphorylation of Ser45, Ser98 and Tyr99 enhance the interaction of H-NS and Mg^{2+}, leading to the 'open' conformation and DNA bridging being favoured (Dilweg and Dame, 2018; Hansen et al., 2013; Lin et al., 2015). A study of H-NS in *Salmonella* revealed that phosphorylation of Thr13 reduces H-NS dimerization and moderately relieves H-NS repression of PhoP/PhoQ-dependent genes (Hu et al., 2019).

Little is known about post-modifications of Lsr2. A phosphoproteomics screen in *S. coelicolor* revealed that the main targets of serine/threonine/tyrosine phosphorylation are proteins involved in sporulation and transcriptional regulation, including Lsr2, which was phosphorylated on Thr78; however, the mechanisms proteins involved these processes remain uncharacterized (Manteca et al., 2011). A study in *M. tuberculosis* showed that Lsr2 can be phosphorylated at four threonine residues (Thr8, Thr22, Thr31 and Thr112), and phosphorylation at theses residues decreases the affinity of Lsr2 for DNA (Alqaseer et al., 2019). Furthermore, phosphorylation at Thr112 is important for *M. tuberculosis* growth under hypoxia conditions (Alqaseer et al., 2019). These observations collectively suggest that nucleoid-associated protein modification represents a new – largely unexplored – level in the control of gene expression in bacteria.

1.7 Outline of this study

In *Streptomyces*, the expression of many antibiotic biosynthetic clusters is controlled by both pathway-specific regulators and more globally-acting regulators; however, there is much that remains to be discovered about the regulators that govern antibiotic production. We have established that the histone-like protein Lsr2 represses antibiotic cluster expression. To understand how this repression is achieved, we focussed our attention on one gene cluster that directs the production of the antibiotic chloramphenicol. We established that Lsr2 shuts down cluster expression by binding DNA at sites both within the cluster and at flanking sites outside of the cluster, and that this repressive effect can be alleviated by a chloramphenicol-specific regulator. These findings suggest that manipulating Lsr2 activity has the potential to promote the expression of antibiotic clusters. This work is described in **Chapter 2** and was published in *mBio* in 2021 (Zhang et al., 2021). To understand how Lsr2 activity is controlled within *Streptomyces* cells, we examined post-translational modification of Lsr2 in *S. venezuelae* and identified interacting partners that could impact Lsr2 regulatory activity. This work is described in **Chapter 3**. Beyond Lsr2, we wanted to develop a comprehensive

understanding of those regulatory proteins that impact biosynthetic gene cluster expression. To define the regulatory protein occupancy of antibiotic clusters (and chromosome-wide), we used '*in vivo* protein occupancy display-high resolution' (IPOD-HR) technology. This work will lay the foundation for establishing a regulatory network map for biosynthetic clusters in *Streptomyces*, and guide future work aimed at stimulating the expression of metabolic clusters of interest in any *Streptomyces* species. This work is described in **Chapter 4**.

CHAPTER 2: INTERPLAY BETWEEN NUCLEOID-ASSOCIATED PROTEINS AND TRANSCRIPTION FACTORS IN CONTROLLING SPECIALIZED METABOLISM IN *STREPTOMYCES*

Xiafei Zhang, Sara N. Andres, Marie A. Elliot

Preface:

This chapter was published in the *mBio* in 2021 (Zhang et al., 2021). Dr. Sara N. Andres (Biochemistry and Biomedical Sciences, McMaster University) assisted with atomic force microscopy data collection and analyses. I performed all other experiments.

2.1 Abstract (Chapter Summary)

Lsr2 is a small nucleoid-associated protein found in actinomycetes. Lsr2 functions similarly to the well-studied H-NS, in that it preferentially binds AT-rich sequences and represses gene expression. In *Streptomyces venezuelae*, Lsr2 represses the expression of many specialized metabolic clusters, including the chloramphenicol antibiotic biosynthetic gene cluster, and deleting lsr2 leads to significant upregulation of chloramphenicol cluster expression. We show here that Lsr2 likely exerts its repressive effects on the chloramphenicol cluster by polymerizing along the chromosome and by bridging sites within and adjacent to the chloramphenicol cluster. CmlR is a known activator of the chloramphenicol cluster, but expression of its associated gene is not upregulated in an *lsr2* mutant strain. We demonstrate that CmlR is essential for chloramphenicol production, and further reveal that CmlR functions to "counter-silence" Lsr2's repressive effects by recruiting RNA polymerase and enhancing transcription, with RNA polymerase effectively clearing bound Lsr2 from the chloramphenicol cluster DNA. Our results provide insight into the interplay between opposing regulatory proteins that govern antibiotic production in *S. venezuelae*, which could be exploited to maximize the production of bioactive natural products in other systems.

2.2 Introduction

Streptomyces species are renowned for their complex life cycle and their ability to produce a wide range of medically useful specialized metabolites, including over two-thirds of the antibiotics in clinical use today. Genome sequencing has revealed that most *Streptomyces* spp. encode 25 to 50 specialized metabolic clusters (Lee et al., 2020; Belknap et al., 2020; Doroghazi and Metcalf, 2013); however, the vast majority of their associated products have yet to be identified. Many of these clusters' genes are poorly transcribed, and consequently, their resulting products have never been detected under laboratory conditions (Gehrke et al., 2019; Yoon and Nodwell, 2014; Zhang et al., 2019). These "cryptic" and "silent" clusters have the potential to produce an impressive array of novel antibiotics (Lee et al., 2020; Xu et al., 2017; Hoshino et al., 2019), and activating their expression is one of the keys to facilitating new antibiotic discovery.

In *Streptomyces*, specialized metabolic clusters are controlled by multiple factors. These include cluster-situated regulators (encoded within their cognate biosynthetic gene clusters) that govern metabolite synthesis by directly binding promoter regions in their associated cluster. Pleiotropic regulators have also been implicated in antibiotic control; these are usually encoded elsewhere on the chromosome and affect the expression of multiple biosynthetic clusters (Bibb, 2005). In recent years, nucleoid-associated proteins have also been found to influence the expression of specialized metabolic clusters (Gehrke et al., 2019; Gao et al., 2012; Swiercz et al., 2013; Yang et al., 2012).

Historically, nucleoid-associated proteins function to promote chromosome organization; however, they can also impact activities like DNA replication, transcription, and chromosome segregation (Badrinarayanan et al., 2015; Song and Loparo, 2015; Szafran et al., 2020). H-NS (histone-like nucleoid-structuring protein) is one of the best-studied nucleoid-associated proteins. It is, however, found in only a subset of Gram-negative bacteria, where it preferentially binds and spreads along and/or bridges distal high-AT-content DNA, compacting the chromosome and/or silencing gene expression (Song and Loparo, 2015; van der Valk et al., 2017; Qin et al., 2020; Qin et al., 2019; Shahul Hameed et al., 2019). The resulting DNA filaments and/or DNA bridges formed by H-NS have the potential to affect gene expression by trapping RNA polymerase and repressing transcription, or by excluding RNA polymerase from promoter regions.

In the streptomycetes, H-NS-like proteins play important roles in regulating antibiotic production. The H-NS-equivalent protein in these bacteria is termed Lsr2, and it is conserved in actinomycetes (Szafran et al., 2020; Gordon et al., 2010). Like H-NS, Lsr2 is a global repressor that preferentially binds high AT-content DNA (Gehrke et al., 2019; Gordon et al., 2010; Chen et al., 2008) and, based on work with the mycobacterial protein, is predicted to silence gene transcription by bridging or oligomerizing along the DNA (van der Valk et al., 2017; Qin et al., 2020; Gordon et al., 2010). Deleting *lsr2* in *Streptomyces venezuelae* leads to significantly upregulated gene expression in a majority of specialized metabolic biosynthetic clusters, including many otherwise cryptic clusters that are not expressed in a wild type background (Gehrke et al., 2019). This suggests that Lsr2 functions to broadly repress specialized metabolism in *Streptomyces* species.

To better understand how Lsr2 repression is both exerted and alleviated in the streptomycetes, we focused our attention on the chloramphenicol biosynthetic cluster. Previous work revealed that loss of Lsr2 results in a dramatic increase in the expression of the chloramphenicol biosynthetic genes, and this effect seems to be a direct one, as an Lsr2 binding site was identified within the gene cluster (Gehrke et al., 2019) (**Figure 2.1**). The chloramphenicol biosynthetic cluster comprises 16 genes (*sven0913* to *sven0928*), with *sven0913*/*cmlR* encoding a pathway-specific transcriptional activator (Fernandez-Martinez et al., 2014). Here, we show that Lsr2 binding to the cluster-internal site, and to an upstream adjacent sequence, leads to Lsr2 polymerization along the DNA and can promote bridging between these two regions. This binding activity limits chloramphenicol production, presumably through the repression of cluster transcription. Lsr2 repression can be relieved through the action of CmlR, which functions as a counter-silencer of Lsr2 activity and is essential for chloramphenicol production. CmlR appears to exert its activity not by competing with Lsr2 for binding but instead by promoting cluster transcription, where the action of RNA polymerase serves to clear Lsr2 from the DNA, alleviating cluster repression.

2.3 Results

2.3.1 Antibiotic production is impacted by Lsr2 binding to sites adjacent to the chloramphenicol cluster

Lsr2 represses the expression of the majority of genes in the chloramphenicol biosynthetic cluster (Gehrke et al., 2019) (**Figure 2.1A**). Intriguingly, the only Lsr2 binding site within the cluster was in the coding sequence of a gene (*sven0926*) located at the 3' end of the cluster (Gehrke et al., 2019) (**Figure 2.1A**). We revisited our chromatin immunoprecipitation sequencing (ChIP-seq) data (Gehrke et al., 2019) and noted that there was a second Lsr2 binding site upstream of the cluster, spanning the genes *sven0904* and *sven0905* (referred to here as *sven0904-0905*), where *sven0904* is predicted to encode a solute binding transport lipoprotein and *sven0905* is predicted to encode a short-chain oxidoreductase (**Figure 2.1A**). We first set out to validate Lsr2 binding to both internal and upstream sites using electrophoretic mobility shifts assays (EMSAs). We found Lsr2 had a much higher affinity for *sven0904-0905* and *sven0926* probes than for a negative-control sequence (within *sven3556*, which was not bound by Lsr2 in our previous ChIP-seq experiments), confirming the specific binding of Lsr2 to these sites within and adjacent to the chloramphenicol cluster (**Figure 2.1B**).

Given the functional similarity shared by Lsr2 and H-NS, we hypothesized that Lsr2 may exert its repressive effects in a manner analogous to that of H-NS, by polymerizing along the DNA and/or bridging distant DNA regions. We considered three mechanisms by which Lsr2 could repress transcription of the chloramphenicol cluster: (i) Lsr2 could bind within *sven0926* and polymerize along the chromosome, repressing expression of the flanking gene clusters; (ii) Lsr2 could bind to both *sven0904-0905* and *sven0926* sites and interact to bridge these sequences and alter the structure of the intervening DNA; or (iii) Lsr2 could both polymerize along the DNA and bridge these disparate sequences. We expected that if Lsr2 repressed transcription of the chloramphenicol cluster by polymerizing only from the *sven0926* binding site, then the *sven0904-0905* binding site would be dispensable for Lsr2 repression, and this region would have no effect on chloramphenicol production. If, however, Lsr2 repression was mediated by bridging these two sites (*sven0926* and *sven0904-0905*), or both polymerizing along the DNA and bridging these two regions, then deleting the upstream/cluster-adjacent binding site would relieve cluster repression and yield increased chloramphenicol levels relative to the wild type strain.

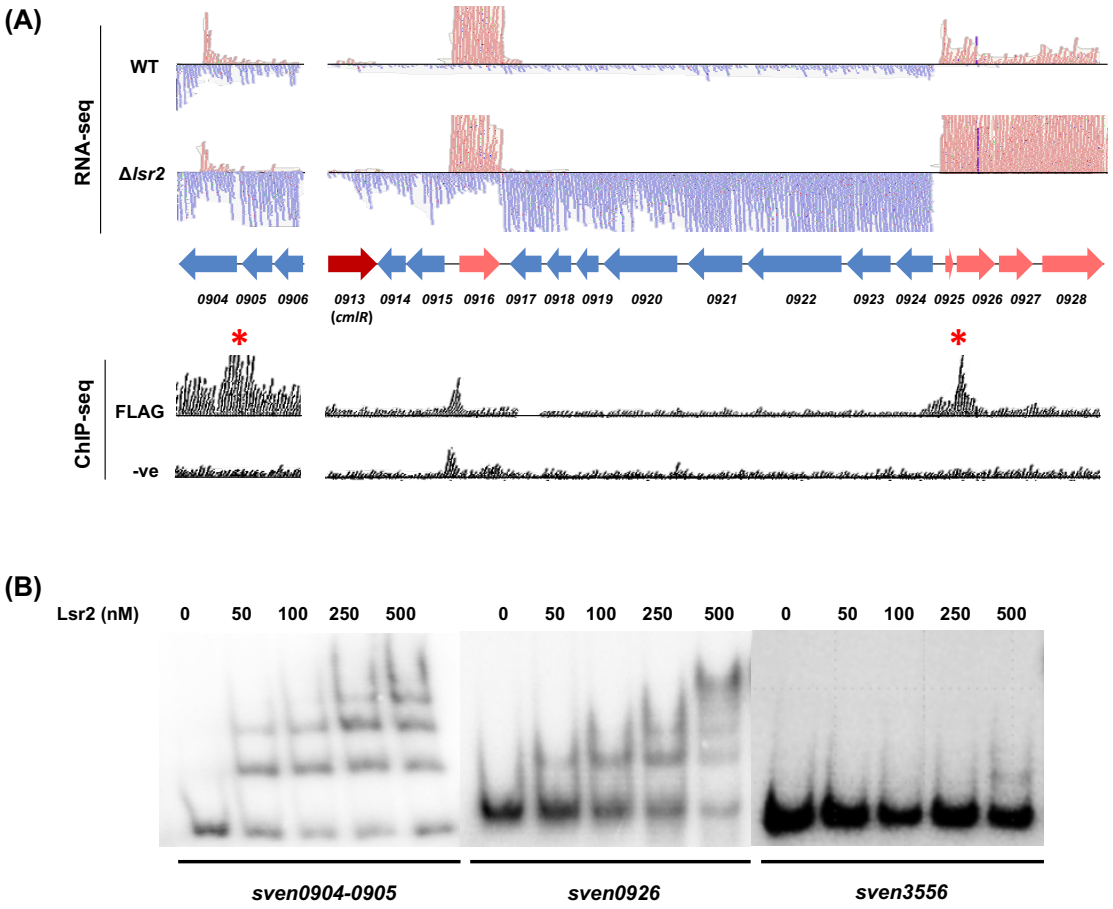

Figure 2.1: Lsr2 binding sites and effect on transcription of the chloramphenicol biosynthetic cluster. (**A**) (Top) RNA-seq analysis of gene expression within and upstream of the chloramphenicol biosynthetic cluster in wild type and *lsr2* mutant strains. Blue reads (and gene arrows) map to the reverse strand, and pink reads (and gene arrows) map to the forward strand; red arrow indicates *cmlR*, the pathway-specific regulator-encoding gene. (Bottom) ChIP-seq analysis of Lsr2 binding sites (using a FLAG-tagged Lsr2 variant), alongside a negative control (expressing untagged Lsr2). Red asterisks indicate statistically significant Lsr2 binding sites at *sven0904-sven0905* and within *sven0926*. (**B**) EMSAs probing Lsr2 binding to sites within and adjacent to the chloramphenicol biosynthetic cluster. Increasing concentrations of Lsr2 (0 to 500 nM) were combined with 1 nM labeled *sven0904-0905* (upstream/adjacent), *sven0926* (internal), or *sven3556* (negative control) probes. The results are representative of two independent biological replicates.

To probe these different scenarios, we compared chloramphenicol production by wild type and Δ*lsr2* strains, alongside a Δ*0904-0905* mutant (where the deletion encompassed the entire coding regions of both *sven0904* and *sven0905*) and a double

Δ*lsr2*Δ*0904-0905* mutant strain using liquid chromatography–mass spectrometry (LC-MS). LC-MS analyses revealed that, relative to the wild type, deleting *sven0904-0905* led to a significant increase (~4-fold) in chloramphenicol production, while deleting both *lsr2* and *sven0904-0905* led to an ~13-fold increase in chloramphenicol production, which was similar to the production levels of the Δ*lsr2* mutant alone (~11-fold) (**Figure 2.2**).

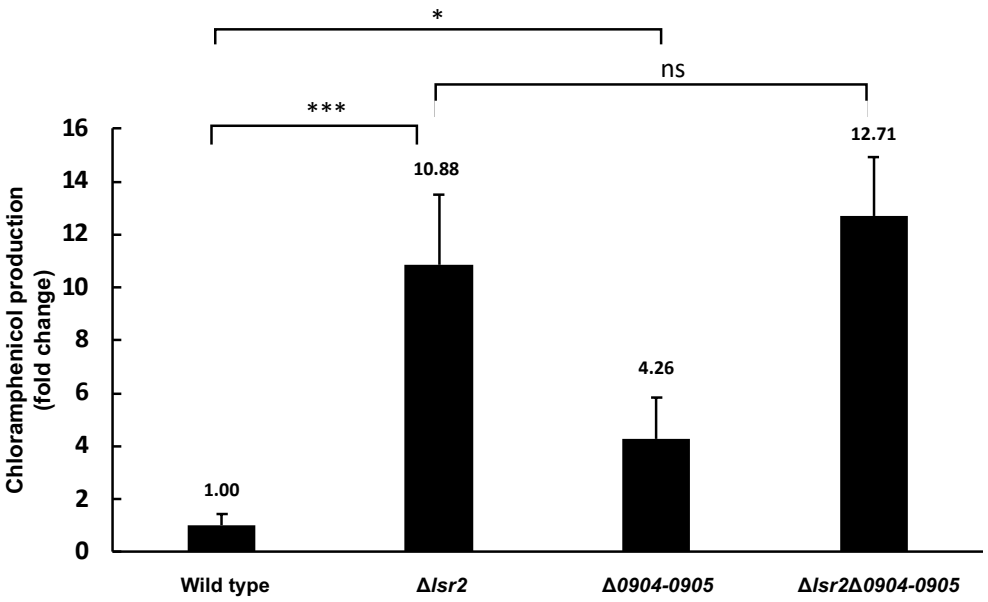

Figure 2.2: Deleting *sven0904-0905* from the chromosome increased chloramphenicol production. *sven0904-0905* were deleted in wild type and Δ*lsr2* backgrounds, and LC-MS analyses were performed on the resulting strains after 2 days' growth in liquid culture, to quantify changes in chloramphenicol production relative to the wild type. Error bars represent standard deviations for three independent biological replicates. *, $P<0.05$; ***, $P<0.005$; ns, no significant difference.

These results were consistent with a possible role for the *sven0904-0905* site in repressing chloramphenicol production through Lsr2 bridging between this site and the internal binding site. It was, however, formally possible that the products of these two upstream genes negatively influenced chloramphenicol production. To test this second possibility, we sought to complement the *sven0904-0905* mutant strains by cloning the operon containing wild type *sven0904-0905* into the integrating plasmid vector pMS82. We reasoned that reintroducing these genes on a plasmid vector that integrated at an independent site in the chromosome should restore wild type levels of chloramphenicol production if their products were important for antibiotic production, whereas no complementation of the mutant phenotype was expected if the locus position was

critical for cluster repression. We introduced the complementation construct into the mutant strains alongside the empty plasmid as a control (in both mutants and the wild type) and assessed chloramphenicol production by these different strains. Complementing the mutants (Δ*0904-0905* and Δ*lsr2*Δ*0904-0905*) with the *sven0904-0906* operon failed to restore production levels to that of the empty plasmid-containing wild type and Δ*lsr2* strains (**Figure 2.3**). This suggested that the position of the *sven0904-0905* locus on the chromosome (and its associated Lsr2-binding site) – and not the function of the SVEN0904 and SVEN0905 gene products – may be important for controlling chloramphenicol production.

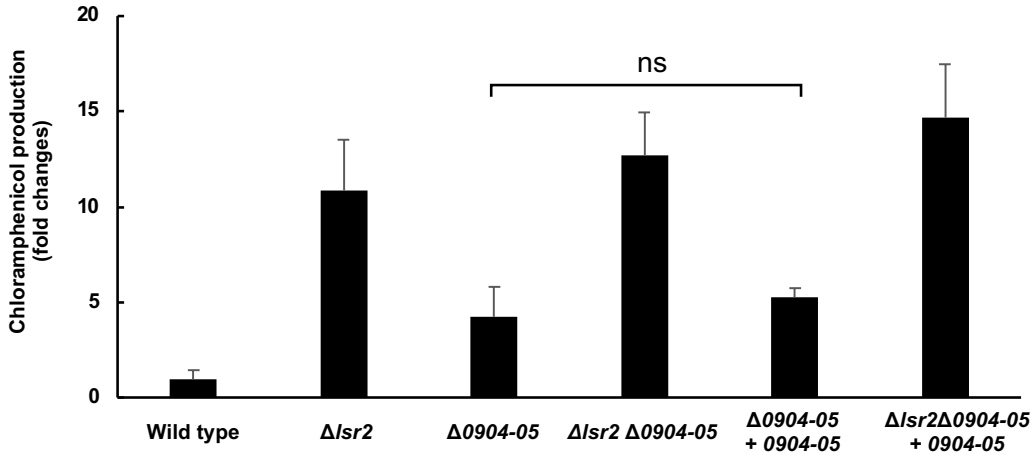

Figure 2.3: Complementing *sven0904-0905* failed to restore chloramphenicol production. *sven0904-0905* was deleted in wild type and Δ*lsr2* backgrounds, and the operon was re-introduced into the mutant strains on an integrating plasmid vector (*+0904-05*). LC-MS analyses were performed to quantify changes in chloramphenicol production, relative to empty plasmid-containing wild type and *lsr2* mutant strains. Error bars represent standard deviation for three independent biological replicates, with ns indicating differences that were not statistically significant (comparisons with other strains were not statistically assessed).

2.3.2 Lsr2 binding leads to polymerization along the DNA and bridging between sites upstream and within the chloramphenicol cluster

To explore the potential bridging capabilities of Lsr2, we employed atomic force microscopy (AFM). The two chloramphenicol cluster-associated Lsr2 binding sites are separated by 24 kb, which would be larger than ideal for use in AFM experiments. We initially opted to bring these two binding sites closer together, such that there was ~1 kb separating the core binding sites (giving a total DNA fragment length of 2,919 bp). Lsr2

was then added, and the resulting products were visualized. If DNA bridging was the sole mechanism by which Lsr2 exerted its regulatory activity, we expected to see a loop formed between the Lsr2 binding sites at either end of the DNA fragment. However, we failed to detect any loop structures and instead observed only DNA molecules that had been coated and compacted by Lsr2, suggesting that Lsr2 could polymerize along the DNA under these *in vitro* conditions.

To better assess the bridging potential of Lsr2, we added an extra 1 kb of sequence between the two Lsr2 binding sites, to give a DNA fragment of ~4 kb. Using AFM, we compared the length of the DNA alone with that of DNA mixed with Lsr2. For the DNA-alone experiments, we needed to supplement the binding buffer with Ni^{2+} to facilitate DNA adherence to the mica slide used for the AFM experiments; Ni^{2+} was not added to the Lsr2-containing samples, as it disrupted DNA binding by Lsr2. For the DNA-alone controls, we observed linear DNA molecules (**Figure 2.4A and B**), with an average length of 1,273.7 nm (*n* = 71) (**Figure 2.4B and C**), consistent with the expected length of 1,200 nm for a 4-kb DNA molecule. In the presence of 250 nM Lsr2, looped molecules were identified alongside linear-appearing DNA-Lsr2 complexes (*n* = 54) (**Figure 2.4A and B**). For the linear-appearing DNA-Lsr2 complexes, Lsr2 polymerization was apparent at one end of the DNA, but no obvious bridging was observed. In contrast, loop structures appeared to result from Lsr2 bridging the two distal regions. Notably, Lsr2 polymerization was also typically observed at each bridging site, where the loop appeared to have been "zipped up" (**Figure 2.4A**). The lengths of both the looped and linear DNA-Lsr2 complexes were measured in the presence of 250 nM Lsr2, and the mean value was found to be 845.7 nm (*n* = 54) (**Figure 2.4B and C**). To ensure that these changes in DNA structure and length stemmed from specific Lsr2 binding and oligomerization and not simply DNA folding back on itself, the height of the observed DNA-alone molecules and Lsr2-bound regions were measured; it was expected that Lsr2 binding to DNA would result in a minimum 3-fold increase in height. The mean values of the height of DNA alone and Lsr2-bound regions were 0.23 nm (*n*=71) and 1.15 nm (*n*=36), respectively (**Figure 2.4B and C**). To further confirm that these DNA structures were the result of specific Lsr2 binding, equivalent experiments were performed using a 4.5 kb DNA fragment that lacked Lsr2 binding sites, based on our previous ChIP-seq analyses (Gehrke et al., 2019). As expected, DNA alone adopted a linear configuration. However, under the conditions used for Lsr2 binding, we consistently failed to detect any DNA, suggesting that Lsr2 was unable to specifically associate with this DNA fragment and tether the DNA to the slide (**Figure 2.5**). In all, the AFM results suggested that Lsr2 could polymerize along the DNA and had the capacity to bridge disparately positioned sites (at least 4 kb apart) and polymerize toward each binding site. These collective actions may serve to downregulate chloramphenicol production by limiting RNA polymerase access/activity within the chloramphenicol biosynthetic cluster in *S. venezuelae*.

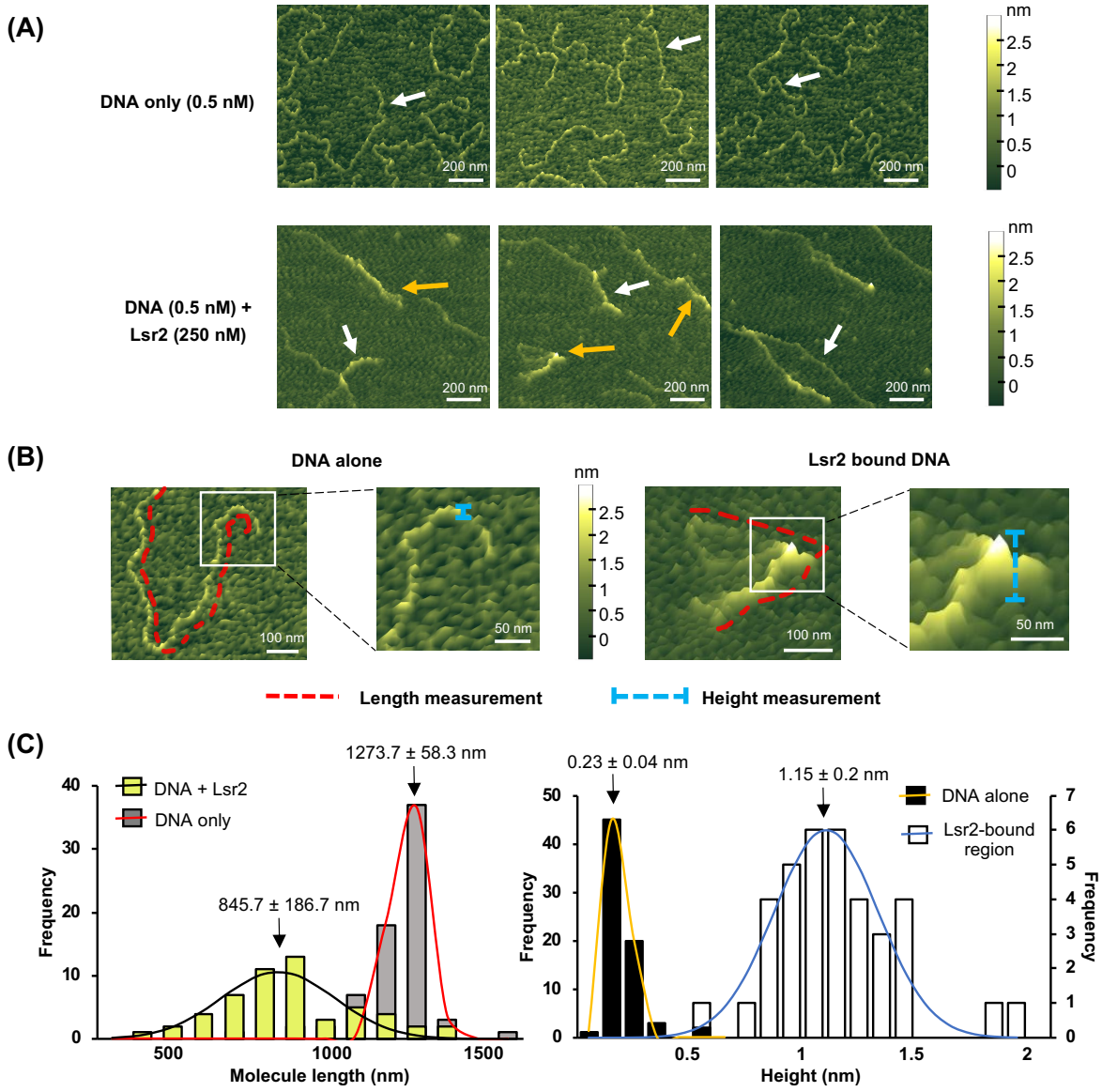

Figure 2.4: Lsr2 binds specific target sequences and can both form polymers along the DNA, and bridge binding sites. (**A**) (Top) AFM images of engineered (target) DNA molecules with two Lsr2 binding sites on either end. (Bottom) AFM images of 0.5 nM target DNA plus 250 nM Lsr2. White arrows indicate linear DNA molecules; orange arrows indicate looped structures. (**B**) Illustration of how length and height measurements of DNA alone and Lsr2-bound regions were taken. (**C**) (Left) Frequency distribution of length of Lsr2-bound/unbound DNA molecules. *n*=71 for DNA only and 54 for DNA plus Lsr2. (Right) Frequency distribution of mean height of DNA alone (frequency axis on the left) and Lsr2-bound regions (frequency axis on the right). *n*=71

for DNA alone and 36 for Lsr2-bound regions. Data are means and standard deviations, calculated from nonlinear Gaussian fit.

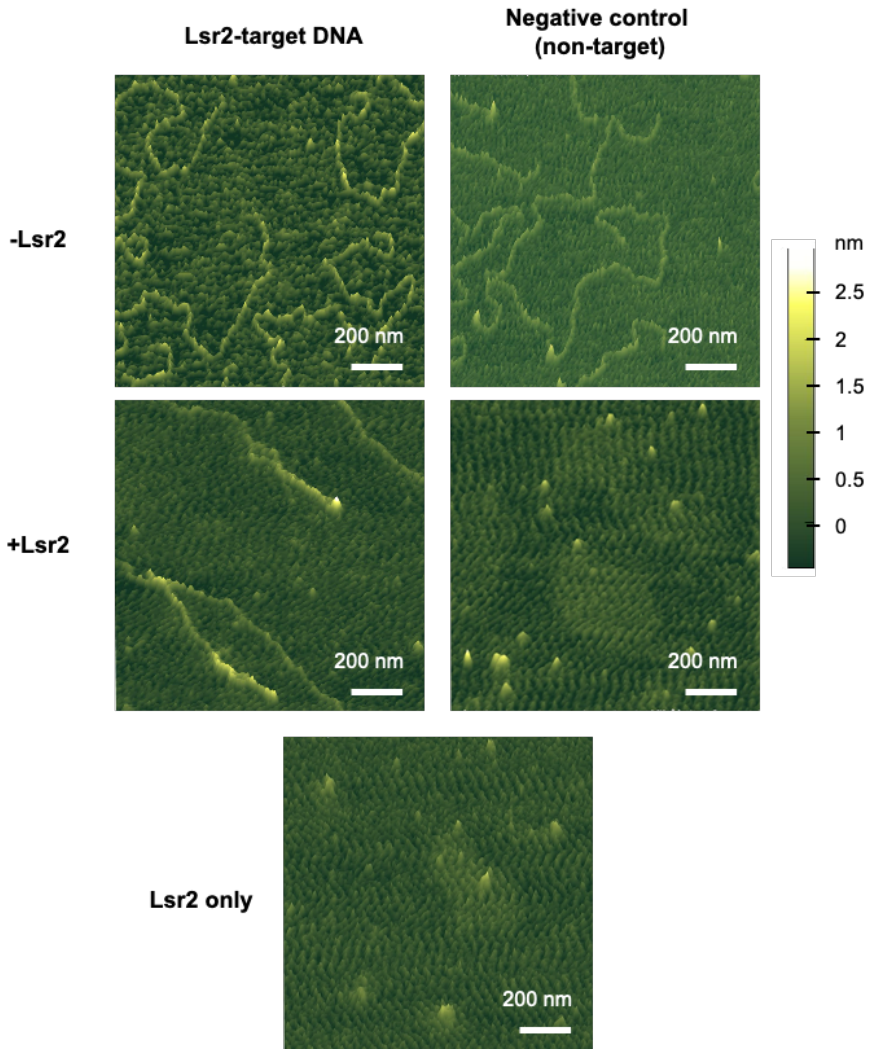

Figure 2.5: Comparing Lsr2 binding to engineered target DNA (two Lsr2 binding sites) and negative control (no Lsr2 binding sites) DNA. Top: AFM images of Lsr2 target-containing DNA (*sven0904-0905-0926*) and negative control DNA (*sven7031*) molecules with nickel added to the buffer. **Middle**: AFM images of 0.5 nM DNA + 250 nM Lsr2, without nickel added to the buffer. **Bottom:** AFM image of 250 nM Lsr2, without nickel added to the buffer. The figure shows representative images from three independent experiments.

2.3.3 The pathway-specific regulator CmlR is essential for chloramphenicol production

We next set out to understand how the cluster-situated regulator CmlR impacted chloramphenicol production. Our previous RNA sequencing results had revealed that the expression of most genes in the chloramphenicol biosynthetic cluster was significantly increased in the absence of Lsr2. A notable exception, however, was *cmlR* (*sven0913*), whose transcript levels were consistent in both wild type and *lsr2* mutant strains (**Figure 2.1A**). Consequently, we wondered whether CmlR might function simply to relieve Lsr2 repression and whether it was dispensable for cluster expression in the absence of Lsr2.

To test this hypothesis, we sought to determine the relative importance of CmlR in wild type and *lsr2* mutant strains of *S. venezuelae*. We created strains in which *cmlR* was deleted from the chromosome and in which it was overexpressed from a strong, constitutive (*ermE**) promoter on an integrating plasmid in both wild type and *lsr2* mutant strains. We then tested chloramphenicol production levels in these different strains using LC-MS analyses. In these experiments, we found that deleting *lsr2* led to an ~8-fold increase in chloramphenicol production relative to the wild type and that deleting *cmlR* abolished chloramphenicol production in all strains. This suggested that CmlR was critical for chloramphenicol biosynthesis beyond simply relieving Lsr2 repression. Consistent with this observation, we found that overexpressing *cmlR* led to a massive increase in chloramphenicol production in wild type strains (102-fold increase relative to plasmid-alone controls), while overexpressing CmlR in the absence of Lsr2 led to even higher chloramphenicol levels (134-fold increase) (**Figure 2.6**). These results suggested that CmlR activity was essential for stimulating chloramphenicol production.

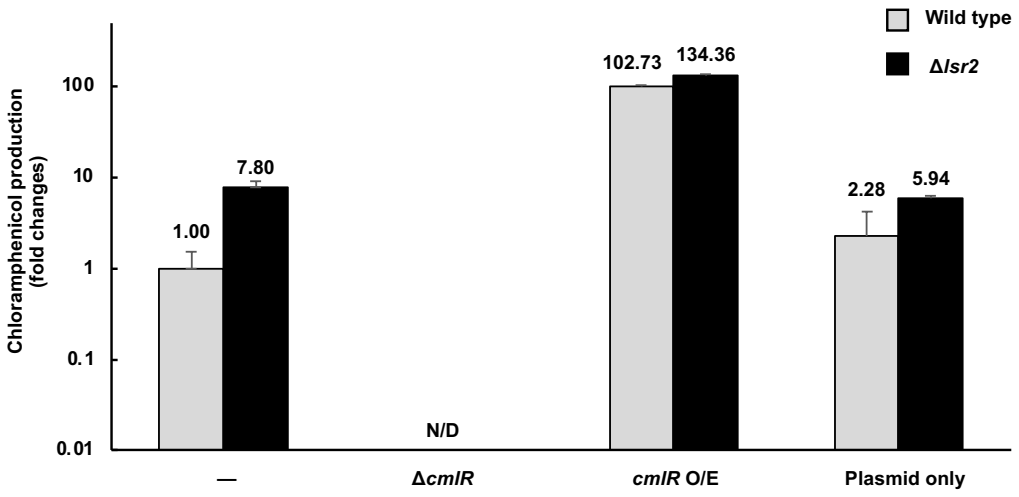

Figure 2.6: CmlR is required for chloramphenicol production in *S. venezuelae*. LC-MS analyses of changes in chloramphenicol production, relative to wild type, are plotted on a logarithmic graph. Gray, wild type background; black, Δ*lsr2* background. N/D, not

detected. Error bars represent standard deviations for two independent biological replicates.

2.3.4 CmlR binds to a divergent promoter region in the chloramphenicol biosynthetic cluster

To begin to understand how CmlR exerted its regulatory effects within the chloramphenicol cluster, we examined its DNA binding capabilities. CmlR shares 44% amino acid sequence identity with StrR (Fernandez-Martinez et al., 2014). which is the pathway-specific activator of the streptomycin biosynthetic gene cluster in *Streptomyces griseus* (Tomono et al., 2005). The StrR target sequence is well-established (5′-GTTCGACTGN$_{11}$CAGTCGAAC-3′) (Tomono et al., 2005), and so we searched for similar sequences in the intergenic/promoter-containing regions of the chloramphenicol cluster. We identified a potential binding site for CmlR between the *sven0924* and *sven0925* promoters, upstream of the Lsr2 binding site within *sven0926* (**Figure 2.7A**). To test whether CmlR specifically bound this sequence, we conducted EMSAs using the predicted binding site as a probe. We found that CmlR directly bound the promoter region with high affinity (**Figure 2.7B**). We confirmed binding specificity using the promoter of a gene outside the chloramphenicol cluster (*sven5133*); there was no binding to this DNA fragment when equivalent concentrations of CmlR were used (**Figure 2.7B**). This implied that CmlR specifically bound a site between the promoters driving the *sven0924*- and *sven0925*-associated operons.

2.3.5 CmlR alleviates Lsr2 repression within the chloramphenicol biosynthetic cluster

Given the relative proximity of the CmlR and Lsr2 binding sites within the chloramphenicol cluster, and that CmlR overexpression appeared to overcome Lsr2-mediated repression of cluster expression, we wanted to determine whether CmlR could act to counter-silence the repressive effects of Lsr2. To address this possibility, we tested whether overexpressing CmlR reduced Lsr2 binding within the chloramphenicol cluster. We introduced our Lsr2-FLAG-tagged expression construct into the *lsr2 cmlR* double- mutant strain and into an *lsr2* mutant strain overexpressing CmlR. Using ChIP to capture DNA sequences bound by Lsr2-FLAG, we then used quantitative PCR (qPCR) to compare the relative amount of target DNA (*sven0926*) bound by Lsr2 in strains lacking or overexpressing CmlR. To ensure that any CmlR-mediated effects were specific to Lsr2 binding within the chloramphenicol cluster, we also assessed Lsr2 binding to another validated Lsr2-binding site positioned outside the chloramphenicol cluster (*sven6264*), alongside negative-control sequences not bound by Lsr2 (based on previous ChIP experiments) (Gehrke et al., 2019).

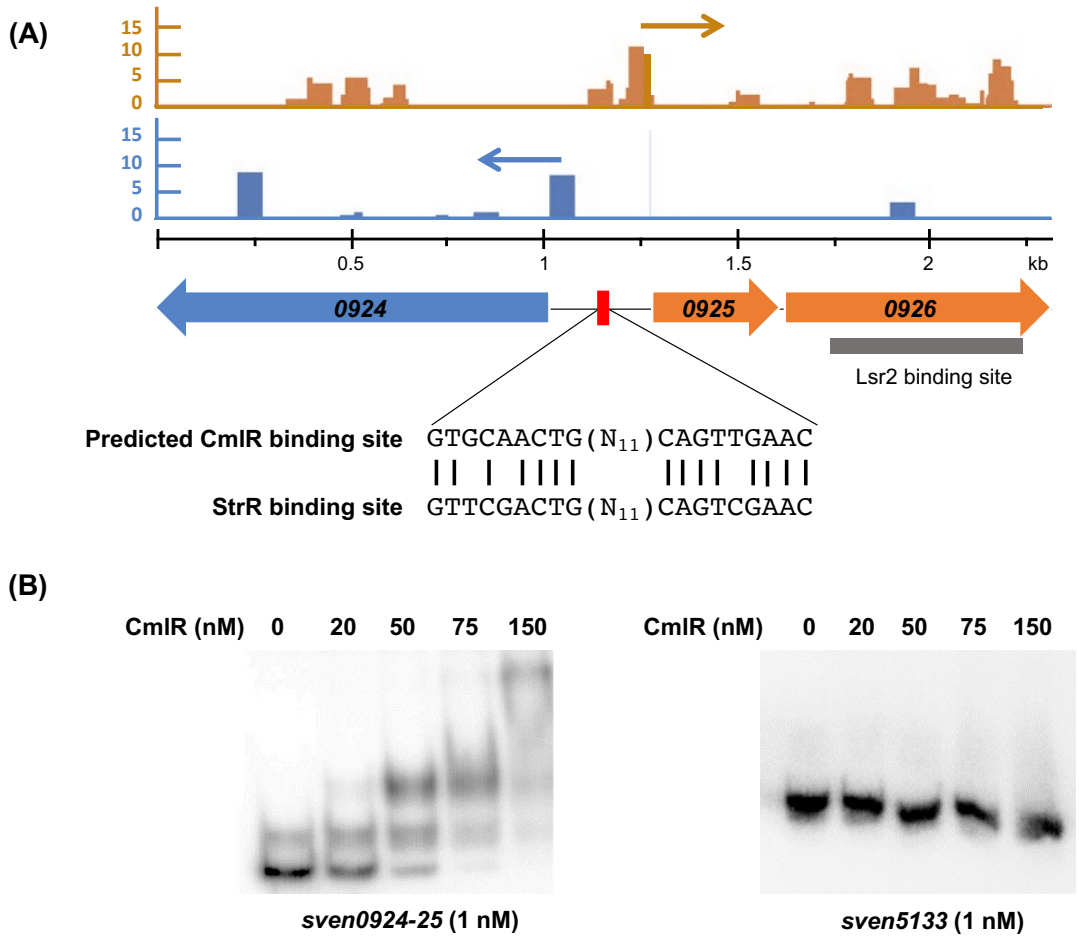

Figure 2.7: CmlR binds promoter regions within the chloramphenicol biosynthetic cluster. (**A**) (Top) Transcription start sites mapped for the *sven0924* and *sven0925* operons, as determined using differential RNA sequencing. (Middle) Schematic diagram showing the predicted CmlR binding site (red bar) within the divergent promoter region upstream of *sven0924* and *sven0925* and the Lsr2 binding site (gray bar) within *sven0926*. The predicted CmlR binding sequence is shown below, together with the analogous StrR binding sequence. Blue reads (and blue arrows) map to the reverse strand; orange reads (and orange arrows) map to the forward strand. (**B**) EMSA using 1 nM labeled *sven0924-0925* or *sven5133* (negative control) promoter regions as probes, together with increasing concentrations (0 to 150 nM) of purified CmlR. Results are representative of two independent mobility shift assays.

Overexpressing CmlR reduced the levels of *sven0926* bound by Lsr2 by 40%, while deleting *cmlR* resulted in >100% increase in *sven0926* bound by Lsr2, relative to that bound by Lsr2 in the presence of wild type levels of CmlR (**Figure 2.8**). Overexpressing and deleting *cmlR* had no obvious effects on the abundance of either the

external Lsr2 target *sven6264* or the negative-control sequence. Taken together, these findings indicated that CmlR activity could influence Lsr2 binding within the chloramphenicol biosynthetic cluster and, in doing so, had the potential to counter the repressive effects of Lsr2.

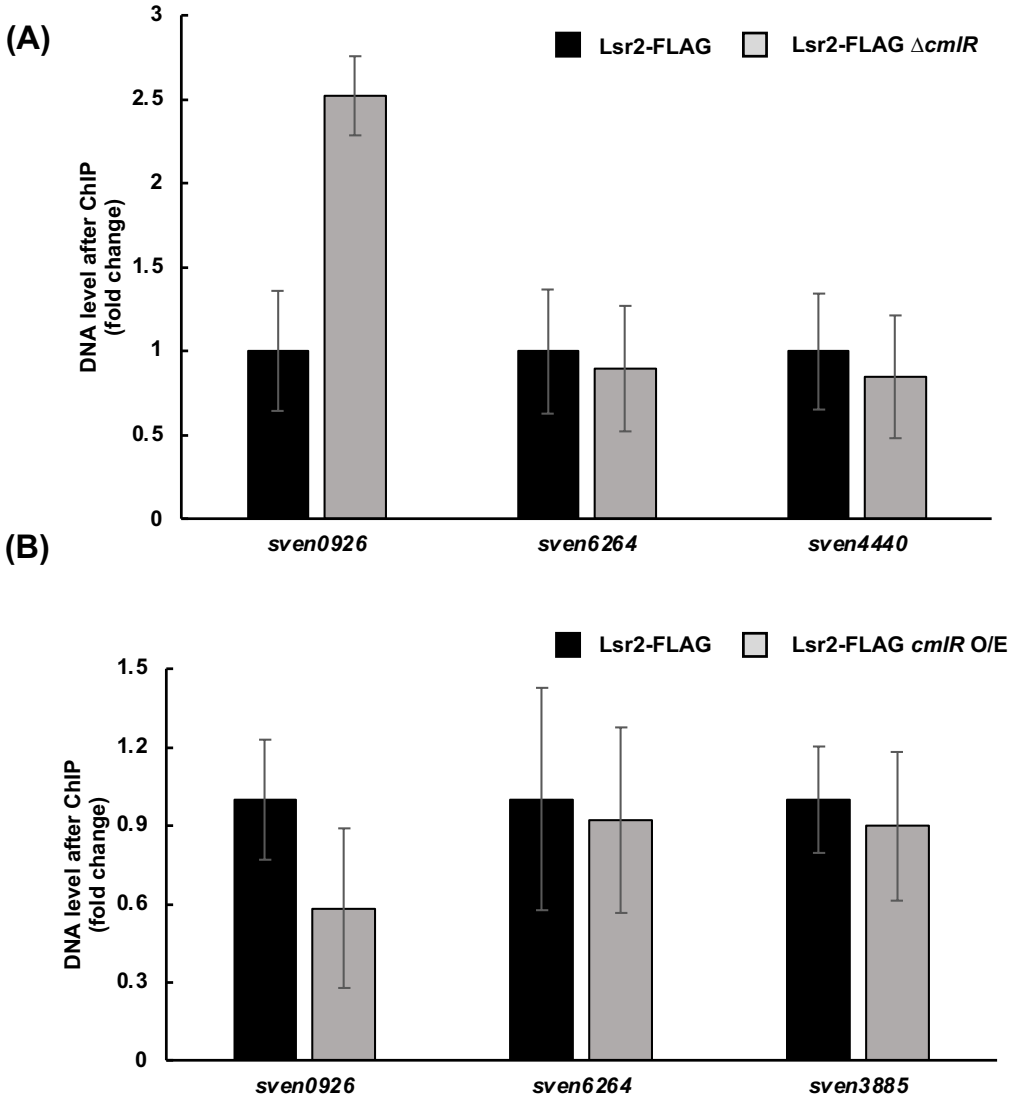

Figure 2.8: CmlR levels affect Lsr2 binding. (**A**) ChIP-qPCR quantification of the relative abundance of *sven0926, sven6264* (Lsr2-binding site positioned outside the chloramphenicol cluster), and *sven4440* (negative control; not bound by Lsr2 in ChIP experiments) bound by Lsr2, in a strain with and without *cmlR* (black and gray bars, respectively). (**B**) qPCR analysis of ChIP DNA samples, quantifying the relative abundance of *sven0926*, *sven6264*, and *sven3885* (negative control; not bound by Lsr2 in ChIP

experiments) in a strain with wild type *cmlR* (black bars) versus a *cmlR* overexpression (O/E) strain (gray bars). For both panels A and B, error bars represent standard errors of the means, for technical triplicate and biological duplicate samples.

2.3.6 CmlR alleviates Lsr2 repression by enhancing transcription

How CmlR impacted Lsr2 binding was not immediately obvious. We hypothesized that CmlR functioned to recruit RNA polymerase and that the act of transcription disrupted the Lsr2 polymers/bridges, thus relieving Lsr2 repression (the CmlR binding site is immediately upstream of the *0925* promoter region) (**Figure 2.7**). To test this possibility, we assessed whether inhibiting transcription affected Lsr2 binding, taking advantage of the fact that RNA polymerase (and correspondingly transcript elongation) could be inhibited by the antibiotic rifampicin (Campbell et al., 2001; Chen et al., 2015).

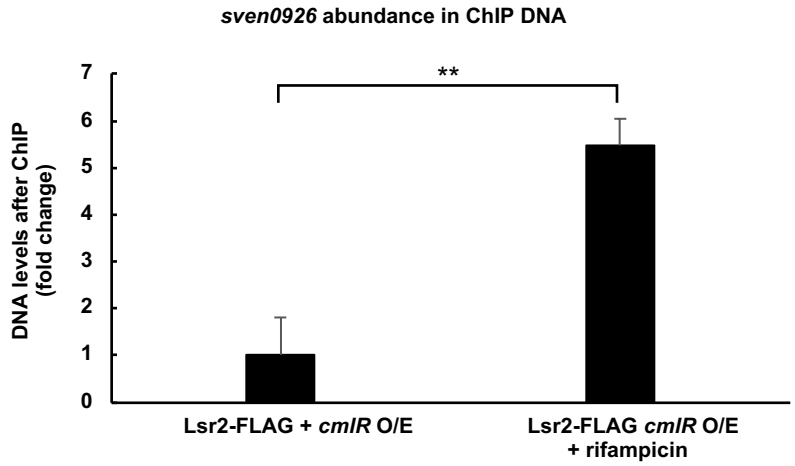

Figure 2.9: Inhibiting transcription enhances Lsr2 binding to its *sven0926* target site. The relative abundance (fold change) of Lsr2-targeted *sven0926* in rifampicin-treated (and untreated) *cmlR* overexpression strains was compared using qPCR, with ChIP-DNA samples as the template. Error bars represent the standard errors of the means, for technical triplicates and biological duplicates. **, $P<0.01$.

Using a strain expressing the FLAG-tagged Lsr2 protein and overexpressing CmlR, we performed ChIP experiments after a 10-min exposure to rifampicin. In parallel, ChIP experiments were done using an untreated control strain. We quantified and compared the levels of *sven0926* bound by Lsr2, both with and without rifampicin treatment, using qPCR. We knew that overexpressing CmlR reduced the levels of *sven0926* bound by Lsr2

(Figure 2.9). Thus, we hypothesized that if CmlR alleviated Lsr2 binding and cluster repression by recruiting RNA polymerase and enhancing transcription, then inhibiting RNA polymerase activity would lead to increased Lsr2 binding to *sven0926*. We found that adding rifampicin to a CmlR-overexpressing strain led to a >500% increase in the amount of *sven0926* bound by Lsr2, relative to untreated controls. This suggested that CmlR relieved Lsr2 silencing by recruiting RNA polymerase, and the resulting increase in transcription served to remove Lsr2 polymers from the chromosome and/or disrupt Lsr2 bridges.

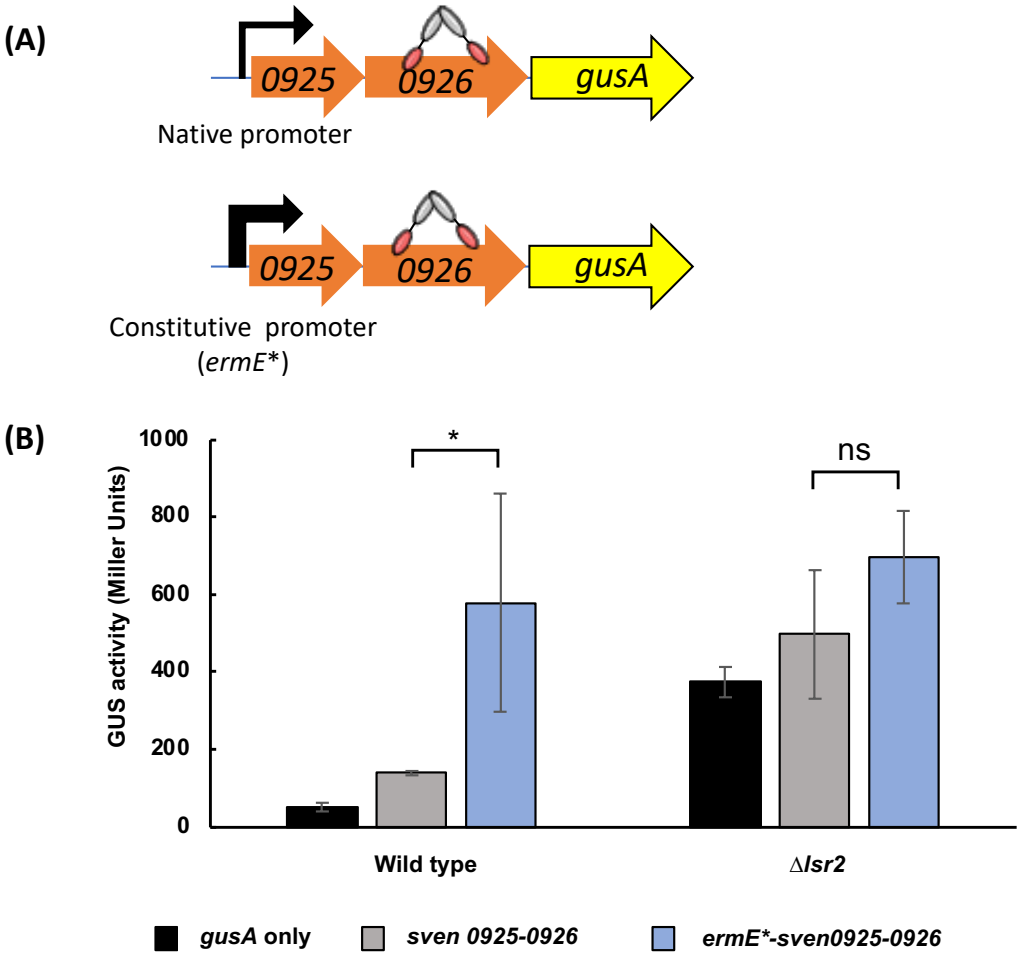

Figure 2.10: Enhancing transcription overcomes the repressive effects of Lsr2. (**A**) Schematic diagram illustrating the *gus* reporter construct design. Top: The CmlR binding site, *sven0925* promoter and downstream *sven0925-0926* coding sequence was cloned upstream of the promoterless *gusA*. Bottom: a constitutive promoter, *ermE**, replaced the CmlR binding site and *sven0925* promoter, upstream of the *sven0925_0926* coding sequence in the promoterless *gusA* reporter construct. (**B**) The constructs from (A) were

tested in wild type and Δ*lsr2* backgrounds. As a negative control, the promoterless *gusA* construct was introduced into both backgrounds. Error bars represent standard deviation of the mean, for biological triplicate samples. * indicates $p<0.05$.

To further test the proposed mechanism of CmlR-mediated counter-silencing of Lsr2 activity, we explored the effects of CmlR using a simplified system in which Lsr2 repression could be exerted only by polymerizing along the chromosome. We employed a transcriptional reporter system and fused two distinct promoter constructs to the *gusA* (β-glucuronidase-encoding) reporter gene (**Figure 2.10A**). The first contained the CmlR binding site and promoter for *sven0925* and extended through to the downstream Lsr2 binding site (within *sven0926*). The second construct was the same, only with the CmlR binding site and *sven0925* promoter replaced with the constitutive *ermE** promoter. These two reporter constructs were introduced into wild type and *lsr2* mutant strains on an integrating plasmid vector, in parallel with a promoterless plasmid control. The active *ermE** promoter led to significantly increased β-glucuronidase activity in the wild type background relative to the CmlR-controlled promoter, suggesting reduced Lsr2 repression. In contrast, in an Δ*lsr2* background, β-glucuronidase activity did not differ significantly for the two reporter constructs, although we note that (for unknown reasons) the activity of the negative control was higher in this background (**Figure 2.10**). Collectively, these results, when taken together with the results of the assays described above, suggested that Lsr2 repression could be alleviated by enhancing transcription.

2.4 Discussion

Lsr2 plays a pivotal role in repressing specialized metabolism in *Streptomyces* species (Gehrke et al., 2019), yet it is assumed that many of these specialized metabolic clusters must be expressed under specific circumstances. Here, we probed the mechanistic basis underlying Lsr2 repression of the chloramphenicol biosynthetic cluster in *S. venezuelae* and found that it appears to function by polymerizing along the chromosome and bridging sites within and adjacent to the biosynthetic cluster. We further explored how Lsr2 repression was alleviated and identified a key counter-silencing function for the cluster-situated regulator CmlR, which enhances transcription, leading to RNA polymerase effectively clearing Lsr2 from the chromosome (**Figure 2.11**).

Unlike most transcription factors, nucleoid-associated proteins typically bind DNA with low affinity and/or specificity, and this is consistent with our observations, where we found that CmlR bound its target sequences with far greater affinity than Lsr2. To date, the counter-silencing of nucleoid-associated protein-mediated repression has been best studied for H-NS. Three main mechanisms having been reported: (i) regulatory proteins remodel the DNA and disrupt the H-NS-DNA complex, facilitating transcription

initiation by RNA polymerase (e.g., VirB alleviates H-NS repression at promoters of virulence genes in *Shigella flexneri*) (Stoebel et al., 2008; Beloin and Dorman, 2003); (ii) DNA-binding proteins compete with H-NS for binding to a given site and in doing so relieve H-NS repression (e.g., in *Vibrio harveyi*, the LuxR transcription factor relieves H-NS repression of bioluminescence by competing with H-NS for binding to the promoter of quorum sensing genes) (Chaparian et al., 2020); and (iii) transcribing RNA polymerase derepresses H-NS by remodeling or disrupting the H-NS complex, ultimately enhancing transcription (e.g., in *Salmonella*, PhoP reduces H-NS binding to horizontally acquired genes by competing with H-NS for binding, and enhancing transcription by recruiting RNA polymerase Rangarajan and Schnetz, 2018; Choi and Groisman, 2020).

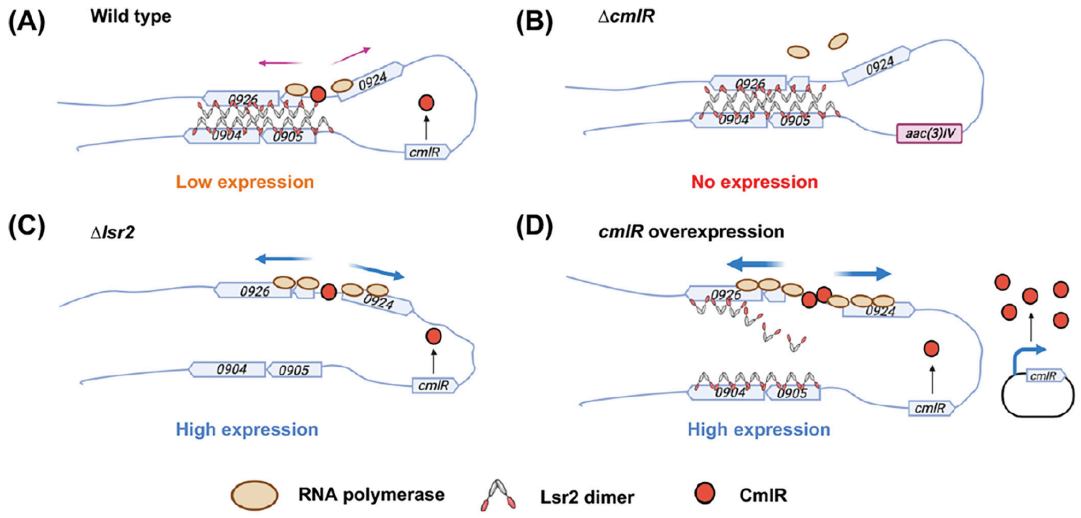

Figure 2.11: Proposed model for Lsr2 repression and CmlR counter-silencing in chloramphenicol cluster expression. (**A**) In the wild type, Lsr2 represses expression of the chloramphenicol cluster by polymerizing along the chromosome and bridging sites between *sven0926* and *sven0904-0905*. Low levels of CmlR bind the divergently expressed promoter region between *sven0924* and *sven0925* and promote baseline cluster expression and low-level production of chloramphenicol. (**B**) Deleting *cmlR* leads to a complete loss of cluster expression and chloramphenicol production. (**C**) In the *lsr2* mutant, the repressing Lsr2 polymers and bridges are absent, allowing CmlR to recruit more RNA polymerase to the divergent promoter region, leading to higher cluster expression and more chloramphenicol production. (**D**) Overexpressed CmlR cooperatively binds the promoter, and its strong recruitment of RNA polymerase, and the associated increase in transcription, serves to remove Lsr2 from the chromosome and neutralizes its repressive effect, leading to high level chloramphenicol production.

Counter-silencing of Lsr2 in *Mycobacterium tuberculosis* has been previously described in relation to iron metabolism (Kurthkoti et al., 2015). The expression of *bfr*, encoding a bacterioferritin, is governed both by Lsr2 and the iron-dependent transcriptional regulator IdeR. Lsr2 binds directly to the promoter of *bfrB*, thereby preventing its transcription. Under iron-replete conditions, IdeR is activated by iron binding and alleviates Lsr2 repression by directly associating with the *bfrB* promoter (Kurthkoti et al., 2015). However, it is not clear whether relief of Lsr2 repression is accomplished through direct competition between IdeR and Lsr2 for binding or by IdeR enhancing transcription levels, as appears to be the case for CmlR and Lsr2 in *S. venezuelae*. Counter-silencing has also been explored for the *Corynebacterium* homologue known as CgpS, using synthetic systems (Wiechert et al., 2020a). These experiments revealed that counter-silencing of Lsr2 bound to a single site/region (i.e., not bridging different sequences) was most effectively achieved through competition for binding by transcription factors at the CgpS nucleation site, presumably serving to limit polymerization along the DNA (Wiechert et al., 2020a). While it is possible that CmlR has a minor role in limiting the bounds of polymerization, our data suggest that its major function is to promote transcription and in doing so to facilitate Lsr2 removal from the chromosome. What controls the expression of *cmlR* remains to be determined, as its expression is unaffected by Lsr2 activity.

Previous work has revealed that Lsr2 binding sites are found in the majority of biosynthetic gene clusters in *S. venezuelae*, including the chloramphenicol cluster (Gehrke et al., 2019). Our data support a model in which Lsr2 employs both an internal and external binding site to downregulate the expression of the chloramphenicol biosynthetic genes (and production of chloramphenicol). We were curious whether such a binding configuration was associated with other Lsr2-targeted clusters. In examining the data of Gehrke et al. (Gehrke et al., 2019), we noted that nine clusters contained more than one Lsr2 binding site, and most of these clusters (7/9) exhibited altered transcription profiles in an *lsr2* mutant. Of the clusters which are associated with a single Lsr2 binding site and which also have altered transcription patterns (6 clusters), all but one have a cluster-adjacent Lsr2 binding site (within 12 genes upstream or downstream), and most of these were oriented such that the binding sites spanned the majority of the cluster (i.e., the external binding site was usually on the side opposite the internal binding site). This suggests that the model we propose for control of the chloramphenicol cluster (polymerization and bridging) may be broadly employed throughout *S. venezuelae* for repression of specialized metabolism. Whether any regulators encoded within these clusters play roles equivalent to that of CmlR in the chloramphenicol cluster, in helping to relieve Lsr2 repression, remains to be seen.

Understanding the different ways in which Lsr2 can exert its repressive effects is central to our ability to effectively manipulate its activity and, in doing so, gain access to the vast cryptic metabolic repertoire of the streptomycetes. Counter-silencing by cluster-situated activators likely represents one of many approaches employed by

Streptomyces spp. to modulate the effects of Lsr2. It will be interesting to determine whether the activity of Lsr2 in the streptomycetes is impacted by environmental factors like H-NS (e.g., temperature) (Shahul Hameed et al., 2019), alternative binding partners like H-NS (e.g., StpA) (Muller et al., 2006) and Lsr2 in *M. tuberculosis* (e.g., HU) (Datta et al., 2019), or posttranslational modification (Alqaseer et al., 2019; Dilweg and Dame, 2018).

2.5 Methods and materials

2.5.1 Bacterial strains and culture conditions.

S. venezuelae strains were grown at 30°C on MYM (maltose, yeast extract, malt extract) agar, or in liquid MYM medium. *Escherichia coli* strains were grown at 37°C on or in LB (lysogeny broth) medium (Kieser and Bibb, 2004). *Streptomyces* and *E. coli* strains that were constructed and used are summarized in **Table 2.1**. Where appropriate, antibiotic selection was used for plasmid maintenance or for screening/selecting during mutant strain construction. For assessing the importance of transcription for Lsr2 counter-silencing, *S. venezuelae* liquid cultures were grown for 16 h, after which they were exposed to the RNA polymerase-targeting antibiotic rifampicin (500 μg/mL) for 10 min.

2.5.2 Mutant/overexpression strain construction

In-frame deletions of *cmlR* and *sven0904-0905* were created using ReDirect technology (Gust et al., 2003). The coding sequence of *cmlR* and the region encompassing *sven0904-0905* in cosmid 4P22 (**Table 2.2**) was replaced with the *aac(3)IV-oriT* apramycin resistance cassette (**Table 2.3**). Mutant cosmids 4P22Δ*cmlR*::*aac(3)IV-oriT* and 4P22Δ*0904_0905*::*aac(3)IV-oriT* were confirmed by PCR before being introduced into the non-methylating *E. coli* strain ET12567/pUZ8002 (MacNeil et al., 1992; Paget et al., 1999) and conjugated into wild type *S. venezuelae* or *lsr2* mutant strains. The sequences of primers used to create the disruption cassettes and to check the integrity of the disrupted cosmids and chromosomal mutations can be found in **Table 2.3**.

The *cmlR* overexpression plasmids were made by cloning the *cmlR* gene and 216 bp of its downstream sequence under the control of the constitutive, highly active *ermE** promoter in the integrating plasmids pIJ82 and pRT801 (**Table 2.2**). For pIJ82, *cmlR* was amplified using primers cmlRfwd1 and cmlRrev1 (**Table 2.3**), digested with BamHI, and cloned into the BamHI site of pIJ82 (**Table 2.2**). For pRT801, *cmlR* was amplified using primers cmlRfwd2 and cmlRrev2 (**Table 2.3**) before being digested with SpeI and cloned into the same site in pRT801 (**Table 2.2**). *cmlR* presence and orientation in both plasmids were checked by PCR using vector- and insert-specific primers (**Table**

2.3), and construct integrity was confirmed by sequencing. The resulting plasmids, alongside empty plasmid controls, were introduced into *S. venezuelae* strains via conjugation from *E. coli* strain ET12567/pUZ8002 (Table 2.1). Strains used for chromatin immunoprecipitation (ChIP) were generated by introducing the pRT801-based *cmlR* overexpression construct into *lsr2* mutant strains complemented with either *lsr2* or *lsr2-3×FLAG* on the integrating plasmid vector pIJ82 and pIJ10706, respectively (Table 2.1) (Gehrke et al., 2019).

Δ*0904-0905* mutants were complemented by cloning the entire *sven0904-0906* operon, including 513 bp upstream and 123 bp downstream sequences (using primers 0904_0906CF and 0904_0906CR [Table 2.3]), into the EcoRV-digested integrating plasmid vector pMS82. The resulting construct was sequenced before being introduced into *E. coli* strain ET12567/pUZ8002, alongside empty vector control plasmids, and conjugated into *S. venezuelae* Δ*0904-0905* and Δ*lsr2* Δ*0904-0905* strains.

2.5.3 Protein overexpression and purification and EMSAs

Lsr2 overexpression and purification was performed as described previously (Gehrke et al., 2019). To overexpress CmlR in *E. coli*, the *cmlR* coding sequence was PCR amplified using primers cmlR O/E fwd and cmlR O/E rev (Table 2.3). The resulting product was digested with NdeI and BamHI before being ligated into the equivalently digested pET15b vector (Table 2.2). After sequencing to confirm construct integrity, the resulting plasmid was introduced into *E. coli* Rosetta 2 cells (Table 2.1). The resulting 6×His-CmlR overexpression strain was grown at 37°C until it reached an optical density at 600 nm (OD_{600}) of 0.6, at which point 0.5 mM isopropyl-β-D-thiogalactopyranoside (IPTG) was added. Cells were then grown at 30°C for 3.5 h before being collected and lysed. The overexpressed protein was purified from the cell extract using nickel-nitrilotriacetic acid (Ni-NTA) affinity chromatography and was washed using increasing concentrations of imidazole (50 mM to 250 mM) before being eluted using 500 mM imidazole. Finally, purified 6×His-CmlR was exchanged to storage buffer suitable for both EMSAs and freezing at -80°C (50 mM NaH_2PO_4, 300 mM NaCl, and 10% glycerol, pH 8).

To test Lsr2-binding specificity, EMSAs were performed using 100- to 222-bp probes amplified by PCR and 5′ end labeled with [γ-^{32}P]dATP (Table 2.3). Lsr2 (0 to 500 nM) was combined with 1 nM probe and binding buffer (10 mM Tris [pH 7.8], 5 mM $MgCl_2$, 60 mM KCl, and 10% glycerol) in 20 μL reaction volumes. Reaction mixtures were incubated at room temperature for 10 min, followed by 30 min on ice. Any resulting complexes were then separated on a 10% native polyacrylamide gel.

To test CmlR binding to the divergent promoter region between *sven0924* and *sven0925*, a 270-bp probe encompassing the predicted binding site (amplified using primers CmlR binding F and CmlR binding R [Table 2.3]) was used for EMSAs. CmlR (0 to 150 nM) was combined with 1 nM probe and binding buffer, as described above for Lsr2.

Reaction mixtures were incubated at 30°C for 30 min before being separated on a 10% native polyacrylamide gel. EMSA gels were exposed to a phosphor screen for 3 h before being imaged using a phosphorimager.

2.5.4 Atomic force microscopy

Lsr2 binding sites, plus considerable flanking sequences, were amplified using AFM0905F and AFM0905R (**Table 2.3**) for *sven0904-0905* (1,612-bp product) and AFM0926F and AFM0926R (**Table 2.3**) for *sven0926* (2,441-bp product). The resulting DNA products were cloned into pBluescript II KS(+) at the EcoRV and SmaI sites, respectively. The orientation of each fragment was assessed by PCR using vector- and insert-specific oligonucleotides (**Table 2.3**) and confirmed by sequencing. The resulting hybrid product was then amplified with AFM0905R and AFM0926R (**Table 2.3**), for use in AFM. Lsr2 was overexpressed and purified as described above. Negative control DNA (sequences not bound by Lsr2 *in vivo*) was amplified from *S. venezuelae* genomic DNA using primers 7031F and 7031R (**Table 2.3**). The DNA-alone samples were prepared in 20 μL reaction volumes and contained 0.5 nM target DNA, 10 mM Tris-HCl (pH 7.6), 5 mM $NiCl_2$, 40 mM HEPES, while the Lsr2+DNA samples, also prepared in 20 μl reaction volumes, contained 0.5 nM target DNA, 250 nM Lsr2, 10 mM Tris (pH 7.8), 5 mM $MgCl_2$, 60 mM KCl, and 10% glycerol. Different buffer conditions were used for DNA alone and Lsr2+DNA because Ni^{2+} was needed for DNA binding to the mica slide; however, it was not compatible with Lsr2 binding, so was excluded from protein-containing reactions. Reaction mixtures were incubated at room temperature for 10 min, followed by 30 min on ice. The DNA or DNA/Lsr2 was then deposited onto freshly cleaved mica surfaces (Ted Pella, Inc.) and rinsed with 1 mL nuclease-free water. Water was removed by blotting with filter paper, after which the mica surface was dried using a stream of nitrogen. AFM was performed as described by Cannavo et al. (Cannavo et al., 2018). Images (2 by 2μm) were captured in air using a Bruker Bioscope Catalyst atomic force microscope with ScanAsyst Air probes. Observed molecules were processed (through plane fit and flattening) and analyzed using Image Metrics version 1.44 (Andres et al., 2019; Li, 2019).

2.5.5 ChIP-qPCR

ChIP-qPCR was performed as described previously (Gehrke et al., 2019). Strains were inoculated in 10 mL of liquid MYM medium and grown overnight, before being subcultured in duplicate in 50 mL of MYM medium. After incubation for 18 h, formaldehyde was added to a final concentration of 1% (vol/vol) to cross-link protein to DNA. The cultures were then incubated for a further 30 min, before glycine was added to a final concentration of 125 mM. Immunoprecipitation of Lsr2-FLAG (or, as a negative control, untagged Lsr2) was performed as described previously (Bush et al., 2013) using

the FLAG M2 antibody (Sigma). To quantify the relative abundance of target genes of interest in the ChIP DNA samples, 20 μL qPCR mixtures were prepared using the LUNA Universal qPCR master mix (New England Biolabs), together with 2.5 μL of ChIP DNA (1:10) as the template. Primer pairs used to amplify the different target DNA sequences are summarized in **Table 2.3**. Target gene levels in ChIP DNA were calculated using data analysis for real-time PCR (DART-PCR) (Peirson et al., 2003) and were normalized to the abundance of the relevant target gene in total DNA as described previously (St-Onge et al., 2015).

2.5.6 Secondary metabolite extraction and LC-MS analysis

Metabolite extraction and LC-MS analyses were performed as described previously (Gehrke et al., 2019), with minor modifications. Strains were grown in triplicate in 30 mL liquid MYM medium at 30°C for 2 days. Cultures were lyophilized and the resulting lyophiles were resuspended in 10 mL methanol and shaken overnight on a rotary shaker at 4°C. After centrifugation to remove particulate matter, the soluble samples were concentrated using a centrifugal vacuum evaporator (Genevac). The resulting products were then dissolved in 50% methanol and centrifuged again to remove residual particulate matter. The resulting soluble extracts were used for LC-MS analyses. The extracts were analyzed using an Agilent 1200 LC coupled to a Bruker micrOTOF II (electrospray ionization-MS [ESI-MS]). One microliter of the injected extracts was separated on a Zorbax Eclipse XDB C_{18} column (100 mm by 2.1 mm by 3.5 mm) at a flow rate of 0.4 mL/min for 22 min. Extracted metabolite separation was achieved using a gradient of 0 to 11 min from 95% to 5% A, 11 to 12 min isocratic 5% A, a gradient of 12 to 21 min from 5% to 95% A, and 21 to 22 min isocratic 95% A, where A is water with 0.1% formic acid (FA) and B is acetonitrile with 0.1% FA. Chloramphenicol was detected using the negative ionization mode, at 321 m/z.

2.5.7 β-Glucuronidase (Gus) reporter assays

To test how promoter activity affected Lsr2 binding, sequences encompassing the CmlR binding site and *sven0925* promoter, through to the Lsr2 binding site in *sven0926*, were amplified and cloned into the KpnI and SpeI sites of pGUS (Myronovskyi et al., 2011) using primers 0925_26 pGUS F and 0925_26 pGUS R (**Table 2.3**). To replace the native promoter of *sven0925* with the constitutive *ermE** promoter, the *ermE** promoter was amplified from plasmid pGUS-*PermE** (**Table 2.3**) using primers ermEF-X and ermER-K **Table 2.3**) and cloned into the XbaI and KpnI sites of pGUS. Into the downstream SpeI site was then cloned the promoterless *sven0925_0926* fragment amplified using 0925_26 pGUS-E*F and 0925_26 pGUS R (**Table 2.3**). The resulting constructs were confirmed by sequencing and were introduced into *S. venezuelae* wild type and *lsr2* mutant strains by conjugation, alongside a promoterless pGUS control

plasmid. The resulting pGUS-containing strains were inoculated into 10 mL MYM medium and grown at 30°C for 18 h, after which 1 mL of culture was removed and assayed for β-glucuronidase activity. Cell pellets were resuspended in lysis buffer (50 mM phosphate buffer [pH 7.0], 0.27% [vol/vol] β-mercaptoethanol, 0.1% [vol/vol] Triton X-100, 1 mg/mL lysozyme) and incubated at 37°C for 30 min. After incubation, the cell lysate was centrifuged, and the resulting supernatant was used in the assay. Fifty microliters of supernatant were added to a 200 μL (total) reaction mixture, together with p-nitrophenyl β–D-glucuronide substrate (PNPG; Sigma-Aldrich) at a concentration of 600 μg/mL. Gus activity was determined by measuring the reaction absorbance at 420 nm and normalizing to the OD_{600} of cultures.

2.6 Tables

Table 2.1 Strains used in this study

Strains	Genotype, characteristics, or use	Reference or source
	Streptomyces	
S. venezuelae NRRL B-65442	Wild type	Gift from M. Buttner; Gomez-Escribano et al., 2021
E327	*S. venezuelae lsr2::acc(3)IV*	Gehrke et al., 2019
E327A	*S. venezuelae* Δ*lsr2*	Gehrke et al., 2019
E332	*S. venezuelae cmlR::acc(3)IV*	This work
E333	*S. venezuelae* Δ*lsr2 cmlR::acc(3)IV*	This work
E334	*S. venezuelae sven0904_0905::acc(3)IV*	This work
E335	*S. venezuelae* Δ*lsr2 sven0904_0905::acc(3)IV*	This work
E336	*S. venezuelae* Δ*lsr2* with pIJ82 carrying wild type *lsr2*	Gehrke et al., 2019
E337	*S. venezuelae* Δ*lsr2* with pIJ10706 carrying *lsr2-3×Gly-3×FLAG*	Gehrke et al., 2019

Escherichia coli		
DH5α	Routine cloning	Hanahan, 1985
SE DH5α	Highly-competent (Subcloning Efficiency™) DH5α cells	Invitrogen
ET12567	*dam, dcm, hsdS, cat tet;* carries *trans*-mobilizing plasmid pUZ8002	MacNeil et al., 1992
Rosetta 2	Protein overexpression host with pRARE2 which supplies 'rare' tRNAs	Novagen

Table 2.2 Plasmids and cosmids used in this study

Cosmid or plasmid	**Description**	**Reference or source**
Cosmid 4P22	*S. venezuelae* cosmid carrying *cmlR* and *sven0904_0905*	Gift from M. Buttner
pIJ82	Integrative cloning vector; *ori* pUC18 *hyg oriT* RK2 *int* ΦC31 *attP* ΦC31	Gift from H. Kieser
pRT801	Integrative cloning vector; *ori* pUC18 *apra oriT* RK2 *int* ΦC31 *attP* ΦC32	Gregory et al., 2003
pMS82	Integrative cloning vector; *hyg oriT int* ΦBT1 *attP* ΦBT1	Gregory et al., 2003
pGUS	Integrative *Streptomyces*-specific reporter vector for transcriptional fusions with the *gusA* gene	Myronovskyi et al., 2011
pGUS-*PermE**	Strong *Streptomyces* promoter, *PermE**, upstream of *gusA*	R. J. St-Onge (unpublished)
pBluescript II KS (+)	Standard cloning vector	Stratagene
pET15b	Overexpression of N-terminally His_6-tagged proteins	Novagen

pMC122	*cmlR* cloned downstream of *ermE** in pIJ82	This study
pMC123	*cmlR* cloned downstream of *ermE** in pRT801	This study
pMC124	pET15b carrying *cmlR* for overexpression with an N-terminal His_6-tag	This study
pMC125	pMS82 carrying *sven0904_0906*	This study
pMC126	pGUS carrying *sven0925_0926*	This study
pMC127	pGUS-*PermE** carrying promoterless *sven0925_0926*	This study

Table 2.3 Oligonucleotides used in this study

Primer	**Sequence (5' - 3')***	**Description**
Gene knockout		
SVEN_0913 FOR	TCCTGTCATCGATGACGTGCGTTCCTGGAGG CATTGATG***ATTCCGGGGATCCGTCGACC***	Replace *cmlR* with an apramycin resistance cassette
SVEN_0913 REV	CGGGCGCCGCCGCTACGGCGGGGCGGCGG TAGGGGATCA***TGTAGGCTGGAGCTGCTTC***	
SVEN_0913 upstream	GCTTAGCGTCACATTTCGGC	Confirm deletion of *cmlR*
SVEN_0913 downstream	TGTACAAGGCGTGGTTCCC	
SVEN_0913 internal	TACGTAATATCCGCAGCGCC	
0904/0905 internal	CTCCACGGCCTCCTTGAGGG	Confirm deletion of *sven0904_0905*
0904/0905 downstream	TACGTCCCAGAACCTACCCG	

0904/0905 upstream	GGCTTCATCGTGACCGAGAT	
0904/0905 Rev	CGCACCGGCCGAAACGGCCGGTGCCGGGA GGTCCTGCTA***TGTAGGCTGGAGCTGCTTC***	Replace *sven0904_0905* with an apramycin resistance cassette
0904/0905 Fwd	CAACTGACGACCGGCAGCGAGAGGAGCAC GGTACCCATG***ATTCCGGGGATCCGTCGACC***	
***cmlR* overexpression**		
cmlRrev1	ATATGGATCCGGGACCTGGCTGGACTTCCG	*cmlR* overexpression in pIJ82
cmlRfwd1	ATATGGATCCCGGAGCCGTACCACCTTTCC	
cmlRrev2	ATATACTAGTGGCGGCGGTAGGGGATC	*cmlR* overexpression in pRT801
cmlRfwd2	ATATACTAGTCGACTCTAGAAGCCCGA	
cmlR O/E rev	CATCATGGATCCATCAGGCCGGGCCCGCGTC	*cmlR* overexpression in pET15b
cmlR O/E fwd	CATCATCATATGATGTCCACGATTTCGGATC TACGAC	
EMSAs		
CmlR binding F	AGACAGAACAGATCGCGTCGC	Amplify CmlR binding site
CmlR binding R	GGCCCACCCCTTCCTTCACT	
sven0926 F	TCGTCGATGAACCATTTCAT	Amplify Lsr2 binding site at *sven0926*
sven0926 R	GGAGACGTTCAGGATCGCGG	
sven0904 F	GGATTTTCCTGAACGCCGGA	Amplify Lsr2 binding site at *sven0904_0905*
sven0904 R	ACTTGAGGCATTCGACGTAT	
sven3556 F	ATATCCTCTAGAGGAGCGACTGGATGTGGA C	Amplify *sven3556* as negative control
sven3556 R	ATATCCGGTACCCCAAGGAAGAGAACAGCT TCCC	

sven5133 F	GGTGGATTCCGTAGTCATGG	Amplify *sven5133* as negative control
sven5133 R	CGAGAATTCGAGAAACAACG	
Gene complementation		
sven0904_0906CF	ATATGGATCCCCGGTGTGGTCGTCTACTG	*sven0904_0905* complementation in pMS82
sven0904_0906CR	ATATGGATCCGGTCACGGTGAACAACCTCC	
qPCR		
0926 qPCR Fwd	CAGGCGATATCCCGTCAGTG	
0926 qPCR Rev	GTGCACACCCCCTAGAAAGA	
4440 qPCR Fwd	ACGACGGATCGACCTGG	
4440 qPCR Rev	AGATCTCACGGGGTTAACTGTC	
6264 qPCR Fwd	GTGATGACATCGACTCCGGG	
6264 qPCR Rev	GGTAGCCGGCCGAGTTGTA	
3885 qPCR Fwd	GGATAACTCCCATCCGCCTG	
3885 qPCR Rev	GATGATCGTACGGAGCAGGG	
AFM		
AFM0905F	GAGCACGGTACCCATGACCAC	Clone *sven0904_0905* into pBlueScript
AFM0905R	CCCTTGTAGGTGGGGTTCT	
AFM0926F	GTGGTCATGGGTACCGTGCTCCGGCGAGGA AGCTGTGGATGT	Clone *sven0924_0926* into pBlueScript
AFM0926R	CCTCGAACCTTCGCAGCAGT	
7032F	CTGCACCACTGGGTCGG	Amplify negative control DNA
7032R	CCGAGCGCTACGCGG	

***gus* constructs**		
0925_26 pGUS F	ATATGGTACCGGATTTCTCGTCCGTGTGGT	Amplify 0925_26 to clone into pGUS
0925_26 pGUS R	ATATACTAGTAACCTTCGCAGCAGTTCGTC	
0925_26 pGUS-E*F	ATATACTAGTGTGCTGGACGGAGGCCTTAA	Amplify 0925_26 to clone into pGUS-P*ermE**

*Underlined: restriction enzyme site; Bold and italics: cassette-specific sequence

CHAPTER 3: IDENTIFICATION OF FACTORS AFFECTING LSR2 ACTIVITY

Xiafei Zhang, Marie A. Elliot

Preface:

This chapter represents unpublished work. Mass spectrometry was performed by the Center for Advanced Proteomics Analyses (Université de Montréal). I performed all the other experiments.

3.1 Abstract (Chapter summary)

In bacteria, nucleoid-associated proteins can function as global regulators and play important roles in a wide range of biological processes, including organizing chromosomes and regulating specialized metabolite biosynthesis. The histone-like nucleoid-structuring protein (H-NS) is a well-studied nucleoid-associated protein but it is only found in a subset of Gram-negative bacteria. Early studies of H-NS in *Escherichia coli* showed that H-NS represses transcription, and its expression and activity are regulated at multiple levels, including post-translational modification, transcriptional regulation, and protein-protein interactions. The first H-NS-like protein to be identified in the Gram-positive bacteria was Lsr2, and it is largely confined to the actinomycetes. In *Streptomyces*, recent work has revealed an important role for Lsr2 in repressing specialized metabolic clusters and has suggested that manipulating Lsr2 activity has the potential to stimulate specialized metabolite production in *Streptomyces.* Unlike H-NS, very little is known about the regulation of Lsr2, except that it represses its own gene transcription. Here, we characterize factors impacting *lsr2* expression and protein activity. Our results suggest that in *Streptomyces venezuelae*, Lsr2 may be subject to multi-level transcriptional regulation, in addition to post-translational control by LsrL, an Lsr2 homologue.

3.2 Introduction

In *Streptomyces* and other actinomycetes, the Lsr2 nucleoid-associated protein appears to be functionally similar to the well-studied H-NS (histone-like nucleoid-structuring) protein in *Escherichia coli*. H-NS is a xenogeneic silencer and global regulator that preferentially binds and spreads along high AT-content DNA to compact the chromosome and/or silence gene expression (Song and Loparo, 2015; Szafran et al., 2020; van der Valk et al., 2017). Like H-NS, Lsr2 preferentially binds high AT-content DNA, and is predicted to silence gene transcription by bridging or oligomerizing along the DNA (Gehrke et al., 2019; Gordon et al., 2010). Deleting *lsr2* in *Streptomyces venezuelae* results in significantly upregulated gene expression in ~2/3 of all biosynthetic clusters, with six clusters showing >80% of their genes to be upregulated. Notably, five of these clusters are transcriptionally silent under laboratory conditions in the wild type strain (Gehrke et al., 2019). In probing the mechanism underlying Lsr2 repression of these clusters, we found that Lsr2 inhibits transcription of the chloramphenicol cluster by binding DNA both within the chloramphenicol biosynthetic cluster, and at flanking sites. We further showed that Lsr2 repression can be relieved by CmlR, the pathway-specific regulator of the chloramphenicol cluster; CmlR functions to recruit RNA polymerase, which in turn effectively clears bound Lsr2 from the chloramphenicol cluster DNA (Zhang et al., 2021). Collectively, these findings provided new insight into biosynthetic gene cluster regulatory networks in the *Streptomyces*, and suggested that

manipulating Lsr2 activity in *Streptomyces* has the potential to impact biosynthetic gene cluster expression.

How Lsr2 activity is controlled more broadly remains unclear. In the case of H-NS, its activity is modulated by post-translational modification. The H-NS binding effects of polymerizing and bridging DNA are heavily influenced by Mg^{2+} (Dillon and Dorman, 2010; Winardhi et al., 2015). In the absence of Mg^{2+}, the DNA-binding domains of H-NS dimers interact with the dimerization domain to form a 'closed' conformation, where H-NS can only bind DNA *in cis*, resulting in H-NS polymerization and formation of a rigid filament. In the presence of Mg^{2+}, the 'closed' conformation transitions to an 'open' conformation, as Mg^{2+} alters H-NS structure and prevents interaction between the dimerization domains and one of the DNA-binding domains. This allows H-NS to bind DNA *in trans* and form a bridge structure (van der Valk et al., 2017). Studies have shown that phosphorylation of Ser45, Ser98 and Tyr99 enhances the interaction of H-NS and Mg^{2+}, promoting the formation of bridge structures (Dilweg and Dame, 2018; Hansen et al., 2013; Lin et al., 2015). in *Mycobacterium* tuberculosis, Lsr2 has been reported to be phosphorylated by PknB at four threonine residues, with phosphorylation decreasing the affinity of Lsr2 for DNA (Alqaseer et al., 2019). Therefore, we were interested in determining whether and how Lsr2 is modified at the post-translational level in *S. venezuelae*.

The regulatory activity of H-NS is also modulated by other proteins. In enteroaggregative *E. coli*, Aar, a virulence regulator, both down-regulates the expression of H-NS and modulates H-NS regulatory properties by binding H-NS (Santiago et al., 2017). StpA, an H-NS paralogue, has a similar oligomerization domain as H-NS and can interact with H-NS to form heterodimers (Muller et al., 2006). Lsr2 functions similarly to H-NS, but little is known about how *lsr2* expression is regulated outside of its auto-regulatory nature. Therefore, we were interested in further defining the regulators of *lsr2* expression and protein activity.

Here, we show that Lsr2 in *S. venezuelae* does not appear to be subject to post-translational modifications under the tested conditions. To probe the regulation of *lsr2,* we developed a plasmid pulldown system and identified multiple candidate regulators of *lsr2* expression in wild type and *lsr2* mutant *S. venezuelae* strains. Furthermore, we found that in *S. venezuelae*, Lsr2 and LsrL, an Lsr2 homologue*,* interact directly with each other, and that their respective DNA-binding activities are impacted by the presence of the other protein.

3.3 Results

3.3.1 Post-translational modification of Lsr2 in *S. venezuelae*

Given that H-NS is subject to post-translational modification, and Lsr2 has been reported to be phosphorylated in *Mycobacterium tuberculosis* (Alqaseer et al., 2019), we

wanted to determine whether Lsr2 in *S. venezuelae* was also subject to post-translational modification. To probe Lsr2 phosphorylation, and to identify conditions under which phosphorylation had occurred, we employed both Zn^{2+}-Phos-tag SDS- PAGE and mass spectrometry post-translational modification analyses using immunoprecipitated Lsr2 samples. The Zn^{2+}-Phos-tag SDS- PAGE method is based on the mobility shift of phosphorylated proteins during SDS-PAGE with polyacrylamide-bound Zn^{2+}-Phos-tag, relative to their mobility during conventional SDS-PAGE (Kinoshita et al., 2006). Zn^{2+} traps the phosphorylated protein during migration, and therefore the phosphorylated proteins run slower in the gel compared with their corresponding non-phosphorylated counterparts (Kinoshita et al., 2006; Kinoshita et al., 2012) (**Figure 3.1A**). *S. venezuelae* strains expressing either Lsr2-FLAG or untagged Lsr2 (negative control) were grown to early (12 hours), mid (16 hours) and late (20 hours) growth stages. Cells were then lysed in phosphatase inhibitor-containing buffer and Lsr2-FLAG (and any cross-reacting proteins) were immunoprecipitated using anti-FLAG agarose beads. Eluted immunoprecipitation samples were separated on both traditional and Zn^{2+}-Phos-tag SDS-PAG, followed by western blotting using anti-FLAG antibodies to visualize phosphorylated and non-phosphorylated Lsr2. If Lsr2 was phosphorylated under the tested conditions, we expected to see a single band corresponding to Lsr2-FLAG in the traditional SDS-PAG and multiple Lsr2-FLAG bands in the Zn^{2+}-Phos-tag SDS- PAG (corresponding to phosphorylated and unphosphorylated proteins). However, the western blot results were identical for both samples, where a single Lsr2-FLAG band was seen in all samples (**Figure 3.1B**). While it was possible that all products were equivalently phosphorylated at all time points, this seemed unlikely relative to what had been observed in other systems (Liu et al., 2021). A more likely interpretation of these results was that Lsr2 was not phosphorylated under the tested conditions.

To complement these studies, mass spectrometry analysis of Lsr2 was also performed to identify any post-translational modifications of Lsr2. Immunoprecipitated Lsr2-FLAG samples from early, mid and late growth stages were run on a 12% SDS-PAG following immunoprecipitation, and the bands corresponding to Lsr2-FLAG were excised and subjected to mass spectrometry analysis to identify any post-translational modifications. These experiments would allow us to determine if Lsr2 was post-translationally modified, as well as which residue(s) of the protein were modified. We did not identify phosphorylated residues in any of the samples, and the only identified Lsr2 modification was deamidation of multiple Asn residues, which was likely caused during sample processing (**Figure 3.2**). Taken together, the Zn^{2+}-Phos-tag SDS- PAGE experiment and mass spectrometry analyses suggested Lsr2 was not phosphorylated – or otherwise modified – in *S. venezuelae* under the tested conditions.

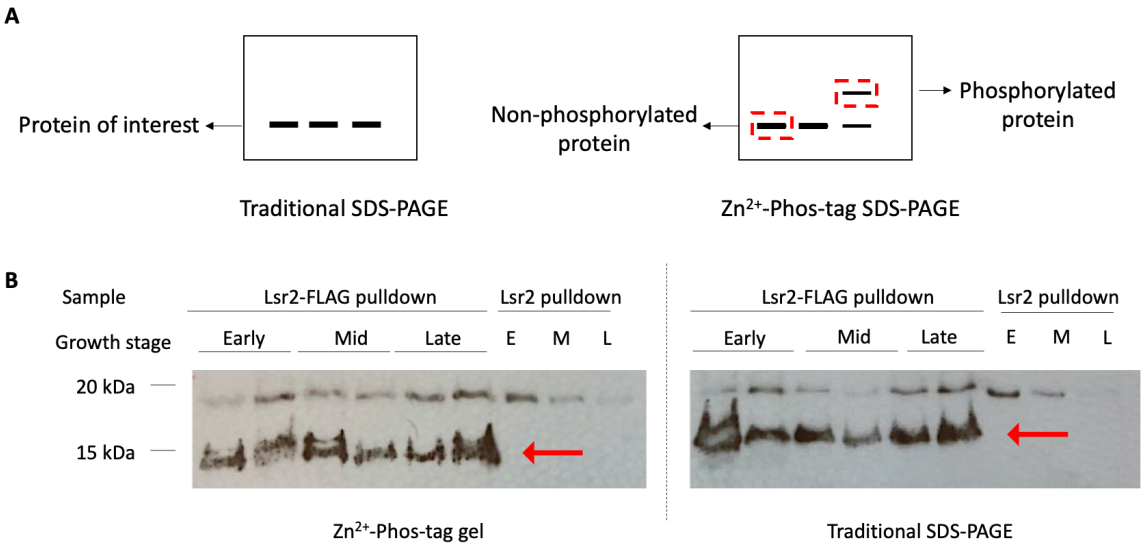

Figure 3.1: Detecting phosphorylation of Lsr2 using Zn^{2+}-Phos-tag SDS-PAGE. (**A**) Principle underlying the detection of protein phosphorylation using Zn^{2+}-Phos-tag SDS-PAGE. (**B**) **Left:** Lsr2-FLAG pulldown samples and control pulldown samples run using Zn^{2+}-Phos-tag SDS-PAGE. **Right:** Lsr2-FLAG pulldown samples and control pulldown samples run using traditional SDS-PAGE. Protein separation by PAGE was followed by western blotting using the anti-FLAG antibodies. Lsr2-FLAG pulldown samples were prepared in biological duplicate. Lsr2-FLAG bands are indicated by red arrows. The upper band seen in all samples is a non-specific band.

Figure 3.2: Lsr2 protein sequence coverage in mass spectrometry analyses. Protein sequence coverage of Lsr2 isolated from early (top panel), mid (middle panel) and late (bottom panel) time points. Residues covered in mass spectrometry analyses are highlighted in yellow. Residues modified by deamidation are in red text. The conserved

Thr78 residue that has been reported to be phosphorylated in *S. coelicolor* is indicated by green triangles.

3.3.2 Identification of regulators of *lsr2* expression in *S. venezuelae*

To identify regulators of *lsr2* expression beyond Lsr2 itself, we sought to create a plasmid construct in which the promoter region of *lsr2* was represented at high(er) copy. We modified the backbone of a non-integrating plasmid vector, such that it could be both conjugated into and replicate in *Streptomyces* species. We further engineered in features that facilitated plasmid capture and isolation of any proteins associated with the plasmid. Specifically, we introduced into the vector a *Streptomyces*-compatible origin of replication, alongside a tandem array of *lacO* binding sites, a constitutively expressed *lacI-FLAG* fusion, and an origin of transfer, together with an apramycin resistance gene. After modifying the backbone, we cloned a dominant allele of *lsr2* (R82A mutant – which is incapable of binding DNA (Gehrke et al., 2019)), together with its native promoter into the plasmid. The modified plasmid without an *lsr2* gene served as a negative control to allow us to differentiate proteins that bound the *lsr2* gene/promoter region, from those that bound the modified plasmid (**Figure 3.3**). These two plasmid constructs (R82A pulldown and control pulldown plasmids) were conjugated into wild type and Δ*lsr2* strains. By comparing the results obtained from the wild type and Δ*lsr2* strains, we could identify regulators of *lsr2* other than itself. Additionally, a plasmid bearing a wild type *lacI* (untagged) was generated and introduced into wild type *S. venezuelae* as a control to identify (and exclude) proteins that non-specifically bound the anti-FLAG resin beads.

For the plasmid pulldown experiment, five strains (wild type+R82A pulldown, wild type+control pulldown, Δ*lsr2*+R82A pulldown, Δ*lsr2*+control pulldown, and wild type+no FLAG control) were grown to mid growth stage (14 hours) in liquid MYM with apramycin to maintain the plasmid in the cell. Regulatory proteins were crosslinked to their target DNA sequences. Following cell lysis, the modified plasmids were isolated using immunoprecipitation, and their associated proteins separated (following cross-linking reversal) and analyzed by mass spectrometry analysis (**Figure 3.4**).

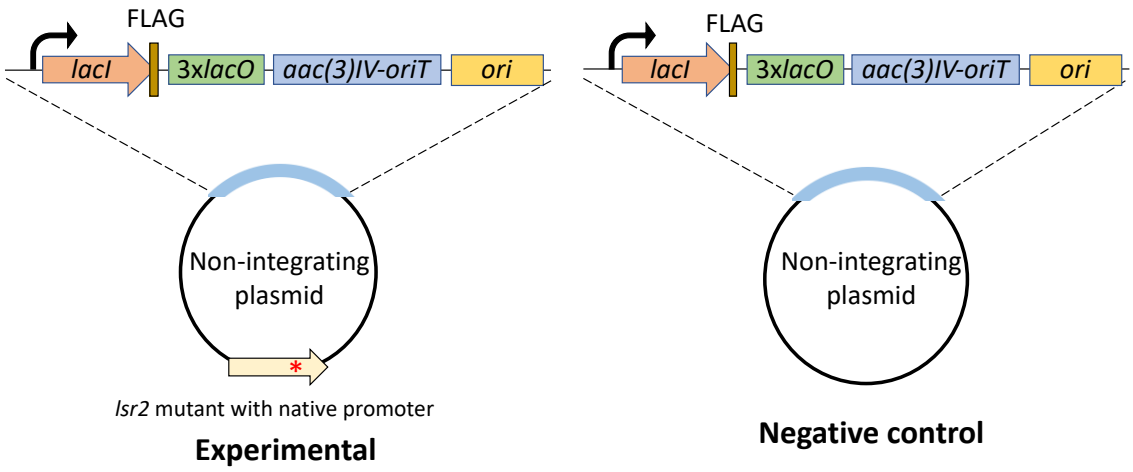

Figure 3.3: Strain construction for R82A plasmid pulldown experiments. To identify direct regulators of *lsr2*, we modified the backbone of a non-integrating plasmid by introducing a *Streptomyces*-compatible origin of replication, a tandem array of *lacO* binding sites, a constitutively expressed *lacI-FLAG* fusion, *oriT*, and an apramycin resistance gene (*aac(3)IV*). R82A, a dominant allele of *lsr2*, with its native promoter was cloned into the experimental plasmid. The modified plasmid without R82A served as a negative control.

By comparing the proteins isolated from the R82A plasmid pulldown, control plasmid pulldown and no FLAG control, we identified proteins that specifically associated with the *lsr2* promoter and/or coding sequences. These experiments were done in quadruplicate, and we focussed our attention on proteins identified in all four experimental replicates but not in any of the controls. Fifteen proteins were associated with *lsr2* in the *lsr2* mutant strain while only two were pulled out in the wild type strain, with one protein (BldM) identified in both conditions. Candidate regulators of *lsr2* identified from the plasmid pulldown experiments are summarized in **Table 3.1**. Notably, this list does not include Lsr2, which is known to bind to its own promoter, as it was identified in the control samples as well. Fourteen out of 16 (all but SVEN_3801 and SVEN_5591) of the identified proteins were conserved in sequenced *Streptomyces*. Importantly, three of the identified proteins, SVEN_4453 (BldM), SVEN_3078 (DNA-binding protein) and SVEN_4914 (Crp family transcriptional regulator), are transcription regulators or contain a DNA binding domain, and thus they have the potential to control *lsr2* expression directly by binding at the promoter region/within *lsr2*. Our result suggested *lsr2* expression may be subject to regulation by a variety of regulators.

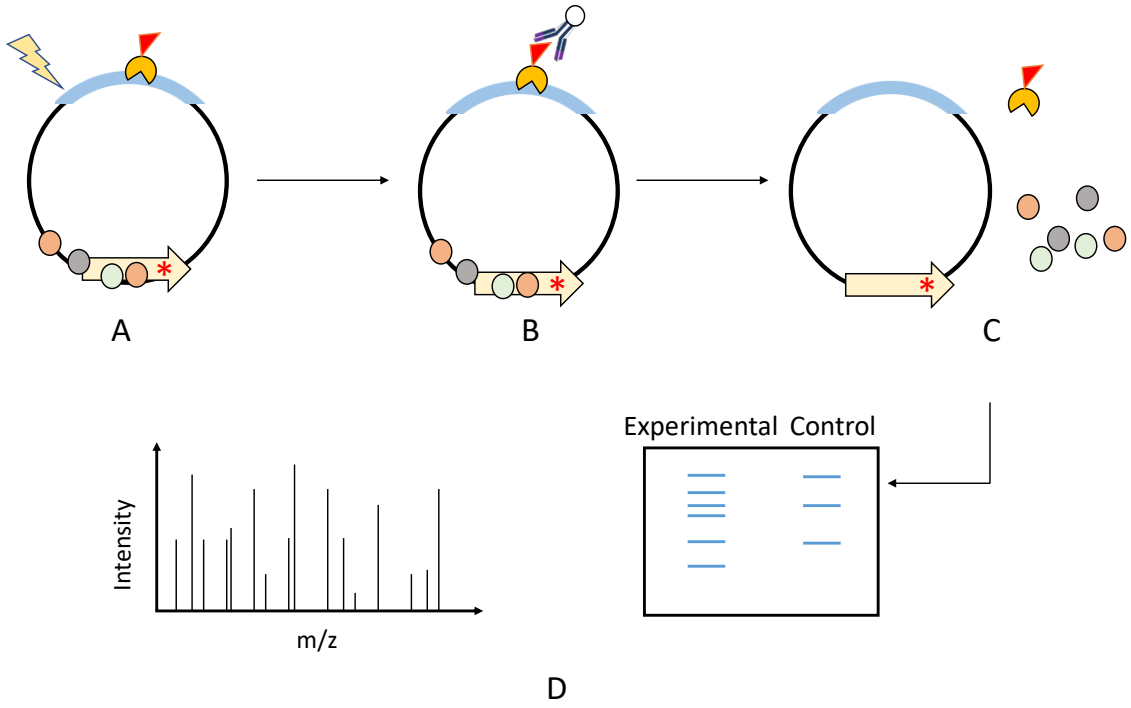

Figure 3.4: Workflow of identification of *lsr2*-binding proteins. (**A**) Regulatory proteins and LacI-FLAG were crosslinked to DNA using formaldehyde. (**B**) Cells were lysed and anti-FLAG resin beads were added to bind LacI-3×FLAG and selectively isolate the plasmids with its associated regulatory proteins bound. (**C**) and (**D**) Plasmid-bound proteins eluted from experimental and control plasmids were separated on an SDS-PAG and then identified using mass spectrometry analyses.

Table 3.1 Regulators of *lsr2* identified in R82A plasmid pulldown experiments

***lsr2*-associated proteins identified from wild type**	
Gene number	**Annotation**
SVEN_3801	NAD(P)H:quinone oxidoreductase
SVEN_4453	BldM (DNA-binding response regulator)
lsr2*-associated proteins identified from Δ*lsr2	
Gene number	**Annotation**
SVEN_0020	Uncharacterized protein

SVEN_0495	Enoyl-CoA hydratase or isomerase
SVEN_1195	InfC - Translation initiation factor
SVEN_1509	Cysteine desulfurase
SVEN_2364	Peptidase_M48 domain-containing protein
SVEN_2576	GlmS - Glutamine--fructose-6-phosphate aminotransferase
SVEN_3078	Putative DNA-binding protein
SVEN_3682	RpsF
SVEN_4283	Gram-pos-anchoring domain-containing protein
SVEN_4453	BldM
SVEN_4826	Putative reductase
SVEN_4914	cAMP-binding protein
SVEN_5591	Uncharacterized protein
SVEN_6165	Putative aminotransferase
SVEN_6166	D-hydantoinase

3.3.3 Lsr2 interacts directly with LsrL in *S. venezuelae*

In parallel, we wanted to determine if Lsr2 activity was impacted by other regulators at a protein level. Given that H-NS activity is controlled by its paralogue StpA, we wondered if Lsr2 activity could be impacted in a similar way. Every streptomycete encodes at least two Lsr2 homologues – Lsr2 and LsrL, and previous work from our lab found that in addition to being autoregulatory, Lsr2 also represses the expression of *lsrL* by binding at its promoter region (Gehrke et al., 2019).

Previous works on Lsr2 in *M. tuberculosis* revealed that the N-terminal domain of $Lsr2_{Mtb}$ consists of three β-strands (green arrows in **Figure 3.5**) and one α-helix (purple rectangles in **Figure 3.5**) (Gordon et al., 2008). Within the N-terminal domain, Asp28 and Arg45 play critical roles in dimerization, functioning to anchor the anti-parallel β-sheet of one monomer and the α-helix of another monomer. Additionally, ten conserved residues are important for dimerization by providing tertiary hydrophobic and H-

bonding interactions (Summers et al., 2012). Following a flexible linker, the C-terminal domain of $Lsr2_{Mtb}$ contains two α-helices connected by a long loop, and the RGR motif (contributing to the 'AT hook') is responsible for DNA binding (Gordon et al., 2010; Gordon et al., 2011; Summers et al., 2012). In *S. venezuelae*, Lsr2 and LsrL share 47% end-to-end amino acid identity, and 60% amino acid similarity. Alignment of Lsr2 from *M. tuberculosis,* and Lsr2 and LsrL from *S. venezuelae* revealed that at the C-terminus, the RGR motif was conserved in Lsr2 and LsrL, while within the N-terminus, the two critical residues (Asp28 and Arg45, corresponding to Asp27 and Arg44 in Lsr2 and LsrL in *S. venezuelae*), alongside nine out of the other 10 residues involved in dimerization were conserved in Lsr2 and LsrL. (**Figure 3.5**). This suggested that LsrL had the potential to interact with Lsr2 via its N-terminal dimerization domain, and possibly function in controlling Lsr2 activity.

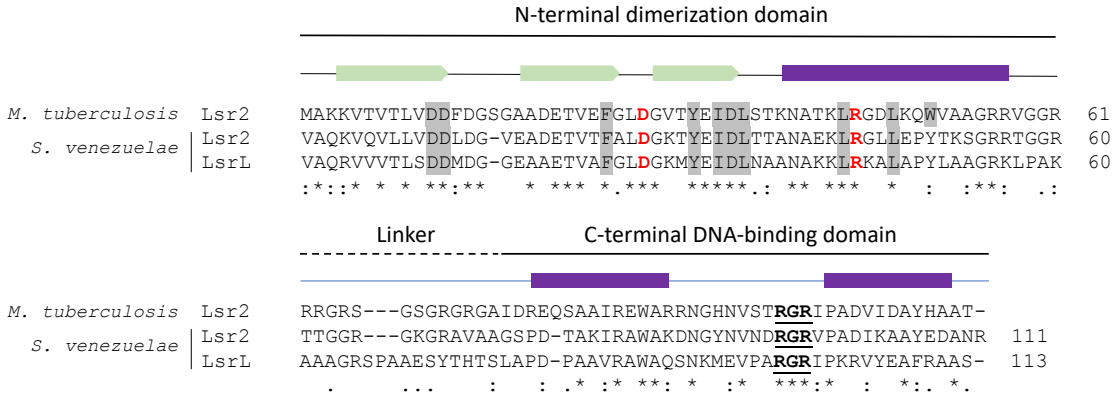

Figure 3.5: Dimerization residues and the RGR AT-hook are conserved in Lsr2 and LsrL. Alignment of Lsr2 from *M. tuberculosis*, and Lsr2 and LsrL from *S. venezuelae.* The green arrows represent β-strands, and the purple rectangles represent α-helices. The two residues implicated in dimerization are highlighted in red text; the residues (ten in Lsr2 in *M. tuberculosis* and nine in Lsr2 and LsrL in *S. venezuelae*) involved in Lsr2 N-terminal dimerization are shaded in grey; the RGR 'AT-hook' residues are bolded and underlined. Asterisks indicate residues that are conserved; colons indicate conservation of residues with strongly similar properties; and periods indicate conservation of residues with weakly similar properties.

Based on these results, we wondered if LsrL interacted with Lsr2 and affected Lsr2 activity, and/or impacted gene expression in *S. venezuelae.* To test these hypotheses, we first tested whether Lsr2 and LsrL could interact using the bacterial adenylate cyclase two-hybrid system. The coding sequences of *lsr2* and *lsrL* were cloned into the four bacterial two-hybrid vectors (pKT25, pKNT25, pUT18, and pUT18C) and the resulting constructs were introduced in pairwise combinations into an *E. coli* reporter

strain. Interactions were assessed on solid medium and using quantitative liquid culture assays, measuring β-galactosidase activity. Lsr2-Lsr2 and Lsr2-T25 plasmid interactions were included as positive and negative controls, respectively. We found that Lsr2 interacted directly with LsrL, based on the blue colonies observed on solid medium and high β-galactosidase activities measured in the quantitative liquid culture assay (**Figure 3.6**).

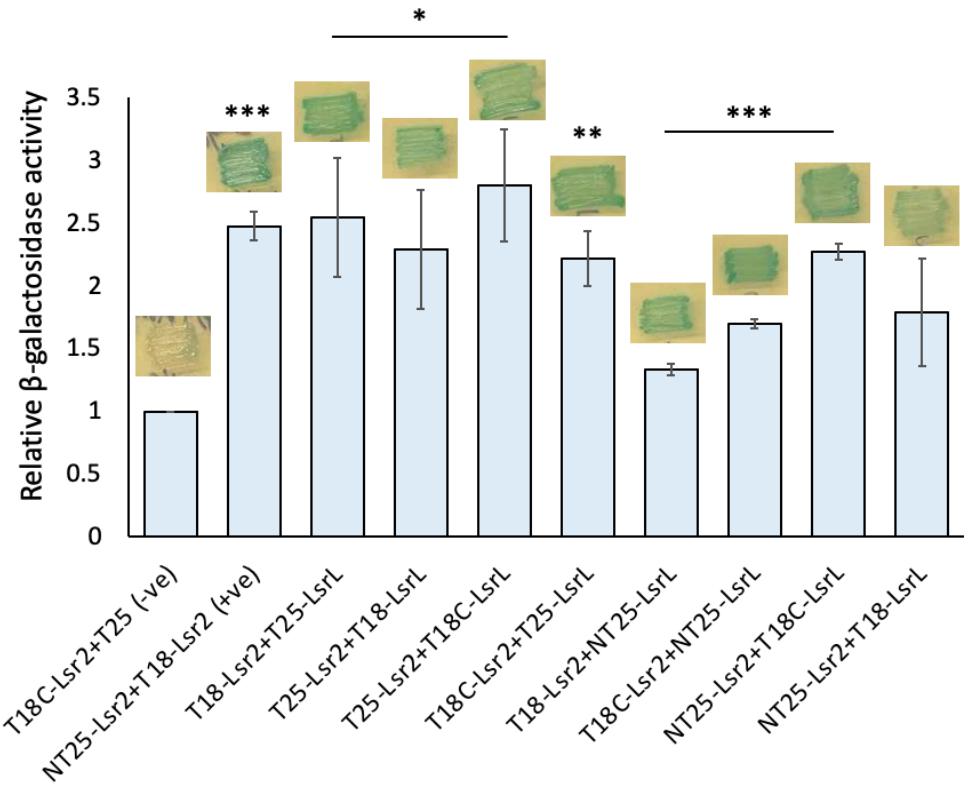

Figure 3.6: Pairwise direct interactions between Lsr2 and LsrL. All interaction orientations between Lsr2 and LsrL were tested. Lsr2-Lsr2 plasmids were included as a positive control and Lsr2-T25 constructs were included as a negative control. Statistical significances between the negative control and other interactions were determined using a Student's t test (* indicates $p<0.05$; ** indicates $p<0.01$; *** indicates $p<0.005$). The error bars represent standard error of mean between three biological replicates (two biological replicates for T25-Lsr2+T18-LsrL and NT25-Lsr2+T18C-LsrL).

To further test the interaction between Lsr2 and LsrL, we co-expressed differentially tagged variants of Lsr2 and LsrL (His-tagged or S-tagged) in *E. coli.* The His-

tagged proteins were then purified, and co-purification of the S-tagged protein was assessed using western blotting. Overexpression and purification of His-tagged Lsr2 only, followed by western blotting using anti-S antibodies was also tested as a negative control to ensure there was no cross-reactivity of the His-tagged Lsr2 with the anti-S antibodies. We found that S-tagged LsrL and S-tagged Lsr2 were effectively co-purified with His-tagged Lsr2 and His-tagged LsrL, respectively (**Figure 3.7**). When co-expressing His-tagged LsrL and S-tagged Lsr2, we observed a strong band of S-tagged Lsr2 in the no induction sample (**Figure 3.7, left**); this was likely due to the leaky expression of S-tagged protein from the T7 promoter. However, the strong band of S-tagged LsrL was absent in the uninduced sample when expressing His-tagged Lsr2 and S-tagged LsrL (**Figure 3.7, middle**). This could be explained by the protein structure of S-tagged Lsr2 and S-tagged LsrL, where upon protein folding, the S-tag fused to Lsr2 might be more accessible to anti-S antibodies compared to the S-tag fused to LsrL. Taken together, our bacterial two-hybrid results and heterologous co-purification observations suggested that Lsr2 and LsrL interact directly with each other when expressed in *E. coli.*

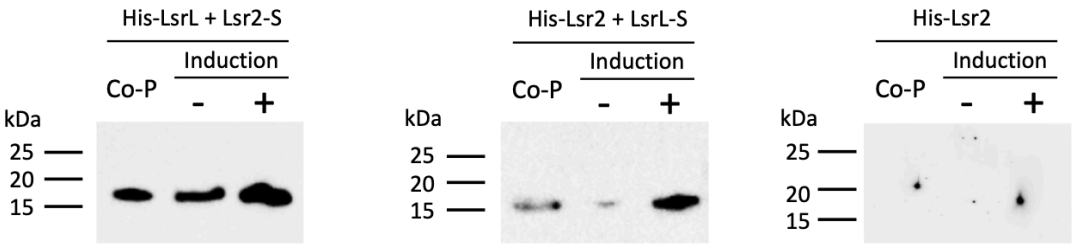

Figure 3.7: Direct interaction of Lsr2 and LsrL through heterologous co-purification. **Left:** Western blot using anti-S-tag antibodies, for S-tagged Lsr2 following co-purification with His-tagged LsrL (Co-P), and cell lysates of uninduced (-) and induced (+) cultures. **Middle:** western blot using anti-S-tag antibodies, for S-tagged LsrL following copurification with His-tagged Lsr2 (Co-P), alongside cell lysates of uninduced (-) and induced (+) cultures. **Right:** western blot using anti-S-tag antibodies, for purified His-tagged Lsr2 (Co-P), and cell lysates of uninduced (-) and induced (+) cultures (negative control, where no-S-tagged protein in present).

To test if Lsr2 and LsrL interacted with each other in *S. venezuelae,* we used an *in vivo* approach to look for proteins that directly interacted with Lsr2 by co-immunoprecipitating Lsr2-FLAG, followed by mass spectrometry analysis of all associated proteins (summarized in **Table 3.2**). We focused on those proteins that were identified in both replicates of Lsr2-FLAG co-immunoprecipitation samples but not in the

Lsr2 (non-tagged) co-immunoprecipitation samples (negative control). And an internal control, we expected to identify Lsr2 (native, untagged) from the Lsr2-FLAG co-immunoprecipitation samples, as Lsr2 oligomerizes with itself. Lsr2 was indeed identified as being abundant in both replicates of Lsr2-FLAG samples; however, it was ultimately excluded from our final list as it was also pulled out from our Lsr2 control samples, but at much lower levels compared to the Lsr2-FLAG samples.

We also identified LsrL, which was reproducibly co-purified with Lsr2-FLAG, and not with the untagged control. These results confirmed our findings from *E. coli* and suggested that Lsr2 and LsrL could interact directly with each other in *S. venezuelae*. SVEN_1508, a MarR (multiple antibiotic resistance repressor) family regulator, was also identified as a candidate interacting protein of interest, alongside three other enzymes/proteins.

Table 3.2: Lsr2 interacting partners identified from *in vivo* co-immunoprecipitation

Gene number	Annotation
SVEN_1508	MarR regulator protein
SVEN_2243	Phospholipase C (membrane associated)
SVEN_3020	Uncharacterized protein
SVEN_3832	LsrL
SVEN_5797	Ornithine carbamoyltransferase

3.3.4 Lsr2 DNA-binding activity is impacted by LsrL

Research in *M. tuberculosis* has revealed that Lsr2 binds DNA specifically in the minor groove via an AT-hook (RGR motif) (Gordon et al., 2011), which is conserved in Lsr2 and LsrL in *S. venezuelae*. Subsequent studies showed that *M tuberculosis* Lsr2 cooperatively binds DNA to form rigid filaments or mediates DNA bridge structure formation. Lsr2 binding causes DNA stiffening, and this change in conformation attracts more Lsr2 for further binding (Qu et al., 2013). In contrast, little is known about the DNA-binding activity of LsrL. To probe this, we overexpressed and purified LsrL, and compared its ability – relative to that of Lsr2 – to bind to two Lsr2 targets identified in previous ChIP-seq and EMSAs: *sven0926* (**Figure 3.8A**) and *sven0904_0905* (**Figure 3.8B**). We determined that both Lsr2 and LsrL bound these target sequences, however, LsrL bound the probes in a different manner compared with Lsr2. Lsr2 bound probes

gradually in a cooperative way that generated multiple shifted bands in EMSAs, whereas LsrL bound DNA in a way that led to one high molecular weight shifted band in EMSAs (**Figure 3.8**).

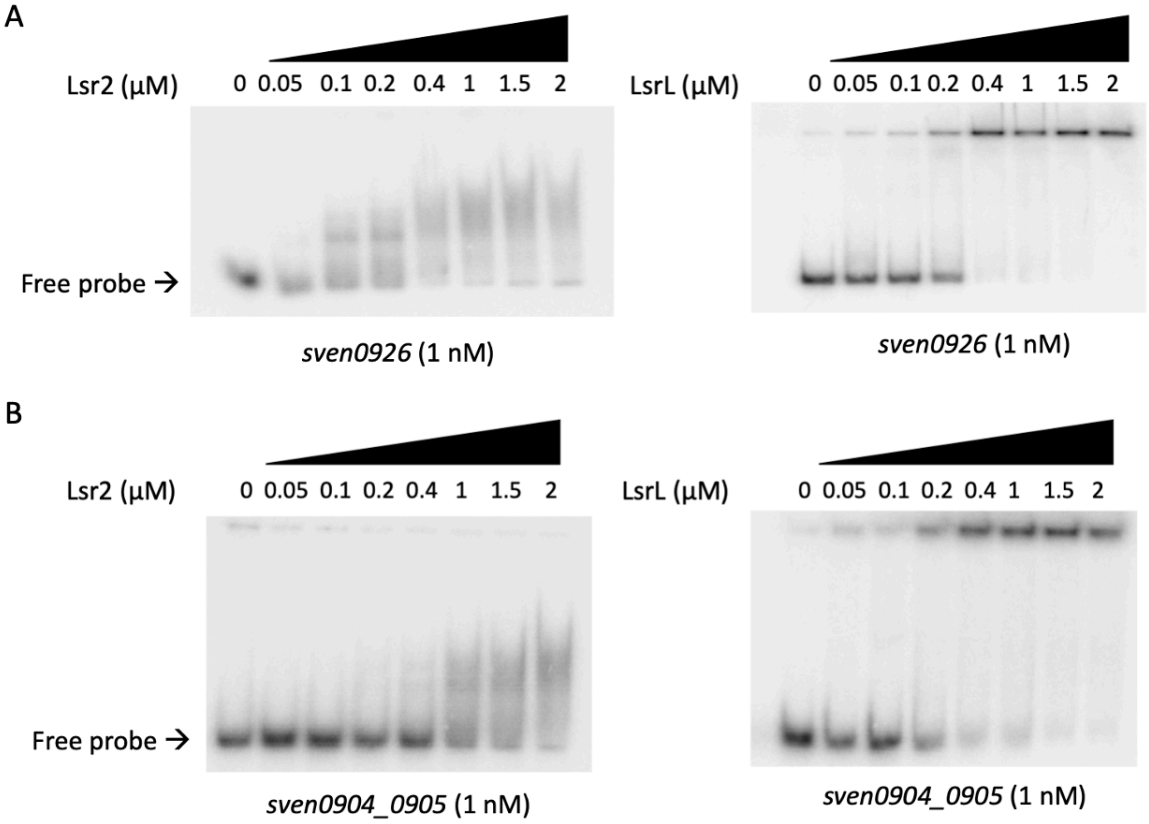

Figure 3.8: Lsr2 and LsrL bind DNA targets differently. EMSAs comparing Lsr2 and LsrL binding to the same probes, (**A**) *sven0926* and (**B**) *sven0904_0905.* 1 nM ^{32}P-labeled *sven0926* and *sven0904_0905* DNA probes were combined with increasing concentrations (0 to 2 μM) of Lsr2 (**left**) and LsrL (**right**). Images are representatives of two independent replicates.

Given that i) Lsr2 and LsrL interact with other, ii) both Lsr2 and LsrL have DNA-binding capabilities, and iii) LsrL binds the tested DNA probes in a different way than Lsr2, we wondered if the DNA binding of Lsr2 might be impacted by LsrL. To test this hypothesis, we pre-incubated purified Lsr2 and LsrL together (Lsr2+LsrL) and performed EMSAs to test the DNA-binding ability of these proteins. We observed that Lsr2+LsrL bound target DNA probes in a way that was more similar to that of Lsr2 than to LsrL (**Figure 3.8 and 3.9**). To examine the affinities of Lsr2, LsrL and Lsr2+LsrL for tested probes, we quantified the intensity of labeled free probes from EMSAs shown in **Figure**

3.8 and 3.9A. We found that the proteins (Lsr2 only, LsrL only and Lsr2+LsrL) had different affinities for the two tested probes (*sven0926* and *sven0904_0905*). Specifically, Lsr2 and LsrL had similar affinity for *sven0926* at high protein concentrations (0.4 – 2 μM); however, Lsr2 bound *sven0926* better than LsrL at low protein concentrations (0.05 – 0.2 μM). In contrast, LsrL had much higher affinity for *sven0904_0905* than Lsr2 at all tested protein concentrations, and Lsr2+LsrL bound *sven0904_0905* probe with an affinity more similar to LsrL than to Lsr2, although the band shifting characteristics were more similar to those of Lsr2. These results suggest that Lsr2 and LsrL interact with DNA differently and their DNA-binding activities may be impacted by each other, where LsrL changes the affinity of Lsr2 for DNA and Lsr2 alters the pattern of LsrL binding to DNA.

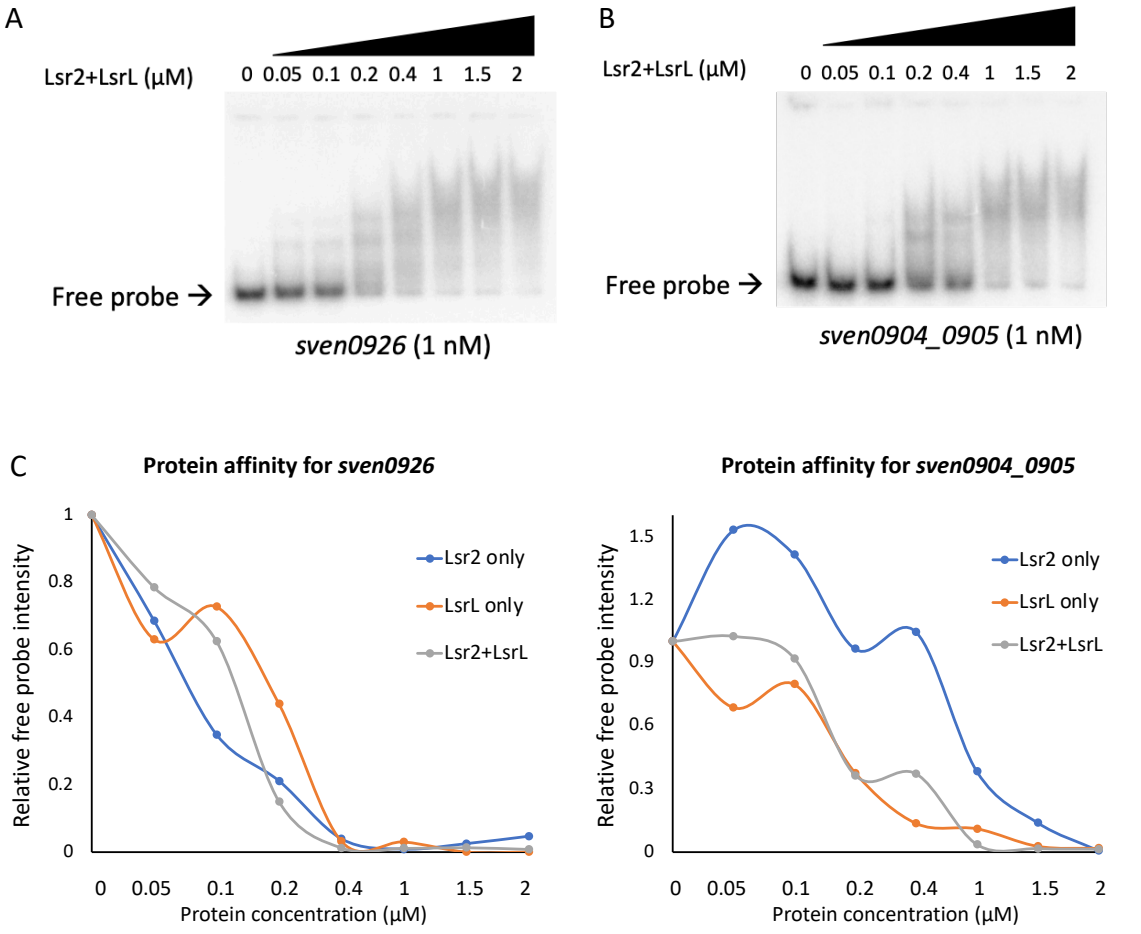

Figure 3.9: Lsr2 and LsrL DNA-binding activities are impacted by each other. EMSAs probing Lsr2+LsrL binding to (**A**) *sven0926* and (**B**) *sven0904_0905.* 1 nM of labeled *sven0926* and *sven0904_0905* DNA probes were combined with increasing concentrations (0 to 2 μM) of pre-incubated Lsr2+LsrL. (**C**) Quantification of labeled free

probe remaining following incubation with increasing concentrations of Lsr2 only (blue), LsrL only (orange) or Lsr2+LsrL (grey) from EMSAs shown in **Figure 3.8 and 3.9A**.

3.4 Discussion

Lsr2 represses specialized metabolite production in *Streptomyces* spp. and manipulating Lsr2 activity has the potential to stimulate the expression of otherwise 'silent' and 'cryptic' specialized metabolic gene clusters (Gehrke et al., 2019; Zhang et al., 2021). Here, we sought to understand the different factors with the potential to directly impact Lsr2 activity in *S. venezuelae*, including post-translational modification, transcriptional regulation, and activity modulation by interacting partners. Our results suggest that Lsr2 is not post-translationally modified under the growth conditions tested here; however, *lsr2* expression and Lsr2 activity may be controlled by a variety of factors.

Previous work in *M. tuberculosis* revealed that $Lsr2_{Mtb}$ can be phosphorylated by the protein kinase PknB at four threonine residues, with phosphorylation decreasing the affinity of Lsr2 for DNA (Alqaseer et al., 2019). Importantly, phosphorylation of one (Thr112) of the four threonine residues appears to be essential for growth under hypoxic conditions (Alqaseer et al., 2019). Lsr2 in *S. venezuelae* lacks Thr112 but has four serine/threonine residues within its C-terminal DNA-binding domain. Furthermore, *S. venezuelae* encodes a serine/threonine protein kinase (SVEN_3632) that shares 54% amino acid identity with PknB in *M. tuberculosis*. Additionally, a phosphoproteomics screen of *S. coelicolor* grown on solid GYM medium (glucose, yeast extract, malt extract) showed that many transcriptional factors were post-translationally modified. One of the phosphorylation targets identified was Lsr2, which was phosphorylated on Thr78, a residue conserved in Lsr2 in *S. venezuelae*; however, no further investigation was undertaken to identify the enzyme responsible, conditions under which phosphorylation occurred, or the downstream effects of this modification. (Parker et al., 2010; Manteca et al., 2011). These results suggest that Lsr2 has the potential to be phosphorylated, and that phosphorylation of Lsr2 may impact the expression of biosynthetic clusters in *S. venezuelae*. However, no phosphorylation was detected in our Zn^{2+}-Phos-tag SDS-PAGE experiments, and no post-translational modifications other than Lsr2 deamidation were identified from our mass spectrometry analyses when *S. venezuelae* was grown in liquid MYM (maltose, yeast extract, malt extract). It is worth noting that not all residues were detected following mass spectrometry, as some of the peptides resulting from trypsin cleavage were too small for analysis and/or were not detected. Notably, Thr78 was covered in our mass spectrometry analysis; however, no phosphorylation was detected (**Figure 3.2**). Our results suggested that under the classical growth conditions (in liquid MYM medium), Lsr2 is not post-translationally modified. It would be interesting to grow *S. venezuelae* under different conditions and assess its post-translational modifications

under these conditions, to better understand how Lsr2 activity is regulated, and to identify any environmental cues that may impact Lsr2 modification.

Lsr2 functions similarly to H-NS, but little is known about the regulatory factors governing Lsr2 activity and gene expression. At a gene expression level, like H-NS, Lsr2 is autoregulatory (Gehrke et al., 2019; Gordon et al., 2010); we were interested in identifying other regulators that might impact *lsr2* expression. We identified multiple proteins associated with the *lsr2* promoter/gene in wild type and Δ*lsr2* mutant strains. Three proteins, SVEN_4453 (BldM), SVEN_3078 (DNA-binding protein) and SVEN_4914 (Crp family transcriptional regulator), were of particular interest as they have known/likely DNA-binding capabilities and may play direct roles in controlling *lsr2* expression.

BldM is an orphaned response regulator containing a ligand binding domain and a helix-turn-helix DNA-binding domain, and has been best studied as a regulator for colony development, with a *bldM* mutant failing to raise aerial hyphae (Molle and Buttner, 2000). BldM is known to exert its regulatory activity by forming either a homodimer or a heterodimer with WhiI (Al-Bassam et al., 2014). Accordingly, ChIP-seq analyses revealed that with BldM binding targets could be divided into two groups (Group I and Group II) based on their WhiI dependencies (Al-Bassam et al., 2014). Group I target promoters are regulated by BldM homodimers and possess a 16 bp palindromic consensus sequence (5′-TCACcCgnncGgGTGA-3′), while Group II target promoters are bound by a BldM-WhiI heterodimer at a non-palindromic sequence (5′-TGnnCCGnnCGGGTGA-3′). *lsr2* was not identified as a binding target in the BldM ChIP-seq experiments, however, by analyzing the *lsr2* promoter and coding sequences, we found a potential BldM-WhiI binding site within the *lsr2* promoter where it overlaps with Lsr2 binding site (**Figure 3.10**). This discrepancy could be explained by the fact that the BldM ChIP-seq experiments were conducted in a wild type strain, where Lsr2 binds its own promoter and effectively prevents the binding of other regulators to the promoter. The plasmid pulldown experiments conducted here were done in both wild type and *lsr2* mutant strains, using *lsr2*R82A (DNA-binding defective variant) with its promoter cloned into a high copy number plasmid. Therefore, regulators with low binding affinity or needing to compete with Lsr2 for binding sites had a higher chance of binding the promoter and were more likely to be identified in our plasmid pulldown experiments than ChIP-seq. Our result suggested that BldM may control *lsr2* expression directly by forming heterodimer with WhiI; however, WhiI was not identified from any of the plasmid pulldown samples. To better understand the regulatory role of BldM, and possibly WhiI, on *lsr2* expression, we will co-overexpress and -purify BldM and WhiI, and perform EMSAs to test the binding of BldM+WhiI (and BldM on its own) to candidate sites within *lsr2*. Given that Lsr2 is a major repressor in controlling specialized metabolism in *Streptomyces*, we are interested in understanding if manipulating activity of BldM has the potential to stimulate specialized metabolites through its effect on *lsr2*

expression. Previous work has revealed that deleting *bldM* increases transcription of the chloramphenicol biosynthetic cluster in *S. venezuelae*; however, no sequence motif corresponding to BldM-WhiI binding was found within the chloramphenicol gene cluster, suggesting that BldM regulates the chloramphenicol gene cluster indirectly by activating the expression of a repressor (Fernandez-Martinez et al., 2014). We have shown that Lsr2 directly represses transcription of the chloramphenicol biosynthetic cluster by binding DNA both within the cluster (Gehrke et al., 2019; Zhang et al., 2021); therefore, it is tempting speculate that *lsr2* could be the target of BldM in regulating transcription of the chloramphenicol gene cluster. To gain better insights into the impact of BldM on *lsr2* expression and specialized metabolic in *S. venezuelae,* we will delete and overexpress *bldM* in wild type and the *lsr2* mutant strains, and measure chloramphenicol production in each strain. If BldM indeed regulates *lsr2* expression, and further has an indirect effect on chloramphenicol production, this would uncover a new level of specialized metabolic control in *Streptomyces* through modulating the activity of nucleoid-associated proteins.

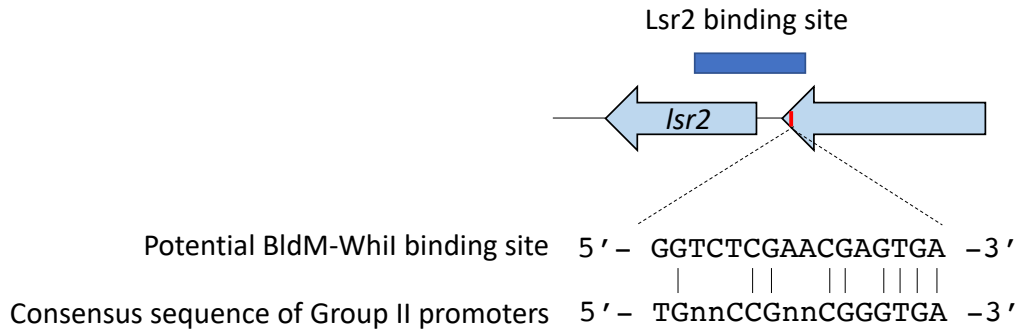

Figure 3.10: BldM-WhiI may regulate *lsr2* expression. Schematic diagram showing the predicted BldM-WhiI binding site and Lsr2 binding site identified from previous ChIP-seq at the promoter region of *lsr2.*

SVEN_3078 is a XRE (xenobiotic response element) family regulator with a helix-turn-helix DNA-binding domain. Studies on its ortholog Scr1 in *S. coelicolor* found that Scr1 and Scr2, a protein encoded by the downstream gene, play important roles in regulating antibiotic production (Santamaria et al., 2018). Overexpression of Scr1/Scr2 induced pigmented antibiotic production in *S. coelicolor*, and Scr2 was needed Scr1 to induce antibiotic production. However, how Scr1 exerts its function remains unknown (Santamaria et al., 2018). Based on our results, a possible mechanism for Scr1 (SVEN_3078 in *S. venezuelae*) in regulating antibiotic production could be through the control of *lsr2*.

Finally, SVEN_4914 is a Crp-like transcription regulator with a well-conserved cAMP-binding domain but a poorly characterized DNA-binding domain. In *S. coelicolor*, Crp is a pleiotropic regulator of antibiotic production with hundreds of associated binding sites identified in the chromosome (Gao et al., 2012). SVEN_4914 could control *lsr2* expression directly by binding its promoter region. Neither SVEN_3078 nor SVEN_4914 have been well characterized compared to BldM, therefore, as a first step towards understanding the impact of SVEN_3078 and SVEN_4914 on *lsr2,* we will overexpress and purify the two proteins, and perform EMSAs to test their binding to the *lsr2* promoter/gene.

Beyond these three DNA-binding proteins, two proteins with links to translation (SVEN_1195 and SVEN_3682) were also pulled out from the *lsr2* mutant strain. In the *lsr2* mutant strain, transcription of *lsr2*R82A in the pulldown plasmid was increased due to the lack of auto-repression, resulting in high mRNA levels. When crosslinking protein to DNA using formaldehyde, mRNA could also be anchored to the plasmid via interactions between DNA and RNA polymerase. Because of coupled transcription-translation in bacteria, translation-associated proteins loaded onto *lsr2*R82A mRNA before transcription was terminated, therefore, translation-associated proteins bound to mRNA could be pulled out with the plasmid during the pulldown process.

At the protein level, our data suggested that Lsr2 and LsrL, a paralogous Lsr2-like protein encoded in all *Streptomyces* genomes (Gehrke et al., 2019), interact directly with each other, suggesting they could form hetero-oligomers. Our EMSA results suggested that Lsr2 and LsrL can bind the same DNA with different affinities and in distinct manners. Lsr2 bound target DNA in a way that yielded multiple shifted bands in EMSAs, while LsrL seemed to bind DNA in a different manner, leading to the formation of large DNA-protein complexes that could not migrate into the gel (**Figure 3.8**). Alignment of Lsr2 and LsrL revealed that these two proteins have the same domain organization, and most of the dimerization/oligomerization residues identified in the protein structure from *M. tuberculosis* (the two implicated residues, Asp27 and Arg44, and nine out of 10 residues involved in dimerization) as well as the RGR motif responsible for DNA-binding, are conserved in both proteins; however, the linker region joining the two domains differed between the proteins, where the Lsr2 linker (TTGGRGKGRAVAA) was more Gly-rich compared with the LsrL linker (AAAGRSPAAESYTHTS), which was more Ala-rich (**Figure 3.5**). Gly-rich linkers are generally flexible and provide good solubility while Ala-rich linkers are more rigid due to restricted conformations and can increase protein stability (Robinson and Sauer, 1998; Chen et al., 2013; Grawe and Stein, 2021). A study using linker libraries showed that altering the composition of Gly/Ala in the linker region can change protein folding rates (Robinson and Sauer, 1998). Specifically, Ala-rich linkers (eight or more Ala in a 19-residue linker) can accelerate protein folding, and can cause protein aggregation during protein purification (Robinson and Sauer, 1998). Therefore, the different DNA-binding activities of Lsr2 and LsrL could be explained by their different linkers: the Gly-rich flexible linker in Lsr2 may promote protein dimerization and

cooperative binding to DNA (**Figure 3.11 top panel**), while the Ala-rich linker in LsrL may facilitate formation of high molecular weight protein oligomers, either before or after DNA binding, to form large DNA-protein complexes (**Figure 3.11 bottom panel**). To test our model for Lsr2 and LsrL DNA-binding activities, we will perform AFM using purified Lsr2 and LsrL, and PCR amplified DNA probes to visualize and compare how Lsr2 and LsrL interact with DNA.

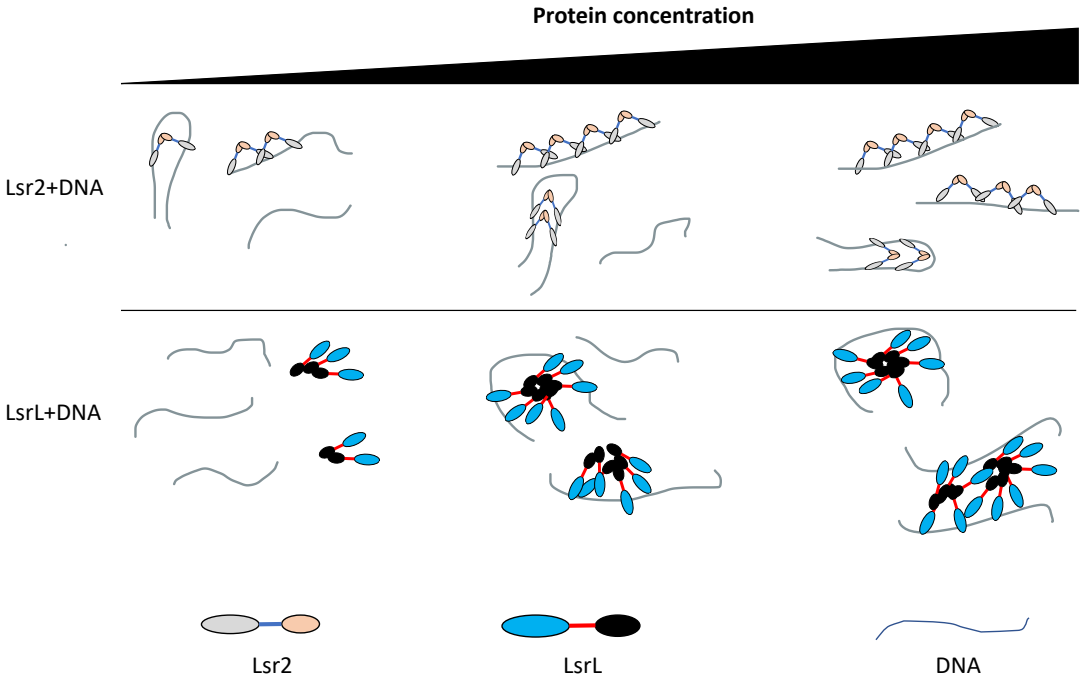

Figure 3.11: Proposed model for the DNA-binding of Lsr2 and LsrL. Top panel: DNA binding of Lsr2 to DNA. At low protein concentration, Lsr2 stiffens bound DNA and this changes the DNA conformation is favored by Lsr2 for further binding. As protein concentrations increase, Lsr2 preferentially oligomerizes on previously bound DNA and also binds free DNA, resulting in DNA-protein complexes having different molecular weights. **Bottom panel**: Due to its more rigid linker, LsrL may preferentially form protein oligomers, which then bind DNA to form large molecular weight DNA-protein complexes.

Additionally, we found that the DNA-binding activities of Lsr2 and LsrL were altered by the presence of the other protein. We considered two main possibilities that could explain these observations: i) LsrL oligomerization was prevented when interacting with Lsr2, and as a result, the Lsr2-LsrL heterodimer bound DNA in a way similar to that of Lsr2; or ii) Lsr2 and LsrL competed for binding to the DNA probes, and since the DNA probes used in the EMSAs were Lsr2 targets previously identified from ChIP-seq, LsrL was outcompeted by Lsr2. To differentiate between these two possibilities, we will perform ChIP-seq to identify LsrL targets and then do EMSAs to test Lsr2, LsrL and

Lsr2+LsrL binding to LsrL targets. We are also interested in examining the impact of potential Lsr2-LsrL interactions *in vivo.* In previous work, we showed that deleting *lsr2* leads to delayed growth and development and altered expression of many biosynthetic clusters. In contrast, deleting *lsrL* had no obvious effect on development and led to minor changes in metabolism. We have previously done ChIP-seq experiments to identify Lsr2-associated DNA. To understand both the direct LsrL regulon, as well as the reciprocal effect of Lsr2 on LsrL and vice versa, in addition to ChIP-seq to identify LsrL-associated DNA, we will also do ChIP-seq to (i) characterize Lsr2 binding in the absence of LsrL, and (ii) identify LsrL binding sites in the absence of Lsr2. This will provide us with key information needed to understand the regulatory interplay between these two proteins.

In addition to LsrL, SVEN_1508, a MarR family regulator, was also identified as a candidate interacting protein of Lsr2. MarR regulators contain a conserved winged helix-turn-helix DNA binding domain and a ligand-binding domain (Guo et al., 2018). MarR regulators typically act as homodimers and bind palindromic sequences within promoters to repress (mostly) or activate transcription. The DNA-binding activity of MarR regulators is impacted by binding of ligands, including small molecules and peptide, however, the natural ligands for MarR regulators are often unknown (Guo et al., 2018; Beggs et al., 2020). It is possible that interaction between Lsr2 and SVEN_1508 can reciprocally impact the DNA binding/regulatory capabilities of each protein.

Taken together, our data show that Lsr2 has the potential to be regulated at different levels by multiple factors. Understanding how Lsr2 is controlled will provide us with important insight into strategies to manipulate Lsr2 expression/activity, so as to access otherwise repressed specialized metabolites in *Streptomyces*.

3.5 Materials and methods

3.5.1 Bacterial strains and culture conditions

S. venezuelae strains were grown at 30°C on MYM (maltose, yeast extract, malt extract) agar, or in liquid MYM medium. *E. coli* strains were grown at 37°C on or in LB medium. *Streptomyces* strains, *E. coli* strains and plasmids that were constructed and used are summarized in **Table 3.3**. Where appropriate, antibiotic selection was used for plasmid maintenance.

3.5.2 Construction of plasmids for bacterial two-hybrid, protein overexpression and plasmid pulldown

To investigate the potential for Lsr2-LsrL protein interaction, *lsr2* and *lsrL* were amplified using primers lsr2B2HF and lsr2B2HR, and lsrlB2HF and lsrlB2HR, respectively

(**Table 3.4**). The resulting products were digested with BamHI and KpnI, and were cloned into the BamHI and KpnI sites in pKT25, pKNT25, pUT18 and pUT18C (**Table 3.3**).

Lsr2 overexpression and purification were performed as described previously (Gehrke et al., 2019). To overexpress LsrL in *E. coli*, the *lsrL* coding sequence was PCR amplified using primers lsrlF_pET15b and lsrlR_pET15b (**Table 3.4**). The resulting product was digested with NdeI and BamHI and was ligated into the equivalently digested pET15b vector. To co-overexpress and -purify 6×His-Lsr2 and LsrL-S, the *lsr2* coding sequence was PCR amplified using primers lsr2F_MCS1 and lsr2R_MCS1 (**Table 3.4**), after which the resulting product was digested with EcoRI and HindIII and cloned into the same sites in pCOLADuet-1. *lsrL* was amplified using primers lsrlF_pET15b and lsrlR_XhoI (**Table 3.4**); the product was then digested with NdeI and XhoI, and was cloned into the NdeI and XhoI site in pCOLADuet-1_6×His-*lsr2* (**Table 3.3**). To co-overexpress and purify 6×His-LsrL and Lsr2-S, *lsrL* was PCR amplified using primers lsrlB2HF and lsrlR_XhoI. The PCR product was then digested with XhoI and BamHI, and was cloned into the SalI (overhangs compatible with XhoI) and BamHI sites in the pCOLADuet-1 vector (**Table 3.3**). The coding sequence of *lsr2* was PCR amplified using primers lsr2F_MCS2 and lsr2R_MCS2. The resulting product was digested with NdeI and KpnI before being cloned into the equivalently digested pCOLADuet-1_6×His-*lsrL* (**Table 3.3**).

To create an appropriate construct for the plasmid pulldown experiments, we modified the backbone of pBlueScript, a non-integrating plasmid vector, to allow it to be conjugated into *Streptomyces* and replicate once introduced. We further engineered in features that facilitated plasmid capture and isolation of the associated proteins. Specifically, a *Streptomyces*-compatible origin of replication was PCR amplified from pKOSi (a plasmid vector containing the pSG5 replicon; **Table 3.3**) using primers oriT_pSG5ori2 and pSG5ori_pBlueScript (**Table 3.4**); a synthetic fragment consisting of a constitutively expressed *lacI-FLAG* fusion and a tandem array of *lacO* binding sites was generated and served as template for PCR amplification using primers pBlueScript_lacI_lacOF and lacI_lacO_oriT1 (**Table 3.4**); the *aac(3)IV-oriT* resistance cassette was amplified from pIJ773 using primers lacI_lacO_oriT2 and oriT_pSG5ori1 (**Table 3.4**). The three fragments were then joined together using overlap extension PCR. The product was then phosphorylated and cloned into the EcoRV site of pBlueScript (**Table 3.3**). After modifying the backbone, a dominant allele of *lsr2* (R82A mutant – which is incapable of binding DNA) with its native promoter was cloned into the plasmid: *lsr2*R82A and its promoter were PCR amplified from pMC132 (an integrating plasmid vector carrying the mutant *lsr2* allele) using primers R82AF and R82AR (**Table 3.4**), after which the resulting product was then phosphorylated and cloned into the EcoRV site of the modified plasmid.

3.5.3 Plasmid pulldown

S. venezuelae strains containing the plasmid pulldown constructs were grown to mid growth stage (14 hours) in liquid MYM with apramycin to maintain the plasmid. Regulatory proteins were crosslinked to their target DNAs by adding formaldehyde to a final concentration of 1% (vol/vol) and incubating for 30 min. Crosslinking reactions were then stopped by adding glycine to a final concentration of 125 mM. Cells were lysed by adding lysozyme [10 mM Tris-HCl pH 8.0, 50 mM NaCl, 14 mg/ml lysozyme, 0.8% Triton X-100, and 1× protease inhibitor (Roche Complete Mini)] and incubating at 37°C for 4 hours. After removing cell debris, the cell lysates were incubated with anti-FLAG resin beads overnight at 4°C to capture the plasmids and bound proteins through binding of anti-FLAG antibodies to LacI-FLAG. Anti-FLAG resin beads with bound plasmids were collected by centrifugation. Plasmid-associated proteins were eluted in 1×SDS loading dye (2% SDS, 10% glycerol, 100 mM DTT, 0.005% bromophenol blue and 50 mM Tris-HCl, pH 6.8) and heated at 95°C for 15 min. The eluted proteins were separated on a 12% SDS-PAG and each sample lane was excised and subjected to mass spectrometry analyses.

3.5.4 Mass spectrometry (MS) analyses

MS analyses were performed by the Center for Advanced Proteomics Analyses (Université de Montréal). To prepare samples for MS, protein samples were reconstituted in 50 mM ammonium bicarbonate with 10 mM TCEP [Tris(2-carboxyethyl) phosphine hydrochloride; Thermo Fisher Scientific], and vortexed for 1 h at 37°C. Samples were then vortexed for another hour at 37°C, together with 55 mM chloroacetamide (Sigma-Aldrich) for alkylation. One microgram of trypsin was added, and protein digestion was performed by incubating samples at 37°C for 8 h. Following trypsin digestion, samples were dried down and solubilized in 4% formic acid (FA).

After sample preparation, peptides were loaded and separated on a home-made reversed-phase column (200 mm long with 150 μm of internal diameter) with a 56-min gradient from 10 to 30% acetonitrile with 0.2% FA at a 600 nL/min flow rate on an Easy nLC-1000 connected to an Orbitrap Fusion (Thermo Fisher Scientific). Each full MS spectrum acquired at a resolution of 120,000 was followed by tandem-MS spectra (MS-MS) acquisition on the most abundant multiply charged precursor ions for a maximum of 3 s. MS-MS experiments were performed using collision-induced dissociation at a collision energy of 30%. The data were processed using PEAKS X Pro (Bioinformatics Solutions, Waterloo, ON) and a Uniprot *S. venezuelae* database (7451 entries). Mass tolerances on precursor and fragment ions were 10 ppm and 0.3 Da, respectively. To analyse post-translational modifications, the following modifications were included in data analyses: carbamidomethyl, oxidation, deamidation, phosphorylation, and

acetylation. The data were visualized using Scaffold 5.0 (99% protein threshold, with at least 2 peptides identified and a false-discovery rate of 1% for peptides).

3.5.5 Western blotting and Zn^{2+}-Phos-tag SDS-PAGE

To check the presence and stability of LacI-3×FLAG, cell lysates were prepared from 10 mL *S. venezuelae* liquid cultures. The protein extracts were separated using 10% SDS-PAGE and were stained with Coomassie Brilliant Blue R-250. Equivalent amounts of total protein were loaded onto a second 10% SDS-PAG and transferred to PVDF membranes. Membranes were blocked for an hour at room temperature with Tris-buffered saline with added Tween 20 (TBS-T, 10 mM Tris, pH 8.0, 100 mM NaCl and 0.1% Tween 20) containing 6% fat-free skim milk. Membranes were then incubated at 4°C overnight in TBS-T containing 6% skim milk with anti-FLAG antibodies (1:6000; Sigma). The membranes were washed six times with TBS-T and incubated in TBS-T containing 6% skim milk with anti-rabbit IgG horseradish peroxidase (HRP)-conjugated secondary antibodies (1:3,000; Cell Signaling) at room temperature for an hour. Blots were developed using an enhanced chemiluminescence system (Bio-Rad).

To probe interactions between Lsr2 and LsrL when expressed in *E. coli*, the His-tagged protein (either Lsr2 or LsrL) was purified, and it and all co-purifying proteins were loaded onto a 10% tricine-SDS-PAG (Haider et al., 2012). Western blotting was then done as described above, only anti-S antibodies (1:10000; Thermo) were used as the primary antibody for immunoblotting.

To detect protein phosphorylation, protein samples were loaded onto a 10% SDS-PAG made with 75.5 μM of phos-tag acrylamide (Fujifilm) and 151 μM of $ZnCl_2$ (Kinoshita et al., 2012). Gel electrophoresis was achieved by running gels in ice-cold MOPS buffer (100 mM Tris-HCl, 100 mM MOPS, 0.1% SDS, 5 mM $NaHSO_3$, pH 7.8). Before transferring to a PVDF membrane, the gel was incubated with 1 mM EDTA to remove the Zn^{2+} (Kinoshita et al., 2006). Following protein transfer to the PVDF membrane, western blotting was done as described above using anti-FLAG antibodies.

3.5.6 Pairwise bacterial two-hybrid interaction test

Competent *E. coli* strain DHM1 was transformed with both T25 and T28 protein fusion plasmids in one step. Following transformation, cells were selected on LB medium containing ampicillin, kanamycin and EZ-Gal, and incubated at 30°C for two days. Representative colonies were streaked onto a fresh LB plate with ampicillin, kanamycin and EZ-Gal, and grown at 30°C for two days prior of phenotypic comparison.

To quantify β-galactosidase activity, strain patches were inoculated into LB liquid medium with ampicillin and kanamycin. After 12 hours of incubation at 30°C, the OD_{600}

of each culture was recorded. Two hundred microlitres of each culture were mixed with 800 µL of Z-buffer (600 mM Na_2HPO_4, 400 mM NaH_2PO_4, 10 mM KCl, 0.1 mM $MgSO_4$, 2.7 mL/L β-mercaptoethanol). To lyse cells, 10 µL of 0.01% SDS, and 20 µL chloroform were added to each tube before vortexing for 10 s. Following vortexing, 50 µL of each lysate were combined with 150 µL of Z-buffer with 40 µL of 0.4% ONPG – the substrate of β-galactosidase. This was repeated in triplicate for each cell culture. The reactions were incubated at 37°C for 1 h, with OD_{420} values recorded every min. The relative β-galactosidase activity was calculated as follows (Battesti and Bouveret, 2012): $OD_{420}/(OD_{600}\times 0.2$ mL of culture$\times$time in min).

3.5.7 Immunoprecipitation and co-immunoprecipitation

To identify any post-translational modifications of Lsr2, an Lsr2-3×FLAG expressing strain was inoculated in 10 mL MYM liquid medium, before being subcultured into 50 mL of MYM in duplicate. After incubating for 8 hours (early growth stage), 16 hours (mid growth stage) and 20 hours (late growth stage), cells were lysed by adding lysozyme (10 mM Tris-HCl pH 8.0, 50 mM NaCl, 14 mg/ml lysozyme, 0.8% Triton X-100, and 1× protease inhibitor (Roche Complete Mini)) and incubating at 37°C for 30 min, followed by sonication. Cell lysates were than incubated with anti-FLAG antibody-coated beads overnight at 4°C to bind Lsr2-3×FLAG. The protein-bound beads were washed three times with immunoprecipitation buffer (50 mM Tris-HCl, 250 mM NaCl, 0.8% Triton X-100, pH 8.0) before the bound proteins were eluted in 1×SDS loading dye. Immunoprecipitated protein samples were then separated on a 12% SDS-PAG, and the bands corresponding to Lsr2-FLAG were excised and analyzed using mass spectrometry analysis to identify any post-translational modifications.

To test for interactions between Lsr2 and other proteins in *S. venezuelae*, Lsr2- (negative control) and Lsr2-3×FLAG-expressing strains were grown for 14 hours before collecting cells and performing co-immunoprecipitation, as described above. After eluting the (co)immunoprecipitated proteins from the anti-FLAG antibody-coated beads, they were separated on a 12% SDS-PAG, and the entire lane for each sample was excised and subjected to mass spectrometry analysis.

3.5.8 Protein overexpression, purification, and EMSAs

To examine the possible interaction of Lsr2 and LsrL in *E. coli*, Rosetta 2 cells expressing 6×His-Lsr2_LsrL-S or 6×His-LsrL_Lsr2-S (**Table 3.3**) were grown at 37°C until the culture reached an OD_{600} of 0.4, after which IPTG was added to a final concentration of 1 mM. Cells were then grown at 30°C for an additional 5 hours before being collected and lysed. Ni-NTA affinity chromatography was used to purify His-tagged proteins and associated interacting partners. Following the application of soluble cell lysate to the Ni-

NTA column, the bound proteins were washed using increasing concentrations of imidazole (10 mM- 200 mM), before being eluted with 250 mM imidazole. After denaturing, the protein samples were subjected to western blotting using anti-S antibodies to assess the interaction between Lsr2 and LsrL.

To overexpress and co-overexpress Lsr2 and LsrL in *E. coli*, their respective plasmids was introduced into *E. coli* Rosetta 2 cells. The resulting 6×His-Lsr2, 6×His-LsrL, 6×His-Lsr2_LsrL-S and 6×His-LsrL_Lsr2-S overexpression strains were grown at 37°C until they reached an OD_{600} of 0.5, at which point 1 mM IPTG was added. Cells were then grown at 30°C for 5 h before being collected and lysed. The overexpressed proteins were purified from the cell extract using Ni-NTA affinity chromatography and were washed using increasing concentrations of imidazole (10 mM – 200 mM), before being eluted using 250 mM imidazole. Finally, purified proteins were exchanged to storage buffer suitable for either EMSAs or freezing at -80°C (20 mM Tris-HCl, 150 mM NaCl, 1.4 mM β-mercaptoethanol, 25% glycerol, pH 8.0).

To test the binding ability of Lsr2 and LsrL, EMSAs were performed using probes amplified by PCR using primers 0926F and 0926R, and 0904F and 0904R (**Table 3.4**), and 5′-end-labelled with [γ-^{32}P]dATP. Lsr2, LsrL and Lsr2+LsrL (0 – 2 μM) were incubated with 1 nM labelled probe in binding buffer (10 mM Tris, pH 7.8, 5 mM $MgCl_2$, 60 mM KCl and 10% glycerol) in 20 μL reaction volumes. EMSA reactions were incubated at room temperature for 10 min, followed by 30 min on ice. The reactions were then running on 10% native polyacrylamide gels. The gels were exposed to a phosphor screen for 45 min and imaged using a Typhoon FLA 9500 phosphorimager.

Table 3.3: *Streptomyces* strains, *E. coli* strains and plasmids

Strains	**Genotype, characteristics, or use**	**Reference or source**
Streptomyces		
S. venezuelae NRRL B-65442	Wild type	Gift from M. Buttner; Gomez-Escribano et al., 2021
E336	*S. venezuelae* Δ*lsr2* with pIJ82 carrying wild type *lsr2*	Gehrke et al., 2019
E337	*S. venezuelae* Δ*lsr2* with pIJ10706 carrying *lsr2-3×Gly-3×FLAG*	Gehrke et al., 2019
E328	*S. venezuelae ΔlsrL::aac(3)IV*	Gehrke et al., 2019

Escherichia coli		
DH5α	Routine cloning	Hanahan, 1985
SE DH5α	Highly-competent (Subcloning Efficiency™) DH5α cells	Invitrogen
ET12567	*dam, dcm, hsdS, cat tet;* carries *trans*-mobilizing plasmid pUZ8002	MacNeil et al., 1992
Rosetta 2	Protein overexpression host with pRARE2 which supplies 'rare' tRNAs	Novagen
DHM1	*cya*$^-$; bacterial two-hybrid reporter strain	Karimova et al., 2001
Plasmids		
pMS82	Integrative cloning vector: *hyg, oriT, int* ΦBT1, *attP* ΦBT1	Gregory et al., 2003
pBluescript II KS (+)	Standard cloning vector	Stratagene
pET15b	Overexpression of N-terminally His_6-tagged proteins	Novagen
pMC109	*lsr2*-R82A mutant variant cloned downstream of *ermE** promoter in pIJ12551	Gehrke et al., 2019
pKT25	Kan^r, *cya* domain T25, multiple cloning site located at C- terminus	Karimova et al., 2001
pKNT25	Kan^r, *cya* domain T25, multiple cloning site located at N- terminus	Karimova et al., 2001
pUT18	Amp^r, *cya* domain T18, multiple cloning site located at N- terminus	Karimova et al., 2001
pUT18C	Amp^r, *cya* domain T18, multiple cloning site located at C- terminus	Karimova et al., 2001
pKT25-*lsr2*	*lsr2* coding sequence cloned into pKT25 at *Bam*HI and *Kpn*I sites	This study

pKT25-*lsrL*	*lsrL* coding sequence cloned into pKT25 at *Bam*HI and *Kpn*I sites	This study
pKNT25-*lsr2*	*lsr2* coding sequence cloned into pKNT25 at *Bam*HI and *Kpn*I sites	This study
pKNT25-*lsrL*	*lsrL* coding sequence cloned into pKNT25 at *Bam*HI and *Kpn*I sites	This study
pUT18-*lsr2*	*lsr2* coding sequence cloned into pUT18 at *Bam*HI and *Kpn*I sites	This study
pUT18-*lsrL*	*lsrL* coding sequence cloned into pUT18 at *Bam*HI and *Kpn*I sites	This study
pUT18C-*lsr2*	*lsr2* coding sequence cloned into pUT18C at *Bam*HI and *Kpn*I sites	This study
pUT18C-*lsrL*	*lsrL* coding sequence cloned into pUT18C at *Bam*HI and *Kpn*I sites	This study
pMC114	pET15b carrying *lsr2* for overexpression with an N-terminal His_6-tag	Gehrke et al., 2019
pMC126	pET15b carrying *lsrL* for overexpression with an N-terminal His_6-tag	This study
pCOLADuet-1	Co-overexpression of N-terminally His_6-tagged protein and C-terminally S-tagged protein	Novagen
pMC127	pCOLADuet-1 carrying *lsr2* with and N-terminal His_6-tag and *lsrL* with a C-terminal S-tag	This study
pMC128	pCOLADuet-1 carrying *lsrL* with and N-terminal His_6-tag and *lsr2* with a C-terminal S-tag	This study
pMC129	pCOLADuet-1 carrying *lsr2* with and N-terminal His_6-tag	This study

pMC130	pBlueScript carrying plasmid pulldown features and *lsr2*-R82A mutant variant	This study
pMC131	pBlueScript carrying plasmid pulldown features	This study
pMC132	*lsr2* with R82A point mutation (with native promoter and terminator) cloned into *Eco*RV site of pIJ82	From Emma J Gehrke
pIJ82	Integrative cloning vector; *ori* pUC18, *hyg*, *oriT*, RK2, *int* ΦC31, *attP* ΦC31	Gift from H. Kieser
pKOSi	Kan^r, pSG5 replicon	Netzker et al., 2016

Table 3.4: Oligonucleotides used in this study

Primers	**Sequence (5' - 3')***	**Use**
lsr2B2HF	ATATGGATCCGGCACAGAAGGTTCAGGTCC	Clone *lsr2* into the pKT25, pKNT25, pUT18 and pUT18C vectors
lsr2B2HR	ATATGGTACCATGCGGTTCGCGTCCTCGTA	
lsrlB2HF	ATATGGATCCAGTGGCTCAGCGTGTGGTGGTC	Clone *lsrL* into the pKT25, pKNT25, pUT18 and pUT18C vectors
lsrlB2HR	ATATGGTACCATACTCGCGGCGCGGAAGGCCT	
lsrlF_pET15b	ATATCATATGGTGGCTCAGCGTGTGGTGGTC	Clone *lsrL* into pET15b
lsrlR_pET15b	ATATGGATCCTCAACTCGCGGCGCGGAAGG	
lsr2F_MCS1	ATATGAATTCAGCACAGAAGGTTCAGGTCC	Clone *lsr2* into pCOLADuet with an N-terminal 6×His-tag
lsr2R_MCS1	ATATAAGCTTTCAGCGGTTCGCGTCCTCG	
lsrlR_XhoI	ATATCTCGAGACTCGCGGCGCGGAAGGCCTC	Clone *lsrL* into pCOLADuet with a C-

		terminal S-tag (with lsrlF)
lsr2F_MCS2	GGGTGCCATATGGCACAGAAGGTTCAGGTCCTT	Clone *lsr2* into pCOLADuet with a C-terminal S-tag
lsr2R_MCS2	ATATGGTACCGCGGTTCGCGTCCTCGTAG	
oriT_pSG5ori2	CGATTGGCTGAGCTCATAAGAATGCCAGGATCAACAGGAC	Amplify pSG5 replicon
pSG5ori_pBluScript	TGATATCGAATTCCTGCAGCCCGGGGGATCTCATCTGGTCAGCGTCAAGG	
pBlueScript_lacI_lacOF	GAGCTCCACCGCGGTGGCGGCCGCTCTAGAAGCCCGACCCGAGCACGCGC	Amplify *ermE*-lacI-FLAG-lacO* fragment
lacI_lacO_oriT1	TGCGAGGCTGGCGGGAACTTTTGTTATCCGCTCACAATTGTTATCCGCTCACAATTG	
lacI_lacO_oriT2	CAATTGTGAGCGGATAACAAAAGTTCCCGCCAGCCTCGCA	Amplify *acc(3)IV* resistance cassette
oriT_pSG5ori1	GTCCTGTTGATCCTGGCATTCTTATGAGCTCAGCCAATCG	
R82AF	TTCCTATGACGAGGGAGTCG	Amplify *lsr2*R82A coding sequence with promoter and terminator
R82AR	GAATGGGGCGGTATCTCG	
0926F	TCGTCGATGAACCATTTCAT	Amplify *sven0926* EMSA probe
0926R	GGAGACGTTCAGGATCGCGG	
0904F	GGATTTTCCTGAACGCCGGA	Amplify *sven0904_0905* EMSA probe
0904R	ACTTGAGGCATTCGACGTAT	

*Restriction sites are underlined in primers.

CHAPTER 4: MAPPING REGULATOR OCCUPANCY WITHIN CLUSTERS IN *S. VENEZUELAE*

Xiafei Zhang, Peter L. Freddolino, Marie A. Elliot

Preface:

This chapter represents unpublished work. Dr. Peter L. Freddolino (Department of Biological Chemistry, University of Michigan Medical School) provided critical advice regarding our IPOD-HR experiments and analyzed our IPOD-HR and ChIP-seq data. I performed all other experiments.

4.1 Abstract (Chapter Summary)

Streptomyces bacteria are noted for their ability to produce an incredible array of bioactive compounds, including over 70% of the antibiotics in clinical use today. Unexpectedly, however, genome sequences of *Streptomyces* species have revealed that these bacteria have the potential to produce far greater numbers of bioactive compounds than have been detected in the lab, and the products of many of these 'cryptic' biosynthetic gene clusters remain unknown. Understanding how the expression of these biosynthetic clusters is controlled is critical to fully accessing the metabolic potential of these bacteria. In *Streptomyces*, the expression of many antibiotic biosynthetic clusters is controlled by both pathway-specific regulators and more globally-acting regulators; however, the mechanism by which clusters are repressed/fail to be activated is largely unknown and there is much that remains to be discovered about the regulators that govern gene expression. Therefore, we sought to develop a comprehensive understanding of those regulatory proteins that impact biosynthetic gene cluster expression. To define the regulatory protein occupancy of antibiotic clusters (and chromosome-wide), we are using '*in vivo* protein occupancy display-high resolution' (IPOD-HR) technology. This work will lay the foundation for establishing a comprehensive regulatory network map for biosynthetic clusters in *Streptomyces*, and guide future work aimed at stimulating the expression of metabolic clusters of interest in any *Streptomyces* species.

4.2 Introduction

Streptomyces bacteria have large chromosomes, ranging in size from 8-12 Mb. They typically possess ~8000 protein-coding genes, with ~12% of these genes encoding regulatory proteins, including transcriptional regulators and σ factors. These regulators play important roles in controlling *Streptomyces* development and metabolism, and their numbers reflect the complexity of regulatory networks in *Streptomyces* (Bentley et al., 2002). *Streptomyces* are well-known for their ability to produce a wide range of bioactive compounds, and analysis of the genome sequences of *Streptomyces* species suggests that these bacteria have the potential to produce far greater numbers of specialized metabolites than have been detected in the lab. The products of many cryptic biosynthetic gene clusters remain unknown, often because their biosynthetic genes are not expressed, or are expressed at very low levels under typical laboratory conditions.

In controlling specialized metabolism, *Streptomyces* species rely heavily on transcriptional regulators, which repress or activate the transcription of their associated target genes. Negative regulators exert their activity by preventing transcription initiation, competing with activators for binding sites, or inhibiting transcription elongation by blocking RNA polymerase progression. Conversely, positive regulators

activate transcription by stabilizing RNA polymerase-promoter complexes during transcription initiation, or promoting repressor dissociation (Lee et al., 2012). Bacterial transcriptional regulators can be divided into specific and pleiotropic regulators, based on their target genes. Pathway-specific regulators are encoded within biosynthetic clusters and often directly control the expression of genes located in that cluster (**Figure 4.1, top panel**). Many, but not all, specialized metabolic clusters in *Streptomyces* contain pathway-specific regulators (Bibb, 2005). In contrast, pleiotropic regulators are usually encoded elsewhere in the chromosome, and affect the production of multiple metabolic pathways (Gao et al., 2012; Kang et al., 2019; Wei et al., 2018) (**Figure 4.1, middle panel**). In bacteria, nucleoid-associated proteins can also function as pleiotropic regulators in governing specialized metabolite biosynthesis. Nucleoid-associated proteins are typically low molecular weight proteins that not only contribute to the overall chromosome structure but also regulate gene expression in both positive and negative manners through bending, bridging, polymerizing and/or wrapping DNA (**Figure 4.1, bottom panel**).

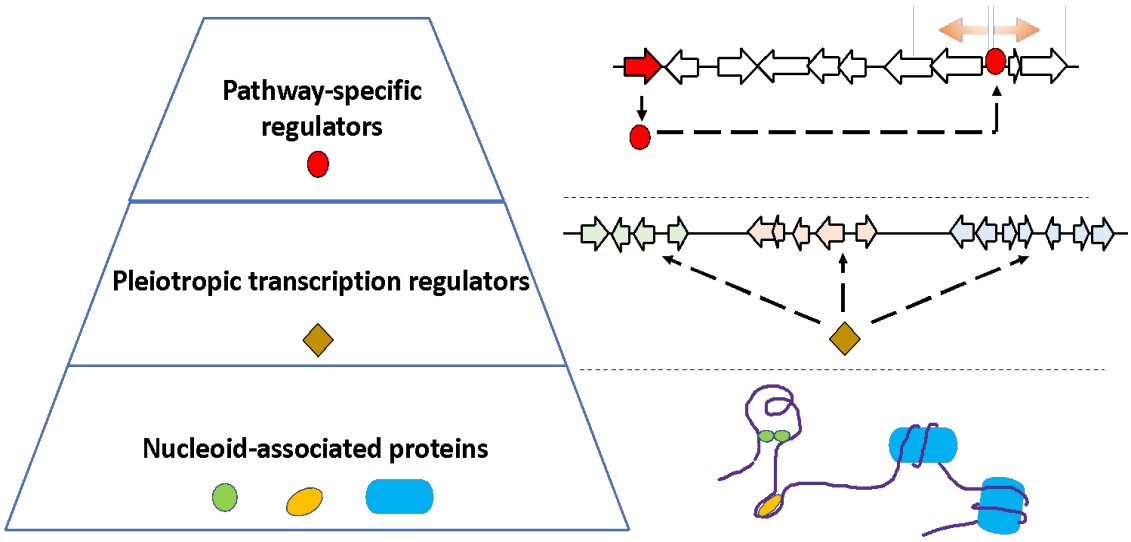

Figure 4.1: The production of specialized metabolites in *Streptomyces* is regulated by multiple factors. Pathway-specific regulators (**top panel**) are frequently encoded within clusters and directly regulate the expression of genes located in the same cluster. In contrast, pleiotropic regulators (**middle panel**) are usually encoded elsewhere in the chromosome and exert their effects by controlling the transcription of multiple metabolic pathways. Nucleoid-associated proteins (**bottom panel**) contribute to both chromosome structure and gene regulation.

Many strategies have been used to stimulate antibiotic production in *Streptomyces*, including manipulating pathway-specific and global regulators (Daniel-

Ivad et al., 2017; Gao et al., 2012; Gehrke et al., 2019), heterologously expressing biosynthetic clusters in chassis strains (Fernandez-Martinez et al., 2014; Myronovskyi et al., 2018; Komatsu et al., 2013; Pait et al., 2018; Thanapipatsiri et al., 2016), and co-culturing with other species or applying elicitors as signals to facilitate metabolism (Xu et al., 2019; Craney et al., 2012; Onaka et al., 2011; Pishchany et al., 2018). Many clusters are, however, not affected by these techniques and remain silent. In considering why many biosynthetic clusters are not transcribed, we proposed two possible hypotheses: i) their genes/promoters are bound by nucleoid-associated proteins and other repressors, which prevents RNA polymerase from binding to promoter regions (**Figure 4.2A**), and/or ii) these clusters are not activated due to the lack of transcriptional activators (**Figure 4.2B**). Establishing regulatory networks of these silent clusters will provide insights that will allow the developing of strategies to stimulate the expression of cryptic clusters.

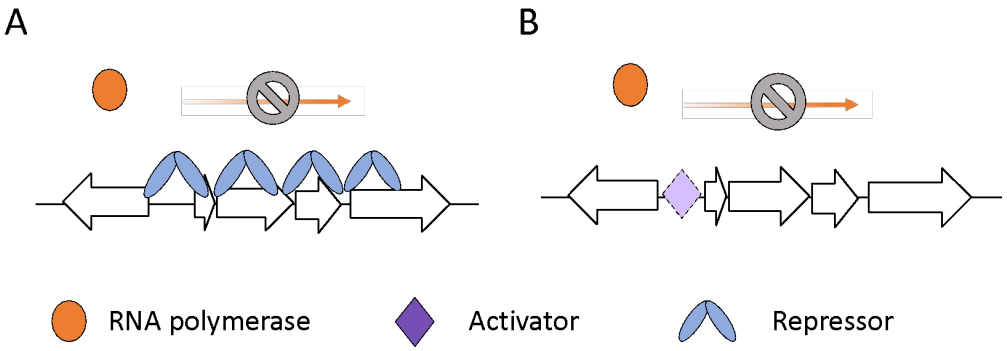

Figure 4.2: Models to explain why many biosynthetic clusters are not transcribed. (**A**) Their genes/promoters are bound by nucleoid-associated proteins and other repressors, preventing RNAP from binding to promoter regions, and/or (**B**) these clusters are not activated due to the lack of transcriptional activators.

Study of the function and targets of transcriptional regulators has benefited from the development of diverse sequencing techniques like chromatin immunoprecipitation sequencing (ChIP-seq), which identifies binding targets of a DNA-binding protein. However, our understanding of the regulatory networks governing specialized metabolism in *Streptomyces* remains limited. A recent work reconstructed the transcriptional regulatory interactions in *S. coelicolor* by collecting and curating reported interactions between transcriptional regulators and their corresponding target genes (Zorro-Aranda et al., 2022). Surprisingly, the analyses done by Zorro-Aranda et al. found that only ~6% of interactions were supported by 'strong' evidence, where the binding of a regulator to the promoter of a target gene was validated using genetic experiments (e.g. EMSAs, *in vitro* transcription assay, ChIP-seq or DNase I footprinting). The majority of the reported interactions between regulators and their associated binding sites are

'weak', meaning no evidence supports direct interaction between the regulator and its targets (Zorro-Aranda et al., 2022). Additionally, commonly used techniques such as ChIP-seq have limitations for understanding systematic regulation in *Streptomyces* since: i) they map binding sites of one particular protein at a time; and ii) they require modification of each regulator with an epitope tag, or an antibody against each regulator of interest.

We have instead opted to pursue *in vivo* protein occupancy display – high resolution (IPOD-HR) technology to characterize the global protein-DNA interactome of *Streptomyces*. IPOD-HR was developed by Freddolino et al. and has been applied in various bacteria to study protein occupancy across the chromosome (Freddolino et al., 2021; Amemiya et al., 2022). The experiment comprises three major steps: i) mapping RNA polymerase occupancy by performing ChIP-seq (**Figure 4.3A**); ii) isolating proteins and their associated DNA regions, followed by sequencing of the bound DNA (**Figure 4.3B**); and iii) data analysis, in which RNA polymerase occupancy signals are subtracted from the overall protein occupancy signals (**Figure 4.3C**). Compared to traditional approaches such as ChIP-seq, DNase footprinting and EMSAs, IPOD-HR technology facilitates understanding the causes of silent biosynthetic clusters in *Streptomyces* by: i) allowing for comprehensive mapping of the protein occupancy landscape on the chromosome without needing extensive genetic manipulation; ii) enabling identification of new binding motifs that could be associated with uncharacterized or poorly characterized regulators; and iii) providing insights into protein occupancy at genomic regions that are transcribed at low levels.

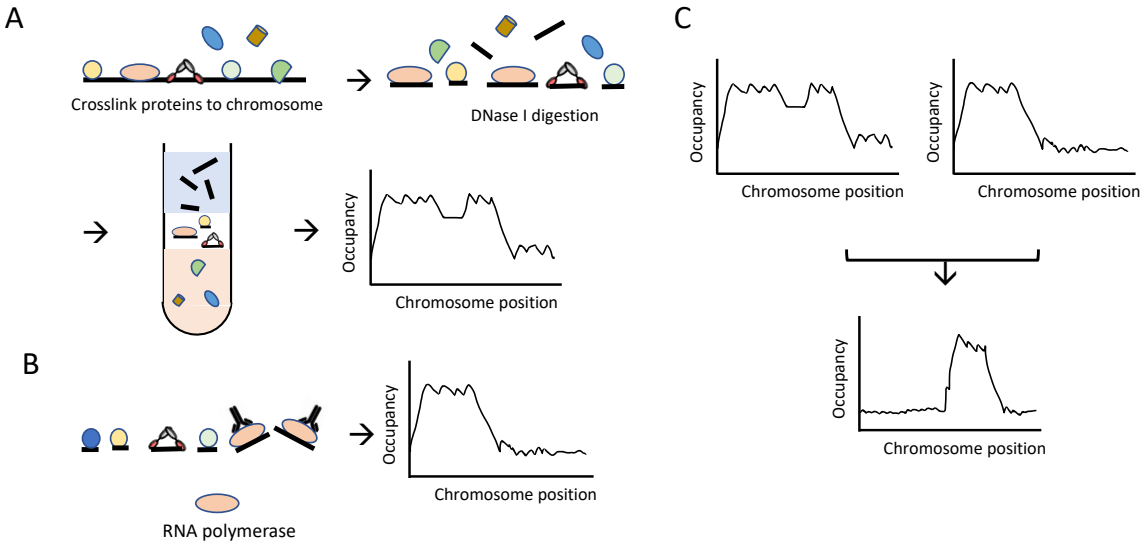

Figure 4.3: Schematic of the IPOD-HR method. (**A**) Generation of overall protein occupancy using IPOD method. (**B**) Identification of RNA polymerase binding site by ChIP-

seq. (**C**) Subtraction of RNA polymerase occupancy signals from raw IPOD signals to create a final IPOD-HR signal.

We adapted the IPOD-HR technology for use in *S. venezuelae*, aiming to probe the regulatory occupancy of specialized metabolic clusters. We have previously identified Lsr2, a nucleoid-associated protein that functions as a global repressor in controlling the expression of biosynthetic gene clusters in *S. venezuelae* (Gehrke et al., 2019). From ChIP-seq and RNA-seq experiments, we found that Lsr2 binds within 17 specialized metabolic clusters and alters the expression of 14 of these clusters (Gehrke et al., 2019). To understand how Lsr2 exerts its repressive effects, we probed its role in governing chloramphenicol production. We found that the expression of the chloramphenicol cluster is controlled by the interplay between Lsr2 and CmlR, the pathway-specific regulator of the chloramphenicol cluster (Zhang et al., 2021). Lsr2 represses transcription of the chloramphenicol cluster and its repression can be relieved by CmlR recruiting RNA polymerase and enhancing transcription (Zhang et al., 2021).

IPOD-HR analyses in *Escherichia coli* identified hundreds of chromosomal regions spanning lengths of over 1 kb that are occupied by protein but without RNA polymerase association (Freddolino et al., 2021). These extended protein occupancy domains (EPOD) were partially bound by nucleoid-associated proteins and some of these domains overlapped with the binding sites of H-NS, an Lsr2 nucleoid-associated protein (Freddolino et al., 2021; Amemiya et al., 2022). In this work, we described our strategy to optimize IPOD-HR technology in *S. venezuelae* in order to map protein occupancy across the chromosome, and discuss the next steps that will be used to identify regulators associated with binding sites of interest. We performed IPOD-HR experiments using both wild type and the *lsr2* mutant strains to assess how DNA occupancy – and RNA polymerase activity – change in the presence and absence of Lsr2. This work lays the foundation to systematically understand the regulation of biosynthetic clusters in *S. venezuelae,* with a particular interest in the clusters that are not controlled by Lsr2 and are silent under normal laboratory conditions.

4.3 Methods and materials

4.3.1 Bacterial strains and culture conditions

S. venezuelae strains were grown at 30°C on MYM (maltose, yeast extract, malt extract) agar, or in liquid MYM medium. For IPOD-HR experiments, *S. venezuelae* wild type and Δ*lsr2* strains were inoculated in 10 mL MYM liquid medium, before being subcultured into 50 mL of MYM in duplicate and grown for 16 hours at 30°C. *E. coli* strains were grown at 37°C in LB (lysogeny broth) medium. *Streptomyces* and *E. coli* strains that were used are summarized in **Table 4.1**.

Table 4.1: *Streptomyces* and *E. coli* strains

Strains	Genotype/characteristics/use	Reference
Streptomyces		
S. venezuelae NRRL B-65442	Wild type	Gift from M. Buttner; Gomez-Escribano et al., 2021
E327A	*S. venezuelae* Δ*lsr2*	Gehrke et al., 2019
Escherichia coli		
DH5α	Control for western blot using anti-RpoB antibodies	Hanahan, 1985

4.3.2 Transcription inhibition and crosslinking

After 16 h of growth, 50 mL of *Streptomyces* cultures were exposed to the RNA polymerase-targeting antibiotic rifampicin (500 µg/mL) and incubated at room temperature for 10 minutes to immobilize RNA polymerase and stop transcription initiation. Crosslinking of proteins to the chromosomal DNA was achieved by mixing the cultures with a formaldehyde/sodium phosphate (pH 7.4) buffer to a final concentration of 10 mM NaH_2PO_4 and 1% v/v formaldehyde. Culture mixtures were then incubated at room temperature for 30 min with shaking. The crosslinking reactions were quenched by adding 2 M glycine to a final concentration of 0.33 M. After a 5 min incubation at room temperature with shaking, the cells were washed three times with 10 mL ice-cold phosphate buffered saline. The fully washed cell pellet was then chilled on ice before cell lysis.

4.3.3 Cell lysis and DNase I treatment

Each cell pellet from the previous step was resuspended in 1.5 mL lysis buffer (10 mM Tris-HCl pH 8.0, 50 mM NaCl, 14 mg/ml lysozyme, 0.8% Triton X-100, and 1× protease inhibitor (Roche Complete Mini)), and incubated at 37°C for 30 min. The reaction tube was cooled on ice before 700 µL IP buffer (50 mM Tris-HCl pH 8.0, 250 mM NaCl, 0.8% Triton X-100, and 1×protease inhibitor) were added. Sonication was then performed at 50% power for 6 cycles of 15 s bursts followed by 45 s incubation on ice. The resulting suspension was clarified by centrifugation for 20 min at 9,600 ×*g* at 4 °C.

As described for previous IPOD-HR experiments with *E. coli*, the *E. coli* chromosome was digested to an average fragment size of less than 200 bp. To optimize the protocol for *Streptomyces* species, we prepared cell lysates of wild type *S. venezuelae* as described above and performed DNase I digestion on the cell-free lysate for 0-90 min. Cell-free supernatant (2.25 mL) was transferred into a 15 mL Falcon tube to which was added 250 µL DNase I buffer (10×), 3.75 µL DNase I (10 U/µL), and 7.5 µL RNase A (10 mg/mL), and incubated at 37 °C. Samples were taken at 0 min (before DNase I digestion; undigested DNA), 20 min after DNase I addition, and then every 10 min thereafter for up to 90 min. At each time-point, a 50 µL aliquot was removed and was mixed with 10 µL of 0.5 M EDTA to quench the digestion reaction before being incubated on ice for the remainder of the time course. All aliquots were then subject to phenol:chloroform extraction. Specifically, 60 µL of 50:50:1 phenol:chloroform:isoamyl alcohol were added into each tube, followed by vortexing and centrifugation for 5 min at 9,600 ×*g* at 4 °C. Five microlitres of the upper phase was mixed with 1 µL of 6× xylene loading dye and run on a 2% agarose gel. Our results suggested that a 90 min of DNase I digestion worked the best and generated DNA fragments centered around 150 bp and ranging in size from 50 bp to 300 bp (**Figure 4.4**).

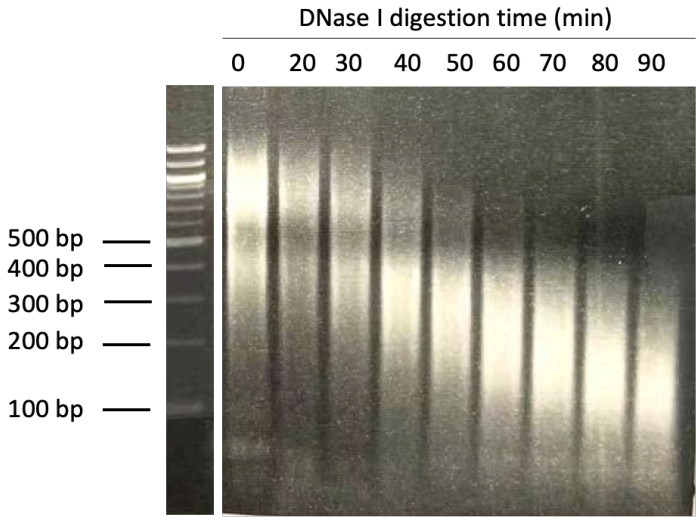

Figure 4.4: **DNase I digestion of protein-crosslinked *S. venezuelae* chromosomal DNA over a 90 min time course.** After sonication, wild type cell lysate was subject to DNase I digestion. Aliquots were taken at 0 min (pre-digestion), and at 20 min, 30 min, 40 min, 50 min, 60 min, 70 min, 80 min, and 90 min after DNase I addition The extracted DNA samples were run on a 2% agarose gel to assess digestion product sizes.

Based on these optimization experiments, we performed DNase I digestions for 90 min for our IPOD-HR experiments with wild type and Δ*lsr2* mutant strains. Cell lysis, DNase I digestion and phenol:chloroform extraction were performed as described

above, only with a 90 min DNase I digestion. After centrifugation, 10 µL of the upper phase was mixed with 2 µL of 6× xylene loading dye and run on a 2% agarose gel. The wild type samples were centered around 150 bp, ranging from 50 – 500 bp in size, while the *lsr2* mutant samples centered around 130 bp, and ranged in size 50 - 200 bp (**Figure 4.5**).

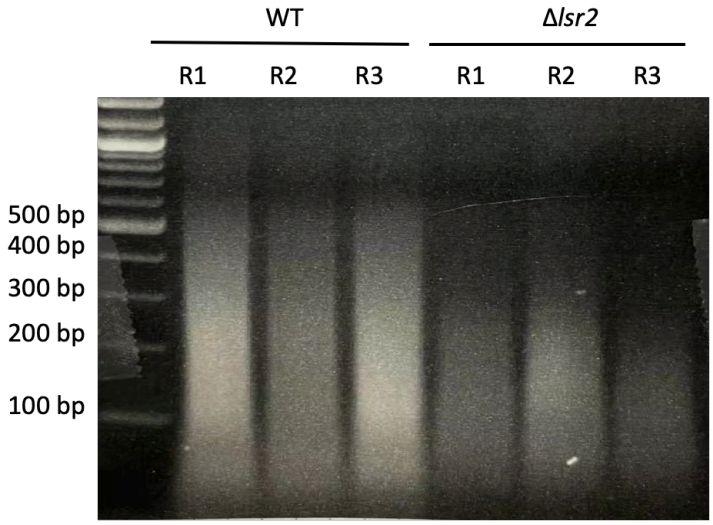

Figure 4.5: DNase I digestion of IPOD-HR samples. DNA aliquots of wild type and Δ*lsr2* samples were run on a 2 % agarose gel after 90 min of DNase I digestion. Wild type samples were digested to fragments centered around 150 bp (~50 - 500 bp), and the Δ*lsr2* samples were digested to fragments centered around 120 bp (~50 - 250 bp).

After DNase I digestion, 50 µL of samples were removed and mixed with 450 µL DNA resuspension buffer (50 mM Tris-HCl, pH 8.0; 10 mM EDTA; 1% SDS). These samples were saved as 'Input samples' and will be used to normalize IPOD-HR and RNA ChIP-seq data. Input samples were kept on ice until the reverse crosslinking step (below). The remaining lysate was divided into two aliquots (1.5 mL per aliquot), where one aliquot was used for the extraction of DNA-protein complexes and the other one was used for RNA polymerase ChIP experiments.

4.3.4 Extraction of DNA-protein complexes for IPOD-HR

In a 15 mL Falcon tube, one aliquot of the cell-free lysate was mixed with 1.5 mL 100 mM Tris base and 3 mL 25:24:1 phenol:chloroform:isoamyl alcohol by vortexing. Following a 10 min incubation at room temperature, the sample was spun at 7,800 ×*g* for 5 min, allowing for the separation of DNA and protein into the aqueous and organic phase, with DNA-protein complexes being enriched in a white disc at the aqueous–

organic interface. After completely removing both aqueous and organic phases, the white interface was washed by resuspending in 350 µL 100 mM Tris base, 350 µL TE buffer (10 mM Tris-HCl pH 7.4, and 1 mM EDTA) and 700 µL 24:1 chloroform:isoamyl alcohol. The suspension was vortexed and centrifuged at 9,600 ×*g* for 5 min. Following removal of the aqueous phases, the white disc was washed again with 1 mL TE buffer and 1 mL 24:1 chloroform:isoamyl alcohol. The mixture was vortexed and spun as above, and the liquid (both aqueous and organic) was removed. The resulting white disc was then washed again exactly as before. After the final wash, the white interface was resuspended in 700 µL of DNA resuspension buffer (described above). The resuspended protein-DNA complexes were kept on ice until the crosslinks were reversed.

4.3.5 Reverse crosslinking and DNA recovery

The DNA from both the 'Input sample' and IPOD-HR samples were recovered using the same procedure. The formaldehyde crosslinks were reversed by incubating the mixture in a 65°C water bath. After 16 h of incubation, the sample was cooled to room temperature, before being mixed with 100 µg of RNase A and incubated at 37°C for another 2 h. Proteinase K (200 µg) was then added, and the mixtures were incubated at 50°C for a further 2 h.

DNA was recovered through phenol:chloroform extraction. Specifically, each sample was mixed with equal volume of 50:50:1 phenol:chloroform:isoamyl alcohol, vortexed and spun at 9,600 ×*g* for 5 min at 4°C, after which the aqueous phase containing DNA was recovered. The sample was subject to phenol:chloroform extraction two more times with equal volumes of 50:50:1 phenol:chloroform:isoamyl alcohol. After the final extraction and recovery of the aqueous phase, the DNA was precipitated by adding two-volume of 95% (v/v) ethanol, 0.1 volume of CH_3COONa/CH_3COOH buffer (5 M, pH 5.20) and glycogen to a final concentration of 0.1 µg/µL. After precipitating at -20°C for 24 h, the sample was centrifuged at 9,600 ×*g* for 30 min at 4°C. The DNA pellet was then washed with ice-cold 95% (v/v) ethanol before being resuspended in 50 µL 10 mM Tris-HCl (pH 8.5). Recovered DNA was quantified using a NanoDrop spectrophotometer.

4.3.6 ChIP of RNA polymerase

4.3.6.1 Western blotting

To check the binding of commercially available anti-RpoB antibodies (Abcam, AB191598; developed against *E. coli* RpoB) to *S. venezuelae* RpoB, we performed western blotting using cell lysates prepared from 10 mL *S. venezuelae* liquid cultures grown for 16 h. As a positive control, *E. coli* cell lysates were also included. The protein concentration of cell lysates was determined by Bradford assay, and 40 µg of each

protein extract were separated using 8% SDS-PAGE and transferred to PVDF membranes. The membranes were blocked for 2 h at room temperature with Tris-buffered saline containing Tween 20 (TBS-T, 10 mM Tris-HCl, pH 8.0, 100 mM NaCl and 0.1% Tween 20) containing 5% bovine serum albumin (BSA). The membranes were then incubated overnight at 4°C in TBS-T containing 2% BSA with anti-RpoB antibodies (1:2000 dilution; Abcam, AB191598). The membrane was washed six times with TBS-T before then being incubated in TBS-T containing 2% BSA with anti-rabbit IgG horseradish peroxidase (HRP)-conjugated secondary antibodies (1:3000 dilution; Cell Signaling) at room temperature for 2 h. Blots were developed using an enhanced chemiluminescence system (Bio-Rad). The western blotting results showed that anti-RpoB antibodies bound RpoB in *S. venezuelae* well, and were therefore appropriate for RNA polymerase ChIP-seq in *S. venezuelae* (**Figure 4.6**).

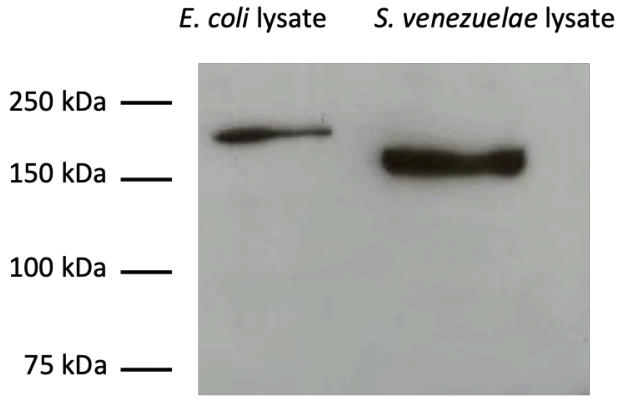

Figure 4.6: Western blotting of RpoB in *S. venezuelae* using anti-RpoB antibodies. Western blot using anti-RpoB antibody (Abcam, AB191598) against cell lysates from wild type *S. venezuelae*, alongside cell lysates from *E. coli* as a positive control. Molecular weight of RpoB in *E. coli*: ~150 kDa; molecular weight of RpoB in *S. venezuelae*: ~128 kDa.

4.3.6.2 Preparation of A-Sepharose beads

In order to immunoprecipitate antibody-bound RpoB (and its associated DNA) from the cell lysate, protein A-coated Sepharose resin was used. For this, 0.125 g A-Sepharose resin was resuspended in 1 ml IP buffer (described above) overnight at 4 °C. The resulting hydrated and swollen A-Sepharose beads were then washed three times with 1 mL IP buffer, and then resuspended in 1 mL 0.5× IP buffer and stored at 4°C.

4.3.6.3 ChIP using anti-RpoB antibodies

One aliquot of cell lysate from **4.3.3** was pre-cleared by incubating with 150 µL of prepared A-Sepharose beads at 4°C for 1 h with mild shaking on a horizontal shaker.

After removing the beads by centrifugation at 8,870 ×*g* for 15 min, 1.35 mL cell lysate was transferred to a 1.5 mL tube, mixed with 10 µL of anti-RpoB antibodies (Abcam, AB191598), and incubated at 4°C overnight with mild shaking. The antibody-lysate mixture was then mixed with 150 µL of A-Sepharose beads and incubated at 4°C for 4 h with mild shaking to recover antibody-protein-DNA complexes. A-Sepharose beads with bound protein-DNA complexes were collected by centrifugation at 2,400 ×*g* for 5 min, and the resulting pellet was washed three times with 0.5× IP buffer. After the final wash and complete removal of supernatant, the beads were resuspended in 150 µL of DNA resuspension buffer (described above).

4.3.6.4 Reverse crosslinking and DNA recovery

The bead suspension was incubated in a 65°C water bath for 16 h to reverse the formaldehyde crosslinks. Following centrifugation at 9,600 ×*g* for 5 min, 150 µL of supernatant was transferred to a 1.5 mL tube. The remaining beads were resuspended again in 50 µL TE buffer and incubated at 65°C for 30 min, after which the beads were pelleted as described above, and 50 µL supernatant were combined with the previous 150 µL, resulting a total volume of 200 µL. This sample containing liberated DNA was then mixed with 60 µg RNase A and incubated at 37°C for 2 h, followed by the addition of 60 µg of Proteinase K and a further incubation at 50°C for 2 h. DNA was recovered from the resulting mixture following phenol:chloroform extraction as described in **4.3.5**. Recovered DNA was quantified using a NanoDrop Spectrophotometer.

4.3.7 Next generation sequencing

Input DNA, IPOD-HR DNA and RNA polymerase ChIP DNA were prepared, as described in **4.3.2** – **4.3.6**, from wild type and Δ*lsr2* strains after 16 h of growth in biological triplicate. Next generation sequencing was conducted by the MOBIX facility at McMaster University. Sequencing was done using paired-end technology on an Illumina NextSeq instrument; this has just been completed and analyses are currently underway.

4.4 Conclusion and next steps

4.4.1 Conclusion

In order to define the protein-DNA interactome in *S. venezuelae*, we adapted and optimized the IPOD-HR technology in *S. venezuelae,* as IPOD-HR has the potential to reveal new information about gene regulation in *Streptomyces* and provide novel insights into the control of biosynthetic clusters. Our IPOD-HR samples (wild type and Δ*lsr2* samples in biological triplicate) have been sequenced and the resulting data are being analysed in collaboration with Dr. Peter Freddolino (University of Michigan). We

have obtained preliminary data analysis results. RNA polymerase ChIP-seq data of wild type samples showed that under the tested condition, the arm regions of the chromosome, which contain over 60% of specialized metabolic clusters, were not transcribed very well compared to the core region (**Figure 4.7**), and IPOD-HR data revealed that the lowly transcribed arm regions were bound by many regulatory proteins, suggesting transcription of these regions might be inhibited by repressors (**Figure 4.7**).

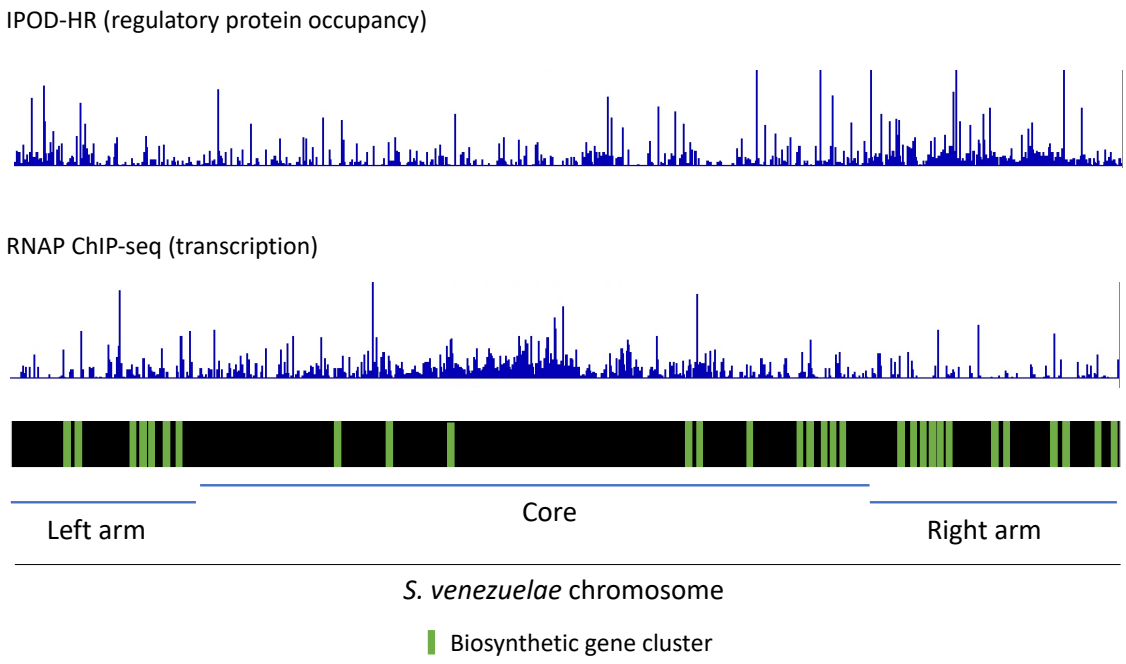

Figure 4.7: IPOD-HR and RNA polymerase ChIP-seq data of wild type *S. venezuelae.* **Top**: IPOD-HR data showing regulatory protein occupancy across the chromosome. **Middle**: RNA polymerase ChIP-seq data showing actively transcribed regions across the chromosome. **Bottom**: *S. venezuelae* chromosome with core and arm regions. Biosynthetic gene clusters are indicated by green lines.

4.4.2 Next steps

The long-term goals of this work are to i) map regulatory occupancy within biosynthetic clusters in *S. venezuelae* (data have been acquired and are currently being assessed); and ii) identify regulatory proteins bound at regulatory regions. The first goal will be achieved by analyzing IPOD-HR and RNA polymerase ChIP-seq data which will provide insight into which regions within a biosynthetic cluster of interest are occupied by regulators, and if these regions are actively transcribed.

To accomplish the second goal, we aim to define the regulators associated with these biosynthetic clusters. To identify the associated DNA-bound proteins within biosynthetic clusters, we will take advantage of the plasmid pulldown system we developed and described in Chapter 3. We modified the backbone of a non-integrating vector to allow it to be conjugated into *Streptomyces* spp. where it can replicate. We further introduced features that facilitated plasmid capture and isolation of the associated proteins. Specifically, we introduced into our vector, a *Streptomyces*-compatible origin of replication, alongside a tandem array of *lacO* binding sites, a constitutively expressed *lacI-FLAG* fusion, and an origin of transfer, together with an apramycin resistance gene. Additionally, a plasmid bearing a wild type *lacI* (untagged) was generated as a control (**Figure 4.8**). We will clone DNA regions of interest (e.g. promote regions within biosynthetic clusters and protein-occupied regions that exclude RNA polymerase) identified from IPOD-HR into the modified non-integrating experimental and control plasmid, and the resulting constructs will be conjugated into *Streptomyces*. Strains will be grown in media containing apramycin to maintain the plasmid in the cell. Regulatory proteins will be crosslinked to their target DNA on the plasmid and pulled out through binding of anti-FLAG antibodies to LacI-FLAG fusion proteins. The proteins will then be identified following plasmid DNA isolation and mass spectrometry analysis. After identifying regulators from the previous step, we will perform electrophoretic mobility shift assays (EMSAs) using purified proteins and PCR amplified DNA sequences of interest to confirm the interactions. Plasmid pulldown experiments coupled with EMSAs will allow us to define a complete regulatory protein-DNA interactome within a biosynthetic cluster.

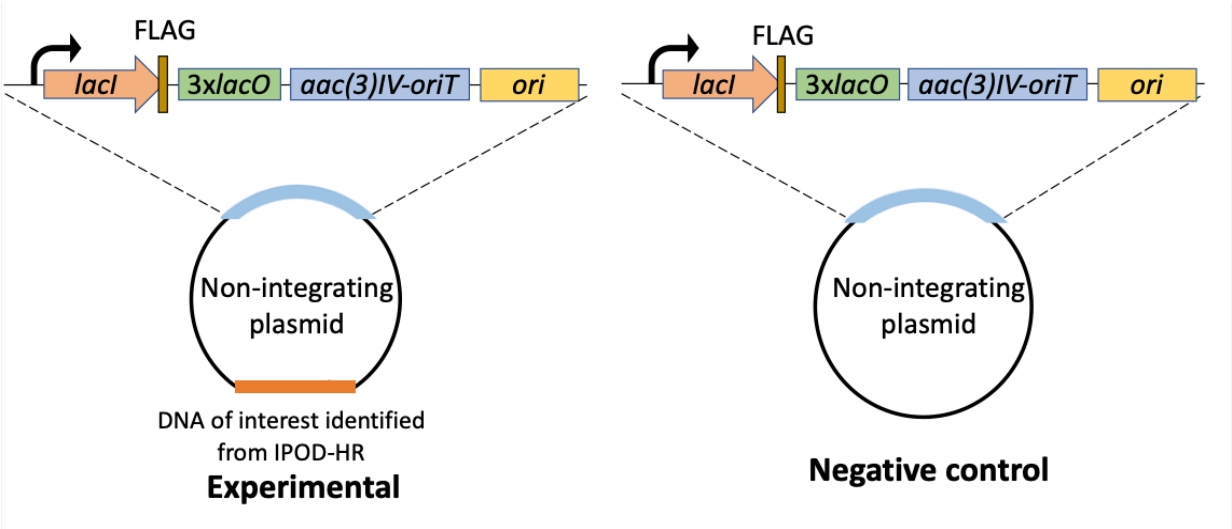

Figure 4.8: Plasmid construction for plasmid pulldown experiments. To identify regulators associated with DNA of interest identified from IPOD-HR, we modified the backbone of a non-integrating plasmid and introduced features that facilitate plasmid replication, conjugation, maintenance, and capture.

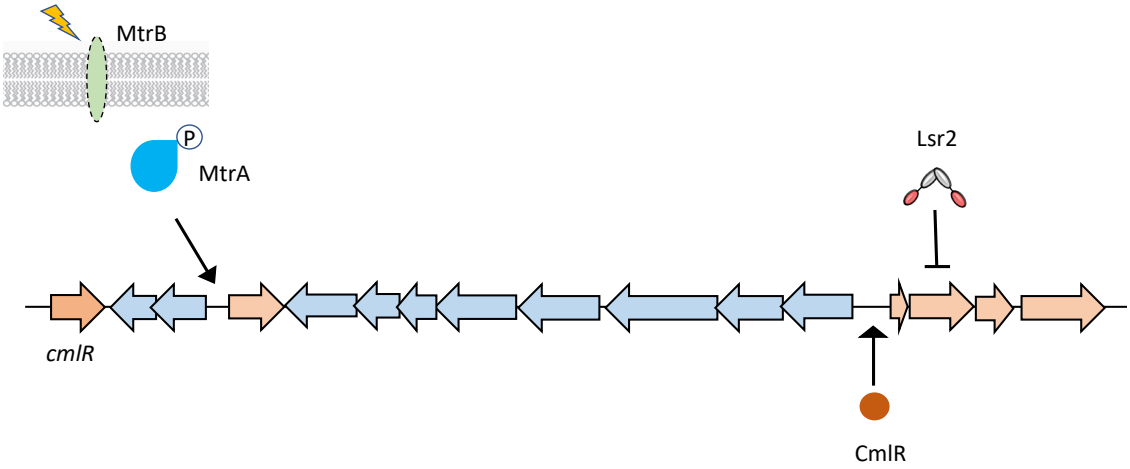

Figure 4.9: Regulators of the chloramphenicol cluster and their binding sites within the cluster. The chloramphenicol cluster is positively regulated by MtrA and CmlR, and negatively regulated by Lsr2.

To test our system, we will first focus on the well-characterized chloramphenicol cluster. The expression of the chloramphenicol cluster is controlled by multiple regulators, including two activators, MtrA (the response regulator of the MtrAB two-component system) and the pathway-specific regulator CmlR, alongside Lsr2, a global repressor (**Figure 4.9**) (Gehrke et al., 2019; Zhang et al., 2021; Fernandez-Martinez et al., 2014; Som et al., 2017b; McLean et al., 2019). The binding sites of these regulators within the chloramphenicol cluster have been well characterized by ChIP-seq and/or EMSAs. We will clone the DNA sequences containing their binding sites into the modified constructs and perform plasmid pulldown experiments to identify associated proteins. Once we have established the appropriate experimental workflow, we will expand our analyses to other biosynthetic clusters in *S. venezuelae*. Identified proteins will be mapped to associated DNA sequences, and the protein binding sites will be predicted based on the binding specificity of protein families. Regulators with unknown binding sites will be overexpressed and purified, and tested for their ability to bind sequences identified from IPOD-HR using EMSAs. For any regulators of particular interest, tagged variants will be generated, and ChIP-seq experiments will be performed. Combining the results from IPOD-HR with our plasmid pulldown experiments, we expect to be able to map different regulators to their specific binding sites within biosynthetic clusters of interest. We will also compare the IPOD-HR profiles of wild type and Δ*lsr2* to identify protein occupancy shifts caused by the loss of Lsr2. This work will establish comprehensive regulatory networks for *S. venezuelae* biosynthetic clusters, and guide future work aimed at stimulating the production of metabolic clusters of interest in *Streptomyces*.

CHAPTER 5: GENERAL CONCLUSION AND FUTURE DIRECTIONS

5.1 Conclusions

In bacteria, nucleoid-associated proteins contribute to chromosome structure organization and gene regulation. Lsr2 is a nucleoid-associated protein that is conserved in actinomycetes and plays an important role in controlling specialized metabolism in *Streptomyces* species. To probe the mechanism of Lsr2 repression of biosynthetic cluster expression, we focused on the chloramphenicol biosynthetic cluster in *S. venezuelae* and established that Lsr2 represses transcription of the chloramphenicol cluster by binding DNA within the cluster and at distal sites. We also revealed that Lsr2 repression within the chloramphenicol cluster can be alleviated by CmlR, a known activator of the chloramphenicol cluster, where CmlR functions to 'counter-silence' Lsr2, enhancing transcription and permitting chloramphenicol production. We have discovered that CmlR exerts its effects on Lsr2 by facilitating RNA polymerase activity. This in turn effectively clears bound Lsr2 from the chloramphenicol cluster (**Chapter 2**).

Beyond counter-silencing of Lsr2 mediated by CmlR, little is known about how Lsr2 is regulated. To understand how Lsr2 expression and protein activity are controlled within *Streptomyces* cells, we identified potential regulators of *lsr2* expression, and interacting proteins that could impact Lsr2 regulatory activity. We found that Lsr2 and LsrL, an Lsr2 homologue that is encoded by all streptomycetes, interact directly with each other, and that their respective DNA-binding activities are altered by the presence of the other protein. This work provides insight into the regulation of Lsr2 in *Streptomyces* (**Chapter 3**).

Beyond Lsr2, we sought to develop a comprehensive understanding of the regulatory proteins that impact biosynthetic gene cluster expression. To define the regulator binding sites associated with biosynthetic clusters (and any locus of interest in the chromosome), we used '*in vivo* protein occupancy display-high resolution' (IPOD-HR) technology to map protein occupancy across the chromosome, and discussed the next steps that will be done to identify regulators associated with DNA sequences of interest identified through our IPOD-HR work. These investigations lay the foundation for establishing a comprehensive regulatory network for biosynthetic clusters in *Streptomyces*, and will guide future work aimed at stimulating the expression of metabolic clusters of interest in any *Streptomyces* species (**Chapter 4**).

5.2 Future directions

5.2.1 Exploring Lsr2 regulatory activities

Nucleoid-associated proteins are known to organize chromosome structure and regulate gene expression by binding DNA; however, several nucleoid-associated proteins, including HU and H-NS, are also able to bind RNA, including mRNA and non-

coding RNA (ncRNA). For example, HU not only impacts gene expression at a transcriptional level by preferentially binding AT-rich regions (e.g. pathogenicity islands and virulence factors encoding genes), it can also act at a post-transcriptional level by binding mRNA and stimulating translation (e.g. Prieto et al., 2012; Balandina et al., 2001; Dorman, 2014; Stojkova et al., 2019). H-NS, which has been best-studied as a global transcriptional repressor, can also regulate translation both positively (e.g. facilitating the translation initiation of *malT* mRNA by relocating ribosomes to more favourable binding sites than the defined Shine-Dalgarno sequence; Brescia et al., 2004) and negatively (e.g. inhibiting RpoS expression by inducing RNA degradation of *rpoS* mRNA and the non-coding RNA DsrA; Park et al., 2010).

Streptomyces bacteria have large chromosomes with great ncRNA potential. A few ncRNAs have been shown to control gene expression and cellular processes in *Streptomyces.* In *S. coelicolor*, Scr4677 is an antisense RNA encoded between the co-transcribed *sco4676-4677* genes, where it appears to promote the degradation of *sco4676* transcripts (Hindra et al., 2014). Another example of RNA-mediated regulation is of the cell wall lytic enzyme-encoding *rpfA* gene, which is under the control of both a riboswitch within its 5′ untranslated region (5′ UTR) and an antisense RNA (scr3097) expressed immediately downstream (St-Onge and Elliot, 2017). The riboswitch responds to cyclic-di-AMP, and upon ligand binding, the structure of the 5′ UTR is altered in a way that leads to premature transcription termination and *rpfA* downregulation; during exponential growth, Scr3097 positively impacts *rpfA* transcript levels and impacts colony development (St-Onge and Elliot, 2017). A recent study showed that the expression of *pepck*, encoding phosphoenolpyruvate carboxykinase, is repressed by the ncRNA Scr5239 (Engel et al., 2019). These studies emphasize the diverse regulatory roles played by ncRNA – but the fact that there are only a handful of other characterized ncRNA regulators in the streptomycetes highlights how much has yet to be discovered regarding ncRNA based control in these bacteria.

We have established that Lsr2 represses the expression of biosynthetic clusters, but RNA-binding activity of Lsr2 has not been reported. Given that Lsr2 is functionally equivalent to H-NS, it will be interesting to determine if Lsr2 can bind mRNA and ncRNA *in vivo* by performing RNA-pulldown experiments followed by RNA sequencing. If we identify any Lsr2-associated RNAs (mRNAs or ncRNA) that interacts with Lsr2, we would first perform EMSAs to confirm Lsr2 binding to the RNA of interest, and then determine the effect of Lsr2 on RNA stability at different growth stages by monitoring RNA abundance in the presence and absence of Lsr2 using RT-qPCR and Northern blotting. After identifying the effect of Lsr2 on any small RNA of interest, we could further determine the expression of products that are transcribed from or controlled by Lsr2-interacting mRNA or ncRNA, respectively. This work has the potential to uncover novel regulatory activities for Lsr2.

In addition to probing the RNA-binding activity of Lsr2, we are interested in investigating possible interactions between Lsr2 and bacteriophage. Bacteria encode multiple phage defense mechanisms, including CRISPR-Cas systems, restriction-modification systems, and xenogeneic gene silencing by nucleoid-associated proteins (e.g. H-NS, MvaT/MvaU and Lsr2) (Pfeifer et al., 2019; Labrie et al., 2010; Dupuis et al., 2013; Singh et al., 2016; Duan et al., 2021). In *Shewanella oneidensis*, the CP4So prophage integrates at the 3′ end of a transfer-messenger RNA (tmRNA)-encoding gene and disrupts its function. Under conditions of heat stress, H-NS represses the expression of the phage excisionase gene *alpA* to inhibit activation of the CP4So prophage; when the temperature decreases, H-NS repression on *alpA* is relieved, allowing simultaneous excision of CP4So and restoration of tmRNA gene integrity (Zeng et al., 2016). Similarly, in *Pseudomonas aeruginosa,* MvaT and MvaU inhibit the production of Pf4 phage by directly binding and repressing the expression of excisionase XisF4 (Li et al., 2019). In *S. venezuelae,* previous work in our lab showed that ~10% of the genes whose expression were altered by Lsr2 are phage-related (Gehrke et al., 2019). Interactions between Lsr2-like protein and phage genomes have also been reported in *Corynebacterium glutamicum.* In this system, CgpS is a novel Lsr2-like protein encoded by the CGP3 prophage. Like other Lsr2-like proteins, it preferentially binds AT-rich regions on the CGP3 genome, and in this case it serves to repress gene expression and maintain the phage lysogenic life cycle (Pfeifer et al., 2016; Wiechert et al., 2020a). In addition to regulating prophage gene expression, CgpS also represses the expression of genes encoding restriction-modification systems that had been acquired through horizontal gene transfer, ultimately interfering with host defense against phage infection (Pfeifer et al., 2016; Jeltsch and Pingoud, 1996; Khan et al., 2010). Further bioinformatics analyses revealed that Lsr2-like protein are widespread in ~35% *Streptomyces* phages (Sharma et al., 2021; Wiechert et al., 2020a). These data suggest the potential for interesting but under-studied regulatory interactions in *Streptomyces*, between host-encoded and phage-encoded Lsr2 proteins. Additionally, studies have shown that the repressive effects of H-NS and MvaT can be counter-silenced by phage-encoded proteins (reviewed in **Chapter 1**; Wagemans et al., 2015; Patterson-West et al., 2021). Therefore, it will be interesting to probe the interplay between host- and phage-encoded Lsr2 proteins in regulating gene expression of prophage and their *Streptomyces* hosts.

5.2.2 Defining the regulation of *lsr2*

In Chapter 3, we identified potential regulators impacting *lsr2* expression by performing plasmid pulldown experiments. We identified three proteins, SVEN_4453 (BldM), SVEN_3078 (a XRE family regulator) and SVEN_4914 (Crp family transcription regulator), that are of particular interest as they may impact *lsr2* expression by directly binding the *lsr2* promoter. BldM is an orphaned response regulator that exerts its regulatory activity by forming a homodimer and binding to a 16 bp palindromic

consensus sequence (5′-TCACcCgnncGgGTGA-3′), or forming a heterodimer with WhiI and associating with a non-palindromic sequence (5′-TGnnCCGnnCGGGTGA-3′) (Molle and Buttner, 2000; Al-Bassam et al., 2014). As the first step towards understanding a possible regulatory role for BldM in controlling *lsr2* expression, we analyzed the *lsr2* promoter and coding sequences, and identified a potential BldM-WhiI binding site within the *lsr2* promoter region, which overlaps with an experimentally validated Lsr2 binding site. It is worth noting that *lsr2* was not identified as a BldM binding target from ChIP-seq experiments (Al-Bassam et al., 2014); however, this could be a result of different protocols being employed (ChIP-seq versus plasmid pulldown) (discussed in **Chapter 3 – 3.3 Discussion**). To experimentally test the binding of BldM, possibly with WhiI, to the *lsr2* promoter, we will perform EMSAs using PCR amplified sequences within *lsr2,* and co-overexpressed and -purified BldM+WhiI (and BldM on its own). If our results support an interaction between *lsr2* and BldM+WhiI (or BldM), we will investigate the impact of BldM on *lsr2* transcription levels by performing RT-qPCR in wild type and *bldM* mutant strains.

Compared to BldM, less is known about SVEN_3078 (a XRE family regulator) and SVEN_4914 (Crp family transcription regulator) (both regulators are conserved amongst a number of streptomycetes). Therefore, we will first test direct binding of SVEN_3078 and SVEN_4914 to *lsr2* by performing EMSAs using PCR amplified sequences within *lsr2* and purified SVEN_3078 and SVEN_4914 proteins. After confirming the interactions between *lsr2* and these two proteins, we would then perform genetic experiments as described above for BldM to assess regulatory roles of SVEN_3078 and SVEN_4914 in *lsr2* expression. If we could establish regulatory effects of these two proteins on *lsr2,* we will perform antibiotic assays and LC-MS analyses to assess specialized metabolism changes in *sven_3078* and *sven_4914* mutant and overexpression strains, and this will allow us to further probe how these two proteins impact specialized metabolism, both generally and through their putative control of *lsr2* in *Streptomyces.*

5.2.3 Investigating LsrL activity and the interaction between Lsr2 and LsrL

LsrL is a Lsr2 paralogue encoded by all *Streptomyces* bacteria, and Lsr2 and LsrL typically share 60% - 65% similarity and ~50% end-to-end protein identity (Gehrke et al., 2019). However, despite the similarities between the two proteins, Lsr2 has been studied for its global repression of biosynthetic clusters, whereas little work has been done on LsrL. Previous studies have revealed that deleting *lsrL* alone did not cause dramatic changes in either development or specialized metabolic profiles compared to wild type (Gehrke et al., 2019). However, it is worth noting that only a limited number of phenotypes have been tested for the *lsrL* mutant strain (Gehrke et al., 2019). In *E. coli*, StpA is a H-NS paralogue that can interact with H-NS to form heterodimers and regulate H-NS activity (Amit et al., 2003; Muller et al., 2006). Previous studies have shown that deleting *stpA* alone does not have an obvious phenotype compared to wild type, but *hns*

and *stpA* double mutant strain shows different metabolic profile compared to Δ*hns* and Δ*stpA*. Furthermore, one of the roles of StpA is to compensate for H-NS loss (Sonden and Uhlin, 1996; Dorman, 2014). Therefore, we are interested in deciphering the regulatory role of LsrL and the interaction between Lsr2 and LsrL in controlling gene expression in *Streptomyces*.

By performing a variety of protein-protein interaction assays, we found that Lsr2 and LsrL interact directly with each other, suggesting Lsr2 and LsrL could form hetero-oligomers. Our *in vitro* studies revealed that Lsr2 and LsrL could bind the same DNA probes with different affinities, and more interestingly, in distinct manners (**Chapter 3**). We have previously optimized and performed atomic force microscopy (AFM) experiments to investigate the structural effects of Lsr2 binding to target DNA sequences (**Chapter 2**) (Zhang et al., 2021). In order to better understand the distinct DNA-binding characteristics of Lsr2 and LsrL, we will perform AFM to visualize how Lsr2 and LsrL interact with DNA using purified proteins, and PCR amplified target DNA probes.

Additionally, we will also investigate the regulatory function of Lsr2-LsrL *in vivo*, and how Lsr2 and LsrL impact the other protein in binding to its associated binding sites. We will identify Lsr2 and LsrL binding sites across the *S. venezuelae* chromosome in the presence and absence of the other protein. We have previously performed ChIP-seq identifying Lsr2-associated proteins (Gehrke et al., 2019); we will perform ChIP-seq to identify i) LsrL binding sites in the presence of Lsr2, ii) LsrL binding sites in the absence of Lsr2, and iii) Lsr2 binding sites in the absence of LsrL. We will also perform RNA-seq on *lsrL* mutant and *lsr2/lsrL* double mutant strains and compare these data to the RNA-seq data for the *lsr2* mutant strain that we had obtained previously (Gehrke et al., 2019). These proposed investigations will provide information on how LsrL interacts with DNA and how the interplay between Lsr2 and LsrL impact gene expression in *Streptomyces.*

5.2.4 Stimulating the expression of silent biosynthetic clusters

5.2.4.1 Establishing regulatory occupancy across S. venezuelae chromosome

Multiple approaches have been applied to stimulate specialized metabolic in *Streptomyces,* including manipulating metabolic regulators, heterologously expressing biosynthetic clusters in chassis strains, applying elicitors, altering nutrient environments, and co-culturing with other species (Nai and Meyer, 2018; Gao et al., 2012; Gehrke et al., 2019; Myronovskyi et al., 2018; Xu et al., 2019). Despite these efforts, many silent clusters are not induced by these techniques. To understand how specialized metabolic clusters are controlled more broadly, we performed IPOD-HR experiments using both *S. venezuelae* wild type and *lsr2* mutant strains, in order to map regulatory protein occupancy in the presence and absence of Lsr2 (described in **Chapter 4**). Our IPOD-HR data are currently being analyzed. We intend to couple these experiments with plasmid

pulldown experiments, to specifically identify regulatory proteins bound at sites identified in our IPOD-HR experiments (discussed in **Chapter 4**). IPOD-HR and plasmid pulldown experiments will allow us to establish the regulatory networks governing the expression of biosynthetic clusters in *S. venezuelae* and provide key information on the control of biosynthetic clusters more generally.

5.2.4.2 Developing strategies to induce the expression of biosynthetic clusters

After defining the regulators of each biosynthetic cluster in *S. venezuelae* using our combined IPOD-HR - plasmid pulldown strategy, we will first categorize the identified regulators based on protein domain annotation and the incidence of pulling out one regulator from multiple clusters. This information will allow us to divide regulators into three groups: pathway-specific regulators, globally-acting regulators and uncharacterized regulators. For pathway-specific regulators, we will focus on the ones that are poorly characterized and/or are associated with clusters that are silent and not impacted by Lsr2. To probe how these regulators control the expression of their respective biosynthetic clusters, we will i) determine their binding sites by performing EMSAs using purified proteins and PCR amplified promoter regions within the biosynthetic clusters, and ii) understand how they affect the production of specialized metabolites by performing LC-MS analyses using strains with the regulator deleted and overexpressed, alongside the wild type strain for comparison. Based on protein conservation, globally-acting regulators can be further divided into two subgroups: species-specific global regulators, and regulators that are conserved throughout the streptomycetes. Our focus for future experiments will be on previously uncharacterized global regulators. To investigate the activity of these global regulators, we will monitor metabolism changes in response to deletion and overexpression of the global regulator of interest, and employ ChIP-seq to identify their binding sites across the chromosome. Uncharacterized regulators will be studied using the same approaches as we have used for global regulators (e.g. Crp, Lsr2). Once we have established the appropriate experimental pipeline in *S. venezuelae*, we will apply the same experiments pipeline (IPOD-HR – plasmid pulldown – genetic approaches to study regulators of interest) to other *Streptomyces* species. The work described here will provide insights into regulatory roles of poorly characterized regulators and their consensus/preference binding sequences, and we aim to combine these data with previously reported regulatory networks in *Streptomyces* to establish a comprehensive database that contains information on classes of regulators (pathway-specific and global) that control specialized metabolism, their potential regulatory functions, and their associated binding sequences. This database could serve as a tool for regulator-binding site predictions that allows researchers to identify potential repressors and activators of a metabolic pathway by analyzing DNA sequences within the biosynthetic gene cluster, and the information obtained from this database will provide guidance for developing genetic approaches aimed at stimulating expression of a biosynthetic cluster of interest in any *Streptomyces* species by manipulating specific regulators.

REFERENCES

Adams, D. W., and Errington, J. (2009). Bacterial cell division: assembly, maintenance and disassembly of the Z ring. *Nat Rev Microbiol, 7*(9), 642-653. doi:10.1038/nrmicro2198

Aigle, B., Lautru, S., Spiteller, D., Dickschat, J. S., Challis, G. L., Leblond, P., et al. (2014). Genome mining of *Streptomyces ambofaciens*. *J Ind Microbiol Biotechnol, 41*(2), 251-263. doi:10.1007/s10295-013-1379-y

Al-Bassam, M. M., Bibb, M. J., Bush, M. J., Chandra, G., and Buttner, M. J. (2014). Response regulator heterodimer formation controls a key stage in *Streptomyces* development. *PLoS Genet, 10*(8), e1004554. doi:10.1371/journal.pgen.1004554

Ali, S. S., Beckett, E., Bae, S. J., and Navarre, W. W. (2011). The 5.5 protein of phage T7 inhibits H-NS through interactions with the central oligomerization domain. *J Bacteriol, 193*(18), 4881-4892. doi:10.1128/JB.05198-11

Ali, S. S., Whitney, J. C., Stevenson, J., Robinson, H., Howell, P. L., and Navarre, W. W. (2013). Structural insights into the regulation of foreign genes in *Salmonella* by the Hha/H-NS complex. *J Biol Chem, 288*(19), 13356-13369. doi:10.1074/jbc.M113.455378

Allfrey, V. G., Faulkner, R., and Mirsky, A. E. (1964). Acetylation and methylation of histones and their possible role in the regulation of RNA synthesis. *Proc Natl Acad Sci U S A, 51*, 786-794. doi:10.1073/pnas.51.5.786

Alqaseer, K., Turapov, O., Barthe, P., Jagatia, H., De Visch, A., Roumestand, C., et al. (2019). Protein kinase B controls *Mycobacterium tuberculosis* growth via phosphorylation of the transcriptional regulator Lsr2 at threonine 112. *Mol Microbiol, 112*(6), 1847-1862. doi:10.1111/mmi.14398

Alva, V., Ammelburg, M., Soding, J., and Lupas, A. N. (2007). On the origin of the histone fold. *BMC Struct Biol, 7*, 17. doi:10.1186/1472-6807-7-17

Amemiya, H. M., Goss, T. J., Nye, T. M., Hurto, R. L., Simmons, L. A., and Freddolino, P. L. (2022). Distinct heterochromatin-like domains promote transcriptional memory and silence parasitic genetic elements in bacteria. *EMBO J, 41*(3), e108708. doi:10.15252/embj.2021108708

Amit, R., Oppenheim, A. B., and Stavans, J. (2003). Increased bending rigidity of single DNA molecules by H-NS, a temperature and osmolarity sensor. *Biophys J, 84*(4), 2467-2473. doi:10.1016/S0006-3495(03)75051-6

Andres, S. N., Li, Z. M., Erie, D. A., and Williams, R. S. (2019). Ctp1 protein-DNA filaments promote DNA bridging and DNA double-strand break repair. *J Biol Chem, 294*(9), 3312-3320. doi:10.1074/jbc.RA118.006759

Arold, S. T., Leonard, P. G., Parkinson, G. N., and Ladbury, J. E. (2010). H-NS forms a superhelical protein scaffold for DNA condensation. *Proc Natl Acad Sci U S A, 107*(36), 15728-15732. doi:10.1073/pnas.1006966107

Ayer, S. W., McInnes, A. G., Thibault, P., Walter, J. A., Doull, J. L., Parnell, T., et al. (1991). Jadomycin, a novel 8H-benz[b]oxazolo[3,2-f]phenanthridine antibiotic from from *Streptomyces venezuelae* ISP5230. *Tetrahedron Letters, 32*(44), 6301-6304. doi:https://doi.org/10.1016/0040-4039(91)80152-V

Badrinarayanan, A., Le, T. B., and Laub, M. T. (2015). Bacterial chromosome organization and segregation. *Annu Rev Cell Dev Biol, 31*, 171-199. doi:10.1146/annurev-cellbio-100814-125211

Balandina, A., Claret, L., Hengge-Aronis, R., and Rouviere-Yaniv, J. (2001). The *Escherichia coli* histone-like protein HU regulates *rpoS* translation. *Mol Microbiol, 39*(4), 1069-1079. doi:10.1046/j.1365-2958.2001.02305.x

Bannister, A. J., and Kouzarides, T. (2011). Regulation of chromatin by histone modifications. *Cell Res, 21*(3), 381-395. doi:10.1038/cr.2011.22

Banos, R. C., Vivero, A., Aznar, S., Garcia, J., Pons, M., Madrid, C., et al. (2009). Differential regulation of horizontally acquired and core genome genes by the bacterial modulator H-NS. *PLoS Genet, 5*(6), e1000513. doi:10.1371/journal.pgen.1000513

Barka, E. A., Vatsa, P., Sanchez, L., Gaveau-Vaillant, N., Jacquard, C., Meier-Kolthoff, J. P., et al. (2016). Taxonomy, physiology, and natural products of Actinobacteria. *Microbiol Mol Biol Rev, 80*(1), 1-43. doi:10.1128/MMBR.00019-15

Bartek, I. L., Woolhiser, L. K., Baughn, A. D., Basaraba, R. J., Jacobs, W. R., Jr., Lenaerts, A. J., et al. (2014). *Mycobacterium tuberculosis* Lsr2 is a global transcriptional regulator required for adaptation to changing oxygen levels and virulence. *mBio, 5*(3), e01106-01114. doi:10.1128/mBio.01106-14

Battesti, A., and Bouveret, E. (2012). The bacterial two-hybrid system based on adenylate cyclase reconstitution in *Escherichia coli. Methods, 58*(4), 325-334. doi:10.1016/j.ymeth.2012.07.018

Bdira, F. B., Erkelens, A. M., Qin, L., Volkov, A. N., Lippa, A. M., Bowring, N., et al. (2021). Novel anti-repression mechanism of H-NS proteins by a phage protein. *Nucleic Acids Res, 49*(18), 10770-10784. doi:10.1093/nar/gkab793

Beggs, G. A., Brennan, R. G., and Arshad, M. (2020). MarR family proteins are important regulators of clinically relevant antibiotic resistance. *Protein Sci, 29*(3), 647-653. doi:10.1002/pro.3769

Belknap, K. C., Park, C. J., Barth, B. M., and Andam, C. P. (2020). Genome mining of biosynthetic and chemotherapeutic gene clusters in *Streptomyces* bacteria. *Sci Rep, 10*(1), 2003. doi:10.1038/s41598-020-58904-9

Bellanger, X., Payot, S., Leblond-Bourget, N., and Guedon, G. (2014). Conjugative and mobilizable genomic islands in bacteria: evolution and diversity. *FEMS Microbiol Rev, 38*(4), 720-760. doi:10.1111/1574-6976.12058

Beloin, C., and Dorman, C. J. (2003). An extended role for the nucleoid structuring protein H-NS in the virulence gene regulatory cascade of *Shigella flexneri*. *Mol Microbiol, 47*(3), 825-838. doi:10.1046/j.1365-2958.2003.03347.x

Bentley, S. D., Chater, K. F., Cerdeno-Tarraga, A. M., Challis, G. L., Thomson, N. R., James, K. D., et al. (2002). Complete genome sequence of the model actinomycete *Streptomyces coelicolor* A3(2). *Nature, 417*(6885), 141-147. doi:10.1038/417141a

Bibb, M. (1996). The regulation of antibiotic production in *Streptomyces coelicolor* A3(2). *Microbiology, 142*(6), 1335-1344. doi:https://doi.org/10.1099/13500872-142-6-1335

Bibb, M. J. (2005). Regulation of secondary metabolism in streptomycetes. *Curr Opin Microbiol, 8*(2), 208-215. doi:10.1016/j.mib.2005.02.016

Bibb, M. J., and Buttner, M. J. (2003). The *Streptomyces coelicolor* developmental transcription factor sigma^{BldN} is synthesized as a proprotein. *J Bacteriol, 185*(7), 2338-2345. doi:10.1128/JB.185.7.2338-2345.2003

Blin, K., Shaw, S., Kloosterman, A. M., Charlop-Powers, Z., van Wezel, G. P., Medema, Marnix H., et al. (2021). antiSMASH 6.0: improving cluster detection and comparison capabilities. *Nucleic Acids Research, 49*(W1), W29-W35. doi:10.1093/nar/gkab335

Bloch, V., Yang, Y., Margeat, E., Chavanieu, A., Auge, M. T., Robert, B., et al. (2003). The H-NS dimerization domain defines a new fold contributing to DNA recognition. *Nat Struct Biol, 10*(3), 212-218. doi:10.1038/nsb904

Bobek, J., Smidova, K., and Cihak, M. (2017). A Waking Review: Old and Novel Insights into the Spore Germination in *Streptomyces*. *Front Microbiol, 8*, 2205. doi:10.3389/fmicb.2017.02205

Boudreau, B. A., Hron, D. R., Qin, L., van der Valk, R. A., Kotlajich, M. V., Dame, R. T., et al. (2018). StpA and Hha stimulate pausing by RNA polymerase by promoting DNA-DNA bridging of H-NS filaments. *Nucleic Acids Res, 46*(11), 5525-5546. doi:10.1093/nar/gky265

Bouffartigues, E., Buckle, M., Badaut, C., Travers, A., and Rimsky, S. (2007). H-NS cooperative binding to high-affinity sites in a regulatory element results in transcriptional silencing. *Nat Struct Mol Biol, 14*(5), 441-448. doi:10.1038/nsmb1233

Bowman, A., Lercher, L., Singh, H. R., Zinne, D., Timinszky, G., Carlomagno, T., et al. (2016). The histone chaperone sNASP binds a conserved peptide motif within the globular core of histone H3 through its TPR repeats. *Nucleic Acids Res, 44*(7), 3105-3117. doi:10.1093/nar/gkv1372

Brautaset, T., Lale, R., and Valla, S. (2009). Positively regulated bacterial expression systems. *Microb Biotechnol, 2*(1), 15-30. doi:10.1111/j.1751-7915.2008.00048.x

Brescia, C. C., Kaw, M. K., and Sledjeski, D. D. (2004). The DNA binding protein H-NS binds to and alters the stability of RNA *in vitro* and *in vivo*. *J Mol Biol, 339*(3), 505-514. doi:10.1016/j.jmb.2004.03.067

Browning, D. F., and Busby, S. J. (2004). The regulation of bacterial transcription initiation. *Nat Rev Microbiol, 2*(1), 57-65. doi:10.1038/nrmicro787

Browning, D. F., Grainger, D. C., and Busby, S. J. (2010). Effects of nucleoid-associated proteins on bacterial chromosome structure and gene expression. *Curr Opin Microbiol, 13*(6), 773-780. doi:10.1016/j.mib.2010.09.013

Bush, M. J., Bibb, M. J., Chandra, G., Findlay, K. C., and Buttner, M. J. (2013). Genes required for aerial growth, cell division, and chromosome segregation are targets of WhiA before sporulation in *Streptomyces venezuelae*. *mBio, 4*(5), e00684-00613. doi:10.1128/mBio.00684-13

Bush, M. J., Gallagher, K. A., Chandra, G., Findlay, K. C., and Schlimpert, S. (2022). Hyphal compartmentalization and sporulation in *Streptomyces* require the conserved cell division protein SepX. *Nat Commun, 13*(1), 71. doi:10.1038/s41467-021-27638-1

Campbell, E. A., Korzheva, N., Mustaev, A., Murakami, K., Nair, S., Goldfarb, A., et al. (2001). Structural mechanism for rifampicin inhibition of bacterial RNA polymerase. *Cell, 104*(6), 901-912. doi:10.1016/s0092-8674(01)00286-0

Cannavo, E., Johnson, D., Andres, S. N., Kissling, V. M., Reinert, J. K., Garcia, V., et al. (2018). Regulatory control of DNA end resection by Sae2 phosphorylation. *Nat Commun, 9*(1), 4016. doi:10.1038/s41467-018-06417-5

Capstick, D. S., Willey, J. M., Buttner, M. J., and Elliot, M. A. (2007). SapB and the chaplins: connections between morphogenetic proteins in *Streptomyces coelicolor. Mol Microbiol, 64*(3), 602-613. doi:10.1111/j.1365-2958.2007.05674.x

Carter, H. E., Gottlieb, D., and Anderson, H. W. (1948). Chloromycetin and streptothricin. *Science, 107*(2770), 113. doi:10.1126/science.107.2770.113-b

Carter, M. Q., Chen, J., and Lory, S. (2010). The *Pseudomonas aeruginosa* pathogenicity island PAPI-1 is transferred via a novel type IV pilus. *J Bacteriol, 192*(13), 3249-3258. doi:10.1128/JB.00041-10

Castang, S., and Dove, S. L. (2010). High-order oligomerization is required for the function of the H-NS family member MvaT in *Pseudomonas aeruginosa. Mol Microbiol, 78*(4), 916-931. doi:10.1111/j.1365-2958.2010.07378.x

Castang, S., McManus, H. R., Turner, K. H., and Dove, S. L. (2008). H-NS family members function coordinately in an opportunistic pathogen. *Proc Natl Acad Sci U S A, 105*(48), 18947-18952. doi:10.1073/pnas.0808215105

Challis, G. L., and Hopwood, D. A. (2003). Synergy and contingency as driving forces for the evolution of multiple secondary metabolite production by *Streptomyces* species. *Proc Natl Acad Sci U S A, 100 Suppl 2*, 14555-14561. doi:10.1073/pnas.1934677100

Chaparian, R. R., Tran, M. L. N., Miller Conrad, L. C., Rusch, D. B., and van Kessel, J. C. (2020). Global H-NS counter-silencing by LuxR activates quorum sensing gene expression. *Nucleic Acids Res, 48*(1), 171-183. doi:10.1093/nar/gkz1089

Chater, K. F. (2001). Regulation of sporulation in *Streptomyces coelicolor* A3(2): a checkpoint multiplex? *Curr Opin Microbiol, 4*(6), 667-673. doi:10.1016/s1369-5274(01)00267-3

Chen, H., Shiroguchi, K., Ge, H., and Xie, X. S. (2015). Genome-wide study of mRNA degradation and transcript elongation in *Escherichia coli. Mol Syst Biol, 11*(5), 808. doi:10.15252/msb.20159000

Chen, J. M., Ren, H., Shaw, J. E., Wang, Y. J., Li, M., Leung, A. S., et al. (2008). Lsr2 of *Mycobacterium tuberculosis* is a DNA-bridging protein. *Nucleic Acids Res, 36*(7), 2123-2135. doi:10.1093/nar/gkm1162

Chen, X., Zaro, J. L., and Shen, W. C. (2013). Fusion protein linkers: property, design and functionality. *Adv Drug Deliv Rev, 65*(10), 1357-1369. doi:10.1016/j.addr.2012.09.039

Choi, J., and Groisman, E. A. (2020). *Salmonella* expresses foreign genes during infection by degrading their silencer. *Proc Natl Acad Sci U S A, 117*(14), 8074-8082. doi:10.1073/pnas.1912808117

Chong, P. P., Podmore, S. M., Kieser, H. M., Redenbach, M., Turgay, K., Marahiel, M., et al. (1998). Physical identification of a chromosomal locus encoding biosynthetic genes for the lipopeptide calcium-dependent antibiotic (CDA) of *Streptomyces coelicolor* A3(2). *Microbiology (Reading), 144 (Pt 1)*, 193-199. doi:10.1099/00221287-144-1-193

Choulet, F., Aigle, B., Gallois, A., Mangenot, S., Gerbaud, C., Truong, C., et al. (2006). Evolution of the terminal regions of the *Streptomyces* linear chromosome. *Mol Biol Evol, 23*(12), 2361-2369. doi:10.1093/molbev/msl108

Chubukov, V., Gerosa, L., Kochanowski, K., and Sauer, U. (2014). Coordination of microbial metabolism. *Nat Rev Microbiol, 12*(5), 327-340. doi:10.1038/nrmicro3238

Claessen, D., Rink, R., de Jong, W., Siebring, J., de Vreugd, P., Boersma, F. G., et al. (2003). A novel class of secreted hydrophobic proteins is involved in aerial hyphae formation in *Streptomyces coelicolor* by forming amyloid-like fibrils. *Genes Dev, 17*(14), 1714-1726. doi:10.1101/gad.264303

Claret, L., and Rouviere-Yaniv, J. (1996). Regulation of HU alpha and HU beta by CRP and FIS in *Escherichia coli. J Mol Biol, 263*(2), 126-139. doi:10.1006/jmbi.1996.0564

Craney, A., Ozimok, C., Pimentel-Elardo, S. M., Capretta, A., and Nodwell, J. R. (2012). Chemical perturbation of secondary metabolism demonstrates important links to primary metabolism. *Chem Biol, 19*(8), 1020-1027. doi:10.1016/j.chembiol.2012.06.013

Cuthbertson, L., and Nodwell, J. R. (2013). The TetR family of regulators. *Microbiol Mol Biol Rev, 77*(3), 440-475. doi:10.1128/MMBR.00018-13

Dame, R. T., Wyman, C., Wurm, R., Wagner, R., and Goosen, N. (2002). Structural basis for H-NS-mediated trapping of RNA polymerase in the open initiation complex at the *rrnB* P1. *J Biol Chem, 277*(3), 2146-2150. doi:10.1074/jbc.C100603200

Dangla-Pelissier, G., Roux, N., Schmidt, V., Chambonnier, G., Ba, M., Sebban-Kreuzer, C., et al. (2021). The horizontal transfer of *Pseudomonas aeruginosa* PA14 ICE PAPI-1 is controlled by a transcriptional triad between TprA, NdpA2 and MvaT. *Nucleic Acids Res, 49*(19), 10956-10974. doi:10.1093/nar/gkab827

Daniel-Ivad, M., Hameed, N., Tan, S., Dhanjal, R., Socko, D., Pak, P., et al. (2017). An engineered allele of *afsQ1* facilitates the discovery and investigation of cryptic natural products. *ACS Chem Biol, 12*(3), 628-634. doi:10.1021/acschembio.6b01002

Datta, C., Jha, R. K., Ahmed, W., Ganguly, S., Ghosh, S., and Nagaraja, V. (2019). Physical and functional interaction between nucleoid-associated proteins HU and Lsr2 of *Mycobacterium tuberculosis*: altered DNA binding and gene regulation. *Mol Microbiol, 111*(4), 981-994. doi:10.1111/mmi.14202

Davies, J. (2006). Are antibiotics naturally antibiotics? *J Ind Microbiol Biotechnol, 33*(7), 496-499. doi:10.1007/s10295-006-0112-5

Davies, J. (2013). Specialized microbial metabolites: functions and origins. *J Antibiot (Tokyo), 66*(7), 361-364. doi:10.1038/ja.2013.61

Dawson, M. A., Foster, S. D., Bannister, A. J., Robson, S. C., Hannah, R., Wang, X., et al. (2012). Three distinct patterns of histone H3Y41 phosphorylation mark active genes. *Cell Rep, 2*(3), 470-477. doi:10.1016/j.celrep.2012.08.016

den Hengst, C. D., Tran, N. T., Bibb, M. J., Chandra, G., Leskiw, B. K., and Buttner, M. J. (2010). Genes essential for morphological development and antibiotic production in *Streptomyces coelicolor* are targets of BldD during vegetative growth. *Mol Microbiol, 78*(2), 361-379. doi:10.1111/j.1365-2958.2010.07338.x

Dilip, C. V., Mulaje, S., and Mohalkar, R. (2013). A review on actinomycetes and their biotechnological application. *International Journal of pharmaceutical sciences and research, 4*(5), 1730.

Dillon, S. C., and Dorman, C. J. (2010). Bacterial nucleoid-associated proteins, nucleoid structure and gene expression. *Nat Rev Microbiol, 8*(3), 185-195. doi:10.1038/nrmicro2261

Dilweg, I. W., and Dame, R. T. (2018). Post-translational modification of nucleoid-associated proteins: an extra layer of functional modulation in bacteria? *Biochem Soc Trans, 46*(5), 1381-1392. doi:10.1042/BST20180488

Ding, P., McFarland, K. A., Jin, S., Tong, G., Duan, B., Yang, A., et al. (2015). A novel AT-rich DNA recognition mechanism for bacterial xenogeneic silencer MvaT. *PLoS Pathog, 11*(6), e1004967. doi:10.1371/journal.ppat.1004967

Dorman, C. J. (2014). Function of nucleoid-associated proteins in chromosome structuring and transcriptional regulation. *J Mol Microbiol Biotechnol, 24*(5-6), 316-331. doi:10.1159/000368850

Doroghazi, J. R., and Metcalf, W. W. (2013). Comparative genomics of actinomycetes with a focus on natural product biosynthetic genes. *BMC Genomics, 14*, 611. doi:10.1186/1471-2164-14-611

Duan, B., Ding, P., Navarre, W. W., Liu, J., and Xia, B. (2021). Xenogeneic silencing and bacterial genome evolution: mechanisms for DNA recognition imply multifaceted roles of xenogeneic silencers. *Mol Biol Evol, 38*(10), 4135-4148. doi:10.1093/molbev/msab136

Dupuis, M. E., Villion, M., Magadan, A. H., and Moineau, S. (2013). CRISPR-Cas and restriction-modification systems are compatible and increase phage resistance. *Nat Commun, 4*, 2087. doi:10.1038/ncomms3087

Ehrlich, J., Bartz, Q. R., Smith, R. M., Joslyn, D. A., and Burkholder, P. R. (1947). Chloromycetin, a new antibiotic from a soil actinomycete. *Science, 106*(2757), 417. doi:10.1126/science.106.2757.417

Elliot, M. A., Bibb, M. J., Buttner, M. J., and Leskiw, B. K. (2001). BldD is a direct regulator of key developmental genes in *Streptomyces coelicolor* A3(2). *Mol Microbiol, 40*(1), 257-269. doi:10.1046/j.1365-2958.2001.02387.x

Elliot, M. A., Karoonuthaisiri, N., Huang, J., Bibb, M. J., Cohen, S. N., Kao, C. M., et al. (2003a). The chaplins: a family of hydrophobic cell-surface proteins involved in aerial mycelium formation in *Streptomyces coelicolor*. *Genes Dev, 17*(14), 1727-1740. doi:10.1101/gad.264403

Elliot, M. A., and Leskiw, B. K. (1999). The BldD protein from *Streptomyces coelicolor i*s a DNA-binding protein. *J Bacteriol, 181*(21), 6832-6835. doi:10.1128/JB.181.21.6832-6835.1999

Elliot, M. A., Locke, T. R., Galibois, C. M., and Leskiw, B. K. (2003b). BldD from *Streptomyces coelicolor* is a non-essential global regulator that binds its own promoter as a dimer. *FEMS Microbiol Lett, 225*(1), 35-40. doi:10.1016/S0378-1097(03)00474-9

Engel, F., Ossipova, E., Jakobsson, P. J., Vockenhuber, M. P., and Suess, B. (2019). sRNA scr5239 involved in feedback loop regulation of *Streptomyces coelicolor* central metabolism. *Front Microbiol, 10*, 3121. doi:10.3389/fmicb.2019.03121

Fang, F. C., and Rimsky, S. (2008). New insights into transcriptional regulation by H-NS. *Curr Opin Microbiol, 11*(2), 113-120. doi:10.1016/j.mib.2008.02.011

Fernandez-Martinez, L. T., Borsetto, C., Gomez-Escribano, J. P., Bibb, M. J., Al-Bassam, M. M., Chandra, G., et al. (2014). New insights into chloramphenicol biosynthesis in *Streptomyces venezuelae* ATCC 10712. *Antimicrob Agents Chemother, 58*(12), 7441-7450. doi:10.1128/AAC.04272-14

Fillenberg, S. B., Friess, M. D., Korner, S., Bockmann, R. A., and Muller, Y. A. (2016). Crystal structures of the global regulator DasR from *Streptomyces coelicolor*: implications for the allosteric regulation of GntR/HutC repressors. *PLoS One, 11*(6), e0157691. doi:10.1371/journal.pone.0157691

Finn, R. D., Tate, J., Mistry, J., Coggill, P. C., Sammut, S. J., Hotz, H. R., et al. (2008). The Pfam protein families database. *Nucleic Acids Res, 36* (Database issue), D281-288. doi:10.1093/nar/gkm960

Flardh, K. (2003). Essential role of DivIVA in polar growth and morphogenesis in *Streptomyces coelicolor* A3(2). *Mol Microbiol, 49*(6), 1523-1536. doi:10.1046/j.1365-2958.2003.03660.x

Flardh, K., and Buttner, M. J. (2009). *Streptomyces* morphogenetics: dissecting differentiation in a filamentous bacterium. *Nat Rev Microbiol, 7*(1), 36-49. doi:10.1038/nrmicro1968

Flores-Rios, R., Quatrini, R., and Loyola, A. (2019). Endogenous and foreign nucleoid-associated proteins of bacteria: occurrence, interactions and effects on mobile genetic elements and host's Biology. *Comput Struct Biotechnol J, 17*, 746-756. doi:10.1016/j.csbj.2019.06.010

Freddolino, P. L., Amemiya, H. M., Goss, T. J., and Tavazoie, S. (2021). Dynamic landscape of protein occupancy across the *Escherichia coli* chromosome. *PLoS Biol, 19*(6), e3001306. doi:10.1371/journal.pbio.3001306

Galagan, J. E., Minch, K., Peterson, M., Lyubetskaya, A., Azizi, E., Sweet, L., et al. (2013). The *Mycobacterium tuberculosis* regulatory network and hypoxia. *Nature, 499*(7457), 178-183. doi:10.1038/nature12337

Gallagher, K. A., Schumacher, M. A., Bush, M. J., Bibb, M. J., Chandra, G., Holmes, N. A., et al. (2020). c-di-GMP arms an anti-sigma to control progression of multicellular differentiation in *Streptomyces. Mol Cell, 77*(3), 586-599 e586. doi:10.1016/j.molcel.2019.11.006

Gao, C., Hindra, Mulder, D., Yin, C., and Elliot, M. A. (2012). Crp is a global regulator of antibiotic production in *Streptomyces*. *mBio, 3*(6). doi:10.1128/mBio.00407-12

Gao, R., and Stock, A. M. (2013). Probing kinase and phosphatase activities of two-component systems in vivo with concentration-dependent phosphorylation profiling. *Proc Natl Acad Sci U S A, 110*(2), 672-677. doi:10.1073/pnas.1214587110

Gao, X., Zou, T., Mu, Z., Qin, B., Yang, J., Waltersperger, S., et al. (2013). Structural insights into VirB-DNA complexes reveal mechanism of transcriptional activation of virulence genes. *Nucleic Acids Res, 41*(22), 10529-10541. doi:10.1093/nar/gkt748

Gehrke, E. J., Zhang, X., Pimentel-Elardo, S. M., Johnson, A. R., Rees, C. A., Jones, S. E., et al. (2019). Silencing cryptic specialized metabolism in *Streptomyces* by the nucleoid-associated protein Lsr2. *Elife, 8*. doi:10.7554/eLife.47691

Glazebrook, M. A., Doull, J. L., Stuttard, C., and Vining, L. C. (1990). Sporulation of *Streptomyces venezuelae* in submerged cultures. *J Gen Microbiol, 136*(3), 581-588. doi:10.1099/00221287-136-3-581

Gomez-Escribano, J. P., Holmes, N. A., Schlimpert, S., Bibb, M. J., Chandra, G., Wilkinson, B., et al. (2021). *Streptomyces venezuelae* NRRL B-65442: genome sequence of a model strain used to study morphological differentiation in filamentous actinobacteria. *Journal of Industrial Microbiology and Biotechnology, 48*(9-10). doi:10.1093/jimb/kuab035

Gordon, B. R., Imperial, R., Wang, L., Navarre, W. W., and Liu, J. (2008). Lsr2 of *Mycobacterium* represents a novel class of H-NS-like proteins. *J Bacteriol, 190*(21), 7052-7059. doi:10.1128/JB.00733-08

Gordon, B. R., Li, Y., Cote, A., Weirauch, M. T., Ding, P., Hughes, T. R., et al. (2011). Structural basis for recognition of AT-rich DNA by unrelated xenogeneic silencing proteins. *Proc Natl Acad Sci U S A, 108*(26), 10690-10695. doi:10.1073/pnas.1102544108

Gordon, B. R., Li, Y., Wang, L., Sintsova, A., van Bakel, H., Tian, S., et al. (2010). Lsr2 is a nucleoid-associated protein that targets AT-rich sequences and virulence genes in *Mycobacterium tuberculosis*. *Proc Natl Acad Sci U S A, 107*(11), 5154-5159. doi:10.1073/pnas.0913551107

Gou, L., Han, T., Wang, X., Ge, J., Liu, W., Hu, F., et al. (2017). A novel TetR family transcriptional regulator, CalR3, negatively controls calcimycin biosynthesis in *Streptomyces chartreusis* NRRL 3882. *Front Microbiol, 8*, 2371. doi:10.3389/fmicb.2017.02371

Grawe, A., and Stein, V. (2021). Linker engineering in the context of synthetic protein switches and sensors. *Trends Biotechnol, 39*(7), 731-744. doi:10.1016/j.tibtech.2020.11.007

Gregory, M. A., Till, R., and Smith, M. C. (2003). Integration site for *Streptomyces* phage phiBT1 and development of site-specific integrating vectors. *J Bacteriol, 185*(17), 5320-5323. doi:10.1128/JB.185.17.5320-5323.2003

Guo, J., Zhang, X., Lu, X., Liu, W., Chen, Z., Li, J., et al. (2018). SAV4189, a MarR-family regulator in *Streptomyces avermitilis*, activates avermectin biosynthesis. *Front Microbiol, 9*, 1358. doi:10.3389/fmicb.2018.01358

Gust, B., Challis, G. L., Fowler, K., Kieser, T., and Chater, K. F. (2003). PCR-targeted *Streptomyces* gene replacement identifies a protein domain needed for biosynthesis of the sesquiterpene soil odor geosmin. *Proc Natl Acad Sci U S A, 100*(4), 1541-1546. doi:10.1073/pnas.0337542100

Guyet, A., Benaroudj, N., Proux, C., Gominet, M., Coppee, J. Y., and Mazodier, P. (2014). Identified members of the *Streptomyces lividans* AdpA regulon involved in differentiation and secondary metabolism. *BMC Microbiol, 14*, 81. doi:10.1186/1471-2180-14-81

Haider, S. R., Reid, H. J., and Sharp, B. L. (2012). Tricine-SDS-PAGE. *Methods Mol Biol, 869*, 81-91. doi:10.1007/978-1-61779-821-4_8

Hanahan, D. (1985). *Techniques for transformation of E. coli.* (Vol. 1). Oxford; Washington, DC: IRL Press.

Hansen, A. M., Chaerkady, R., Sharma, J., Diaz-Mejia, J. J., Tyagi, N., Renuse, S., et al. (2013). The *Escherichia coli* phosphotyrosine proteome relates to core pathways and virulence. *PLoS Pathog, 9*(6), e1003403. doi:10.1371/journal.ppat.1003403

Hardisson, C., Manzanal, M. B., Salas, J. A., and Suarez, J. E. (1978). Fine structure, physiology and biochemistry of arthrospore germination in *Streptomyces antibioticus*. *J Gen Microbiol, 105*(2), 203-214. doi:10.1099/00221287-105-2-203

Hempel, A. M., Cantlay, S., Molle, V., Wang, S. B., Naldrett, M. J., Parker, J. L., et al. (2012). The Ser/Thr protein kinase AfsK regulates polar growth and hyphal branching in

the filamentous bacteria *Streptomyces*. *Proc Natl Acad Sci U S A, 109*(35), E2371-2379. doi:10.1073/pnas.1207409109

Hindra, Moody, M. J., Jones, S. E., and Elliot, M. A. (2014). Complex intra-operonic dynamics mediated by a small RNA in *Streptomyces coelicolor*. *PLoS One, 9*(1), e85856. doi:10.1371/journal.pone.0085856

Ho, C. H., Wang, H. C., Ko, T. P., Chang, Y. C., and Wang, A. H. (2014). The T4 phage DNA mimic protein Arn inhibits the DNA binding activity of the bacterial histone-like protein H-NS. *J Biol Chem, 289*(39), 27046-27054. doi:10.1074/jbc.M114.590851

Holowka, J., and Zakrzewska-Czerwinska, J. (2020). Nucleoid associated proteins: the small organizers that help to cope with stress. *Front Microbiol, 11*, 590. doi:10.3389/fmicb.2020.00590

Hopwood, D. A., Chater, K. F., and Bibb, M. J. (1995). Genetics of antibiotic production in *Streptomyces coelicolor* A3(2), a model streptomycete. *Biotechnology, 28*, 65-102. doi:10.1016/b978-0-7506-9095-9.50009-5

Hoshino, S., Onaka, H., and Abe, I. (2019). Activation of silent biosynthetic pathways and discovery of novel secondary metabolites in actinomycetes by co-culture with mycolic acid-containing bacteria. *J Ind Microbiol Biotechnol, 46*(3-4), 363-374. doi:10.1007/s10295-018-2100-y

Hoskisson, P. A., and Rigali, S. (2009). Variation in form and function the helix-turn-helix regulators of the GntR superfamily. *Adv Appl Microbiol, 69*, 1-22. doi:10.1016/S0065-2164(09)69001-8

Hu, L., Kong, W., Yang, D., Han, Q., Guo, L., and Shi, Y. (2019). Threonine phosphorylation fine-tunes the regulatory activity of histone-like nucleoid structuring protein in *Salmonella* transcription. *Front Microbiol, 10*, 1515. doi:10.3389/fmicb.2019.01515

Huang, R., Liu, H., Zhao, W., Wang, S., Wang, S., Cai, J., et al. (2022). AdpA, a developmental regulator, promotes epsilon-poly-L-lysine biosynthesis in *Streptomyces albulus*. *Microb Cell Fact, 21*(1), 60. doi:10.1186/s12934-022-01785-6

Hutchings, M. I., Hong, H.-J., and Buttner, M. J. (2006). The vancomycin resistance VanRS two-component signal transduction system of *Streptomyces coelicolor*. *Molecular Microbiology, 59*(3), 923-935. doi:https://doi.org/10.1111/j.1365-2958.2005.04953.x

Ibarra, J. A., Perez-Rueda, E., Segovia, L., and Puente, J. L. (2008). The DNA-binding domain as a functional indicator: the case of the AraC/XylS family of transcription factors. *Genetica, 133*(1), 65-76. doi:10.1007/s10709-007-9185-y

Ikeda, H., Ishikawa, J., Hanamoto, A., Shinose, M., Kikuchi, H., Shiba, T., et al. (2003). Complete genome sequence and comparative analysis of the industrial microorganism *Streptomyces avermitilis. Nat Biotechnol, 21*(5), 526-531. doi:10.1038/nbt820

Ito, T. (2007). Role of histone modification in chromatin dynamics. *J Biochem, 141*(5), 609-614. doi:10.1093/jb/mvm091

Jakimowicz, D., Brzostek, A., Rumijowska-Galewicz, A., Zydek, P., Dolzblasz, A., Smulczyk-Krawczyszyn, A., et al. (2007). Characterization of the mycobacterial chromosome segregation protein ParB and identification of its target in *Mycobacterium smegmatis. Microbiology (Reading), 153*(Pt 12), 4050-4060. doi:10.1099/mic.0.2007/011619-0

Jakimowicz, D., Gust, B., Zakrzewska-Czerwinska, J., and Chater, K. F. (2005). Developmental-stage-specific assembly of ParB complexes in *Streptomyces coelicolor* hyphae. *J Bacteriol, 187*(10), 3572-3580. doi:10.1128/JB.187.10.3572-3580.2005

Jakimowicz, D., and van Wezel, G. P. (2012). Cell division and DNA segregation in *Streptomyces:* how to build a septum in the middle of nowhere? *Mol Microbiol, 85*(3), 393-404. doi:10.1111/j.1365-2958.2012.08107.x

Jeltsch, A., and Pingoud, A. (1996). Horizontal gene transfer contributes to the wide distribution and evolution of type II restriction-modification systems. *J Mol Evol, 42*(2), 91-96. doi:10.1007/BF02198833

Jiang, M., Yin, M., Wu, S., Han, X., Ji, K., Wen, M., et al. (2017). GdmRIII, a TetR family transcriptional regulator, controls geldanamycin and elaiophylin biosynthesis in *Streptomyces autolyticus* CGMCC0516. *Sci Rep, 7*(1), 4803. doi:10.1038/s41598-017-05073-x

Jones, S. E., and Elliot, M. A. (2017). *Streptomyces* exploration: competition, volatile communication and new bacterial behaviours. *Trends Microbiol, 25*(7), 522-531. doi:10.1016/j.tim.2017.02.001

Jones, S. E., Ho, L., Rees, C. A., Hill, J. E., Nodwell, J. R., and Elliot, M. A. (2017). *Streptomyces* exploration is triggered by fungal interactions and volatile signals. *Elife, 6*. doi:10.7554/eLife.21738

Kang, Y., Wang, Y., Hou, B., Wang, R., Ye, J., Zhu, X., et al. (2019). $AdpA_{lin}$, a pleiotropic transcriptional regulator, is involved in the cascade regulation of lincomycin biosynthesis in *Streptomyces lincolnensis*. *Front Microbiol, 10*, 2428. doi:10.3389/fmicb.2019.02428

Karimova, G., Ullmann, A., and Ladant, D. (2001). Protein-protein interaction between *Bacillus stearothermophilus* tyrosyl-tRNA synthetase subdomains revealed by a bacterial

two-hybrid system. *J Mol Microbiol Biotechnol, 3*(1), 73-82. Retrieved from https://www.ncbi.nlm.nih.gov/pubmed/11200232

Karoonuthaisiri, N., Weaver, D., Huang, J., Cohen, S. N., and Kao, C. M. (2005). Regional organization of gene expression in *Streptomyces coelicolor. Gene, 353*(1), 53-66. doi:10.1016/j.gene.2005.03.042

Khan, F., Furuta, Y., Kawai, M., Kaminska, K. H., Ishikawa, K., Bujnicki, J. M., et al. (2010). A putative mobile genetic element carrying a novel type IIF restriction-modification system (PluTI). *Nucleic Acids Res, 38*(9), 3019-3030. doi:10.1093/nar/gkp1221

Kieser, T., and Bibb, M. J. (2004). *Practical streptomyces genetics*. Norwich, England: John Innes Centre.

Kim, H. J., Calcutt, M. J., Schmidt, F. J., and Chater, K. F. (2000). Partitioning of the linear chromosome during sporulation of *Streptomyces coelicolor* A3(2) involves an oriC-linked parAB locus. *J Bacteriol, 182*(5), 1313-1320. doi:10.1128/JB.182.5.1313-1320.2000

Kim, I. K., Lee, C. J., Kim, M. K., Kim, J. M., Kim, J. H., Yim, H. S., et al. (2006). Crystal structure of the DNA-binding domain of BldD, a central regulator of aerial mycelium formation in *Streptomyces coelicolor* A3(2). *Mol Microbiol, 60*(5), 1179-1193. doi:10.1111/j.1365-2958.2006.05176.x

Kim, W., Lee, N., Hwang, S., Lee, Y., Kim, J., Cho, S., et al. (2020). Comparative genomics determines strain-dependent secondary metabolite production in *Streptomyces venezuelae* strains. *Biomolecules, 10*(6). doi:10.3390/biom10060864

Kinoshita, E., Kinoshita-Kikuta, E., and Koike, T. (2012). Phos-tag SDS-PAGE systems for phosphorylation profiling of proteins with a wide range of molecular masses under neutral pH conditions. *Proteomics, 12*(2), 192-202. doi:10.1002/pmic.201100524

Kinoshita, E., Kinoshita-Kikuta, E., Takiyama, K., and Koike, T. (2006). Phosphate-binding tag, a new tool to visualize phosphorylated proteins. *Mol Cell Proteomics, 5*(4), 749-757. doi:10.1074/mcp.T500024-MCP200

Kirby, R. (2011). Chromosome diversity and similarity within the Actinomycetales. *FEMS Microbiol Lett, 319*(1), 1-10. doi:10.1111/j.1574-6968.2011.02242.x

Kolodziej, M., Lebkowski, T., Plocinski, P., Holowka, J., Pasciak, M., Wojtas, B., et al. (2021a). Lsr2 and its novel paralogue mediate the adjustment of *Mycobacterium smegmatis* to unfavorable environmental conditions. *mSphere, 6*(3). doi:10.1128/mSphere.00290-21

Kolodziej, M., Trojanowski, D., Bury, K., Holowka, J., Matysik, W., Kakolewska, H., et al. (2021b). Lsr2, a nucleoid-associated protein influencing mycobacterial cell cycle. *Sci Rep, 11*(1), 2910. doi:10.1038/s41598-021-82295-0

Komatsu, M., Komatsu, K., Koiwai, H., Yamada, Y., Kozone, I., Izumikawa, M., et al. (2013). Engineered *Streptomyces avermitilis* host for heterologous expression of biosynthetic gene cluster for secondary metabolites. *ACS Synth Biol, 2*(7), 384-396. doi:10.1021/sb3001003

Kotlajich, M. V., Hron, D. R., Boudreau, B. A., Sun, Z., Lyubchenko, Y. L., and Landick, R. (2015). Bridged filaments of histone-like nucleoid structuring protein pause RNA polymerase and aid termination in bacteria. *Elife, 4*. doi:10.7554/eLife.04970

Kotowska, M., Swiat, M., Zareba-Paslawska, J., Jaworski, P., and Pawlik, K. (2019). A GntR-Like Transcription factor HypR regulates expression of genes associated with L-hydroxyproline utilization in *Streptomyces coelicolor* A3(2). *Front Microbiol, 10*, 1451. doi:10.3389/fmicb.2019.01451

Kriel, N. L., Gallant, J., van Wyk, N., van Helden, P., Sampson, S. L., Warren, R. M., et al. (2018). Mycobacterial nucleoid associated proteins: An added dimension in gene regulation. *Tuberculosis (Edinb), 108*, 169-177. doi:10.1016/j.tube.2017.12.004

Kurthkoti, K., Tare, P., Paitchowdhury, R., Gowthami, V. N., Garcia, M. J., Colangeli, R., et al. (2015). The mycobacterial iron-dependent regulator IdeR induces ferritin (*bfrB*) by alleviating Lsr2 repression. *Mol Microbiol, 98*(5), 864-877. doi:10.1111/mmi.13166

Labrie, S. J., Samson, J. E., and Moineau, S. (2010). Bacteriophage resistance mechanisms. *Nat Rev Microbiol, 8*(5), 317-327. doi:10.1038/nrmicro2315

Lang, B., Blot, N., Bouffartigues, E., Buckle, M., Geertz, M., Gualerzi, C. O., et al. (2007). High-affinity DNA binding sites for H-NS provide a molecular basis for selective silencing within proteobacterial genomes. *Nucleic Acids Res, 35*(18), 6330-6337. doi:10.1093/nar/gkm712

Lata, S., Mahatha, A. C., Mal, S., Gupta, U. D., Kundu, M., and Basu, J. (2022). Unraveling novel roles of the *Mycobacterium tuberculosis* transcription factor Rv0081 in regulation of the nucleoid-associated proteins Lsr2 and EspR, cholesterol utilization, and subversion of lysosomal trafficking in macrophages. *Mol Microbiol*. doi:10.1111/mmi.14895

Le Moigne, V., Bernut, A., Cortes, M., Viljoen, A., Dupont, C., Pawlik, A., et al. (2019). Lsr2 is an important determinant of intracellular growth and virulence in *Mycobacterium abscessus*. *Front Microbiol, 10*, 905. doi:10.3389/fmicb.2019.00905

Lee, D. J., Minchin, S. D., and Busby, S. J. (2012). Activating transcription in bacteria. *Annu Rev Microbiol, 66*, 125-152. doi:10.1146/annurev-micro-092611-150012

Lee, E.-J., Karoonuthaisiri, N., Kim, H.-S., Park, J.-H., Cha, C.-J., Kao, C. M., et al. (2005). A master regulator σ^B governs osmotic and oxidative response as well as differentiation via a network of sigma factors in *Streptomyces coelicolor*. *Molecular Microbiology, 57*(5), 1252-1264. doi:https://doi.org/10.1111/j.1365-2958.2005.04761.x

Lee, N., Hwang, S., Kim, J., Cho, S., Palsson, B., and Cho, B. K. (2020). Mini review: Genome mining approaches for the identification of secondary metabolite biosynthetic gene clusters in *Streptomyces*. *Comput Struct Biotechnol J, 18*, 1548-1556. doi:10.1016/j.csbj.2020.06.024

Leonard, T. A., Butler, P. J., and Lowe, J. (2005). Bacterial chromosome segregation: structure and DNA binding of the Soj dimer--a conserved biological switch. *EMBO J, 24*(2), 270-282. doi:10.1038/sj.emboj.7600530

Li, Y., Liu, X., Tang, K., Wang, P., Zeng, Z., Guo, Y., et al. (2019). Excisionase in Pf filamentous prophage controls lysis-lysogeny decision-making in *Pseudomonas aeruginosa*. *Mol Microbiol, 111*(2), 495-513. doi:10.1111/mmi.14170

Li, Z. (2019). Developing new AFM imaging technique and software for DNA mismatch repair. (PhD PhD thesis). University of North Carolina, Chapel Hill, NC,

Lim, C. J., Lee, S. Y., Kenney, L. J., and Yan, J. (2012). Nucleoprotein filament formation is the structural basis for bacterial protein H-NS gene silencing. *Sci Rep, 2*, 509. doi:10.1038/srep00509

Lin, M. H., Sugiyama, N., and Ishihama, Y. (2015). Systematic profiling of the bacterial phosphoproteome reveals bacterium-specific features of phosphorylation. *Sci Signal, 8*(394), rs10. doi:10.1126/scisignal.aaa3117

Lioy, V. S., Lorenzi, J. N., Najah, S., Poinsignon, T., Leh, H., Saulnier, C., et al. (2021). Dynamics of the compartmentalized *Streptomyces* chromosome during metabolic differentiation. *Nat Commun, 12*(1), 5221. doi:10.1038/s41467-021-25462-1

Liu, M., Zhu, X., Zhang, C., and Zhao, Z. (2021). LuxQ-LuxU-LuxO pathway regulates biofilm formation by *Vibrio parahaemolyticus*. *Microbiol Res, 250*, 126791. doi:10.1016/j.micres.2021.126791

Liu, Y., Chen, H., Kenney, L. J., and Yan, J. (2010). A divalent switch drives H-NS/DNA-binding conformations between stiffening and bridging modes. *Genes Dev, 24*(4), 339-344. doi:10.1101/gad.1883510

Luger, K., Rechsteiner, T. J., Flaus, A. J., Waye, M. M., and Richmond, T. J. (1997). Characterization of nucleosome core particles containing histone proteins made in bacteria. *J Mol Biol, 272*(3), 301-311. doi:10.1006/jmbi.1997.1235

MacNeil, D. J., Gewain, K. M., Ruby, C. L., Dezeny, G., Gibbons, P. H., and MacNeil, T. (1992). Analysis of *Streptomyces avermitilis* genes required for avermectin biosynthesis utilizing a novel integration vector. *Gene, 111*(1), 61-68. doi:10.1016/0378-1119(92)90603-m

Madrid, C., Balsalobre, C., Garcia, J., and Juarez, A. (2007). The novel Hha/YmoA family of nucleoid-associated proteins: use of structural mimicry to modulate the activity of the H-NS family of proteins. *Mol Microbiol, 63*(1), 7-14. doi:10.1111/j.1365-2958.2006.05497.x

Malpartida, F., Niemi, J., Navarrete, R., and Hopwood, D. A. (1990). Cloning and expression in a heterologous host of the complete set of genes for biosynthesis of the *Streptomyces coelicolor* antibiotic undecylprodigiosin. *Gene, 93*(1), 91-99. doi:10.1016/0378-1119(90)90141-d

Manteca, A., and Yagüe, P. (2019). *Streptomyces as a Source of Antimicrobials: Novel Approaches to Activate Cryptic Secondary Metabolite Pathways*. In (Ed.), Antimicrobials, Antibiotic Resistance, Antibiofilm Strategies and Activity Methods. IntechOpen.

Manteca, A., Ye, J., Sanchez, J., and Jensen, O. N. (2011). Phosphoproteome analysis of *Streptomyces* development reveals extensive protein phosphorylation accompanying bacterial differentiation. *J Proteome Res, 10*(12), 5481-5492. doi:10.1021/pr200762y

Martin, J. F., and Liras, P. (2010). Engineering of regulatory cascades and networks controlling antibiotic biosynthesis in *Streptomyces. Curr Opin Microbiol, 13*(3), 263-273. doi:10.1016/j.mib.2010.02.008

Martínez, L. F., Bishop, A., Parkes, L., Del Sol, R., Salerno, P., Sevcikova, B., et al. (2009). Osmoregulation in *Streptomyces coelicolor*: modulation of SigB activity by OsaC. *Molecular Microbiology, 71*(5), 1250-1262. doi:https://doi.org/10.1111/j.1365-2958.2009.06599.x

McCormick, J. R., and Flardh, K. (2012). Signals and regulators that govern *Streptomyces* development. *FEMS Microbiol Rev, 36*(1), 206-231. doi:10.1111/j.1574-6976.2011.00317.x

McLean, T. C., Wilkinson, B., Hutchings, M. I., and Devine, R. (2019). Dissolution of the disparate: co-ordinate regulation in antibiotic biosynthesis. *Antibiotics (Basel), 8*(2). doi:10.3390/antibiotics8020083

Merrick, M. J. (1976). A morphological and genetic mapping study of bald colony mutants of *Streptomyces coelicolor. J Gen Microbiol, 96*(2), 299-315. doi:10.1099/00221287-96-2-299

Miller, J. L., and Grant, P. A. (2013). The role of DNA methylation and histone modifications in transcriptional regulation in humans. *Subcell Biochem, 61*, 289-317. doi:10.1007/978-94-007-4525-4_13

Molle, V., and Buttner, M. J. (2000). Different alleles of the response regulator gene bldM arrest *Streptomyces coelicolor* development at distinct stages. *Mol Microbiol, 36*(6), 1265-1278. doi:10.1046/j.1365-2958.2000.01977.x

Muller, C. M., Dobrindt, U., Nagy, G., Emody, L., Uhlin, B. E., and Hacker, J. (2006). Role of histone-like proteins H-NS and StpA in expression of virulence determinants of uropathogenic *Escherichia coli. J Bacteriol, 188*(15), 5428-5438. doi:10.1128/JB.01956-05

Myronovskyi, M., Rosenkranzer, B., Nadmid, S., Pujic, P., Normand, P., and Luzhetskyy, A. (2018). Generation of a cluster-free *Streptomyces albus* chassis strains for improved heterologous expression of secondary metabolite clusters. *Metab Eng, 49*, 316-324. doi:10.1016/j.ymben.2018.09.004

Myronovskyi, M., Welle, E., Fedorenko, V., and Luzhetskyy, A. (2011). Beta-glucuronidase as a sensitive and versatile reporter in actinomycetes. *Appl Environ Microbiol, 77*(15), 5370-5383. doi:10.1128/AEM.00434-11

Nai, C., and Meyer, V. (2018). From axenic to mixed cultures: technological advances accelerating a paradigm shift in microbiology. *Trends Microbiol, 26*(6), 538-554. doi:10.1016/j.tim.2017.11.004

Navarre, W. W., Porwollik, S., Wang, Y., McClelland, M., Rosen, H., Libby, S. J., et al. (2006). Selective silencing of foreign DNA with low GC content by the H-NS protein in *Salmonella*. *Science, 313*(5784), 236-238. doi:10.1126/science.1128794

Netzker, T., Schroeckh, V., Gregory, M. A., Flak, M., Krespach, M. K. C., Leadlay, P. F., et al. (2016). An efficient method to generate gene deletion mutants of the rapamycin-producing bacterium *Streptomyces iranensis* HM 35. *Appl Environ Microbiol, 82*(12), 3481-3492. doi:10.1128/AEM.00371-16

Nguyen, C. T., Dhakal, D., Pham, V. T. T., Nguyen, H. T., and Sohng, J. K. (2020). Recent advances in strategies for activation and discovery/characterization of cryptic biosynthetic gene clusters in *Streptomyces. Microorganisms, 8*(4). doi:10.3390/microorganisms8040616

Oberto, J., Nabti, S., Jooste, V., Mignot, H., and Rouviere-Yaniv, J. (2009). The HU regulon is composed of genes responding to anaerobiosis, acid stress, high osmolarity and SOS induction. *PLoS One, 4*(2), e4367. doi:10.1371/journal.pone.0004367

Ohnishi, Y., Ishikawa, J., Hara, H., Suzuki, H., Ikenoya, M., Ikeda, H., et al. (2008). Genome sequence of the streptomycin-producing microorganism *Streptomyces griseus* IFO 13350. *J Bacteriol, 190*(11), 4050-4060. doi:10.1128/JB.00204-08

Ohnishi, Y., Yamazaki, H., Kato, J. Y., Tomono, A., and Horinouchi, S. (2005). AdpA, a central transcriptional regulator in the A-factor regulatory cascade that leads to morphological development and secondary metabolism in *Streptomyces griseus*. *Biosci Biotechnol Biochem, 69*(3), 431-439. doi:10.1271/bbb.69.431

Olanrewaju, O. S., and Babalola, O. O. (2019). *Streptomyces*: implications and interactions in plant growth promotion. *Appl Microbiol Biotechnol, 103*(3), 1179-1188. doi:10.1007/s00253-018-09577-y

Onaka, H., Mori, Y., Igarashi, Y., and Furumai, T. (2011). Mycolic acid-containing bacteria induce natural-product biosynthesis in *Streptomyces* species. *Appl Environ Microbiol, 77*(2), 400-406. doi:10.1128/AEM.01337-10

Paget, M. S. (2015). Bacterial sigma factors and anti-sigma factors: structure, function and distribution. *Biomolecules, 5*(3), 1245-1265. doi:10.3390/biom5031245

Paget, M. S., Chamberlin, L., Atrih, A., Foster, S. J., and Buttner, M. J. (1999). Evidence that the extracytoplasmic function sigma factor sigmaE is required for normal cell wall structure in *Streptomyces coelicolor* A3(2). *J Bacteriol, 181*(1), 204-211. doi:10.1128/JB.181.1.204-211.1999

Pait, I. G. U., Kitani, S., Roslan, F. W., Ulanova, D., Arai, M., Ikeda, H., et al. (2018). Discovery of a new diol-containing polyketide by heterologous expression of a silent biosynthetic gene cluster from *Streptomyces lavendulae* FRI-5. *J Ind Microbiol Biotechnol, 45*(2), 77-87. doi:10.1007/s10295-017-1997-x

Pandey, S. D., Choudhury, M., Yousuf, S., Wheeler, P. R., Gordon, S. V., Ranjan, A., et al. (2014). Iron-regulated protein HupB of *Mycobacterium tuberculosis* positively regulates siderophore biosynthesis and is essential for growth in macrophages. *J Bacteriol, 196*(10), 1853-1865. doi:10.1128/JB.01483-13

Park, H. S., Ostberg, Y., Johansson, J., Wagner, E. G., and Uhlin, B. E. (2010). Novel role for a bacterial nucleoid protein in translation of mRNAs with suboptimal ribosome-binding sites. *Genes Dev, 24*(13), 1345-1350. doi:10.1101/gad.576310

Parker, J. L., Jones, A. M., Serazetdinova, L., Saalbach, G., Bibb, M. J., and Naldrett, M. J. (2010). Analysis of the phosphoproteome of the multicellular bacterium *Streptomyces coelicolor* A3(2) by protein/peptide fractionation, phosphopeptide enrichment and high-accuracy mass spectrometry. *Proteomics, 10*(13), 2486-2497. doi:10.1002/pmic.201000090

Parthun, M. R. (2007). Hat1: the emerging cellular roles of a type B histone acetyltransferase. *Oncogene, 26*(37), 5319-5328. doi:10.1038/sj.onc.1210602

Patterson-West, J., Tai, C. H., Son, B., Hsieh, M. L., Iben, J. R., and Hinton, D. M. (2021). Overexpression of the bacteriophage T4 *motB* gene alters H-NS dependent repression of specific host DNA. *Viruses, 13*(1). doi:10.3390/v13010084

Peirson, S. N., Butler, J. N., and Foster, R. G. (2003). Experimental validation of novel and conventional approaches to quantitative real-time PCR data analysis. *Nucleic Acids Res, 31*(14), e73. doi:10.1093/nar/gng073

Perez-Rueda, E., Collado-Vides, J., and Segovia, L. (2004). Phylogenetic distribution of DNA-binding transcription factors in bacteria and archaea. *Comput Biol Chem, 28*(5-6), 341-350. doi:10.1016/j.compbiolchem.2004.09.004

Persson, J., Chater, K. F., and Flardh, K. (2013). Molecular and cytological analysis of the expression of *Streptomyces* sporulation regulatory gene whiH. *FEMS Microbiol Lett, 341*(2), 96-105. doi:10.1111/1574-6968.12099

Peterson, C. L., and Laniel, M. A. (2004). Histones and histone modifications. *Curr Biol, 14*(14), R546-551. doi:10.1016/j.cub.2004.07.007

Pfeifer, E., Hunnefeld, M., Popa, O., and Frunzke, J. (2019). Impact of xenogeneic silencing on phage-host interactions. *J Mol Biol, 431*(23), 4670-4683. doi:10.1016/j.jmb.2019.02.011

Pfeifer, E., Hunnefeld, M., Popa, O., Polen, T., Kohlheyer, D., Baumgart, M., et al. (2016). Silencing of cryptic prophages in *Corynebacterium glutamicum*. *Nucleic Acids Res, 44*(21), 10117-10131. doi:10.1093/nar/gkw692

Pioro, M., and Jakimowicz, D. (2020). Chromosome segregation proteins as coordinators of cell cycle in response to environmental conditions. *Front Microbiol, 11*, 588. doi:10.3389/fmicb.2020.00588

Pishchany, G., Mevers, E., Ndousse-Fetter, S., Horvath, D. J., Jr., Paludo, C. R., Silva-Junior, E. A., et al. (2018). Amycomicin is a potent and specific antibiotic discovered with

a targeted interaction screen. *Proc Natl Acad Sci U S A, 115*(40), 10124-10129. doi:10.1073/pnas.1807613115

Plachetka, M., Krawiec, M., Zakrzewska-Czerwinska, J., and Wolanski, M. (2021). AdpA positively regulates morphological differentiation and chloramphenicol biosynthesis in *Streptomyces venezuelae*. *Microbiol Spectr, 9*(3), e0198121. doi:10.1128/Spectrum.01981-21

Podgornaia, A. I., and Laub, M. T. (2013). Determinants of specificity in two-component signal transduction. *Curr Opin Microbiol, 16*(2), 156-162. doi:10.1016/j.mib.2013.01.004

Prieto, A. I., Kahramanoglou, C., Ali, R. M., Fraser, G. M., Seshasayee, A. S., and Luscombe, N. M. (2012). Genomic analysis of DNA binding and gene regulation by homologous nucleoid-associated proteins IHF and HU in *Escherichia coli* K12. *Nucleic Acids Res, 40*(8), 3524-3537. doi:10.1093/nar/gkr1236

Procopio, R. E., Silva, I. R., Martins, M. K., Azevedo, J. L., and Araujo, J. M. (2012). Antibiotics produced by *Streptomyces*. *Braz J Infect Dis, 16*(5), 466-471. doi:10.1016/j.bjid.2012.08.014

Qin, L., Bdira, F. B., Sterckx, Y. G. J., Volkov, A. N., Vreede, J., Giachin, G., et al. (2020). Structural basis for osmotic regulation of the DNA binding properties of H-NS proteins. *Nucleic Acids Res, 48*(4), 2156-2172. doi:10.1093/nar/gkz1226

Qin, L., Erkelens, A. M., Ben Bdira, F., and Dame, R. T. (2019). The architects of bacterial DNA bridges: a structurally and functionally conserved family of proteins. *Open Biol, 9*(12), 190223. doi:10.1098/rsob.190223

Qu, Y., Lim, C. J., Whang, Y. R., Liu, J., and Yan, J. (2013). Mechanism of DNA organization by *Mycobacterium tuberculosis* protein Lsr2. *Nucleic Acids Res, 41*(10), 5263-5272. doi:10.1093/nar/gkt249

Raivio, T. L., and Silhavy, T. J. (1997). Transduction of envelope stress in *Escherichia coli* by the Cpx two-component system. *Journal of bacteriology, 179*(24), 7724-7733. doi:10.1128/jb.179.24.7724-7733.1997

Ramos, J. L., Martinez-Bueno, M., Molina-Henares, A. J., Teran, W., Watanabe, K., Zhang, X., et al. (2005). The TetR family of transcriptional repressors. *Microbiol Mol Biol Rev, 69*(2), 326-356. doi:10.1128/MMBR.69.2.326-356.2005

Ramos-Leon, F., Bush, M. J., Sallmen, J. W., Chandra, G., Richardson, J., Findlay, K. C., et al. (2021). A conserved cell division protein directly regulates FtsZ dynamics in filamentous and unicellular actinobacteria. *Elife, 10*. doi:10.7554/eLife.63387

Rangarajan, A. A., and Schnetz, K. (2018). Interference of transcription across H-NS binding sites and repression by H-NS. *Mol Microbiol, 108*(3), 226-239. doi:10.1111/mmi.13926

Ray, S., Maitra, A., Biswas, A., Panjikar, S., Mondal, J., and Anand, R. (2017). Functional insights into the mode of DNA and ligand binding of the TetR family regulator TylP from *Streptomyces fradiae*. *J Biol Chem, 292*(37), 15301-15311. doi:10.1074/jbc.M117.788000

Rigali, S., Nothaft, H., Noens, E. E., Schlicht, M., Colson, S., Muller, M., et al. (2006). The sugar phosphotransferase system of *Streptomyces coelicolor* is regulated by the GntR-family regulator DasR and links *N*-acetylglucosamine metabolism to the control of development. *Mol Microbiol, 61*(5), 1237-1251. doi:10.1111/j.1365-2958.2006.05319.x

Robinson, C. R., and Sauer, R. T. (1998). Optimizing the stability of single-chain proteins by linker length and composition mutagenesis. *Proc Natl Acad Sci U S A, 95*(11), 5929-5934. doi:10.1073/pnas.95.11.5929

Rodriguez, H., Rico, S., Diaz, M., and Santamaria, R. I. (2013). Two-component systems in *Streptomyces*: key regulators of antibiotic complex pathways. *Microb Cell Fact, 12*, 127. doi:10.1186/1475-2859-12-127

Romero, D., Traxler, M. F., Lopez, D., and Kolter, R. (2011). Antibiotics as signal molecules. *Chem Rev, 111*(9), 5492-5505. doi:10.1021/cr2000509

Romero-Rodriguez, A., Robledo-Casados, I., and Sanchez, S. (2015). An overview on transcriptional regulators in *Streptomyces. Biochim Biophys Acta, 1849*(8), 1017-1039. doi:10.1016/j.bbagrm.2015.06.007

Rudd, B. A., and Hopwood, D. A. (1979). Genetics of actinorhodin biosynthesis by *Streptomyces coelicolor* A3(2). *J Gen Microbiol, 114*(1), 35-43. doi:10.1099/00221287-114-1-35

Ryding, N. J., Kelemen, G. H., Whatling, C. A., Flärdh, K., Buttner, M. J., and Chater, K. F. (1998). A developmentally regulated gene encoding a repressor-like protein is essential for sporulation in *Streptomyces coelicolor* A3(2). *Mol Microbiol, 29*(1), 343-357. doi:10.1046/j.1365-2958.1998.00939.x

Salerno, P., Larsson, J., Bucca, G., Laing, E., Smith, C. P., and Flardh, K. (2009). One of the two genes encoding nucleoid-associated HU proteins in *Streptomyces coelicolor i*s developmentally regulated and specifically involved in spore maturation. *J Bacteriol, 191*(21), 6489-6500. doi:10.1128/JB.00709-09

Santamaria, R. I., Sevillano, L., Martin, J., Genilloud, O., Gonzalez, I., and Diaz, M. (2018). The XRE-DUF397 protein pair, Scr1 and Scr2, acts as a strong positive regulator of antibiotic production in *Streptomyces. Front Microbiol, 9*, 2791. doi:10.3389/fmicb.2018.02791

Santiago, A. E., Yan, M. B., Hazen, T. H., Sauder, B., Meza-Segura, M., Rasko, D. A., et al. (2017). The AraC negative regulator family modulates the activity of histone-like proteins in pathogenic bacteria. *PLoS Pathog, 13*(8), e1006545. doi:10.1371/journal.ppat.1006545

Santos, C. L., Tavares, F., Thioulouse, J., and Normand, P. (2009). A phylogenomic analysis of bacterial helix-turn-helix transcription factors. *FEMS Microbiol Rev, 33*(2), 411-429. doi:10.1111/j.1574-6976.2008.00154.x

Schlimpert, S., Wasserstrom, S., Chandra, G., Bibb, M. J., Findlay, K. C., Flardh, K., et al. (2017). Two dynamin-like proteins stabilize FtsZ rings during *Streptomyces* sporulation. *Proc Natl Acad Sci U S A, 114*(30), E6176-E6183. doi:10.1073/pnas.1704612114

Schumacher, M. A., Zeng, W., Findlay, K. C., Buttner, M. J., Brennan, R. G., and Tschowri, N. (2017). The *Streptomyces* master regulator BldD binds c-di-GMP sequentially to create a functional $BldD_2$-$(c\text{-}di\text{-}GMP)_4$ complex. *Nucleic Acids Res, 45*(11), 6923-6933. doi:10.1093/nar/gkx287

Shahul Hameed, U. F., Liao, C., Radhakrishnan, A. K., Huser, F., Aljedani, S. S., Zhao, X., et al. (2019). H-NS uses an autoinhibitory conformational switch for environment-controlled gene silencing. *Nucleic Acids Res, 47*(5), 2666-2680. doi:10.1093/nar/gky1299

Sharma, V., Hardy, A., Luthe, T., and Frunzke, J. (2021). Phylogenetic distribution of WhiB- and Lsr2-type regulators in actinobacteriophage genomes. *Microbiol Spectr, 9*(3), e0072721. doi:10.1128/Spectrum.00727-21

Shepherdson, E. M. F., Netzker, T., Stoyanov, Y., and Elliot, M. A. (2022). Exploratory growth in *Streptomyces venezuelae* involves a unique transcriptional program, enhanced oxidative stress response, and profound acceleration in response to glycerol. *J Bacteriol, 204*(4), e0062321. doi:10.1128/jb.00623-21

Shindo, H., Iwaki, T., Ieda, R., Kurumizaka, H., Ueguchi, C., Mizuno, T., et al. (1995). Solution structure of the DNA binding domain of a nucleoid-associated protein, H-NS, from *Escherichia coli*. *FEBS Lett, 360*(2), 125-131. doi:10.1016/0014-5793(95)00079-o

Singh, K., Milstein, J. N., and Navarre, W. W. (2016). Xenogeneic silencing and its impact on bacterial genomes. *Annu Rev Microbiol, 70*, 199-213. doi:10.1146/annurev-micro-102215-095301

Skoko, D., Wong, B., Johnson, R. C., and Marko, J. F. (2004). Micromechanical analysis of the binding of DNA-bending proteins HMGB1, NHP6A, and HU reveals their ability to form highly stable DNA-protein complexes. *Biochemistry, 43*(43), 13867-13874. doi:10.1021/bi048428o

Solorzano, C., Srikumar, S., Canals, R., Juarez, A., Paytubi, S., and Madrid, C. (2015). Hha has a defined regulatory role that is not dependent upon H-NS or StpA. *Front Microbiol, 6*, 773. doi:10.3389/fmicb.2015.00773

Som, N. F., Heine, D., Holmes, N. A., Knowles, F., Chandra, G., Seipke, R. F., et al. (2017a). The MtrAB two-component system controls antibiotic production in *Streptomyces coelicolor* A3(2). *Microbiology (Reading), 163*(10), 1415-1419. doi:10.1099/mic.0.000524

Som, N. F., Heine, D., Holmes, N. A., Munnoch, J. T., Chandra, G., Seipke, R. F., et al. (2017b). The conserved actinobacterial two-component system MtrAB coordinates chloramphenicol production with sporulation in *Streptomyces venezuelae* NRRL B-65442. *Front Microbiol, 8*, 1145. doi:10.3389/fmicb.2017.01145

Sonden, B., and Uhlin, B. E. (1996). Coordinated and differential expression of histone-like proteins in *Escherichia coli*: regulation and function of the H-NS analog StpA. *EMBO J, 15*(18), 4970-4980. Retrieved from https://www.ncbi.nlm.nih.gov/pubmed/8890170

Song, D., and Loparo, J. J. (2015). Building bridges within the bacterial chromosome. *Trends Genet, 31*(3), 164-173. doi:10.1016/j.tig.2015.01.003

St-Onge, R. J., and Elliot, M. A. (2017). Regulation of a muralytic enzyme-encoding gene by two non-coding RNAs. *RNA Biol, 14*(11), 1592-1605. doi:10.1080/15476286.2017.1338241

St-Onge, R. J., Haiser, H. J., Yousef, M. R., Sherwood, E., Tschowri, N., Al-Bassam, M., et al. (2015). Nucleotide second messenger-mediated regulation of a muralytic enzyme in *Streptomyces*. *Mol Microbiol, 96*(4), 779-795. doi:10.1111/mmi.12971

Stoebel, D. M., Free, A., and Dorman, C. J. (2008). Anti-silencing: overcoming H-NS-mediated repression of transcription in Gram-negative enteric bacteria. *Microbiology (Reading), 154*(Pt 9), 2533-2545. doi:10.1099/mic.0.2008/020693-0

Stojkova, P., Spidlova, P., and Stulik, J. (2019). Nucleoid-associated protein HU: a lilliputian in gene regulation of bacterial virulence. *Front Cell Infect Microbiol, 9*, 159. doi:10.3389/fcimb.2019.00159

Stone, J. B., and Withey, J. H. (2021). H-NS and ToxT inversely control cholera toxin production by binding to overlapping DNA sequences. *J Bacteriol, 203*(18), e0018721. doi:10.1128/JB.00187-21

Summers, E. L., Meindl, K., Uson, I., Mitra, A. K., Radjainia, M., Colangeli, R., et al. (2012). The structure of the oligomerization domain of Lsr2 from *Mycobacterium tuberculosis* reveals a mechanism for chromosome organization and protection. *PLoS One, 7*(6), e38542. doi:10.1371/journal.pone.0038542

Sun, D., Liu, C., Zhu, J., and Liu, W. (2017). Connecting metabolic pathways: sigma factors in *Streptomyces* spp. *Front Microbiol, 8*, 2546. doi:10.3389/fmicb.2017.02546

Swiatek-Polatynska, M. A., Bucca, G., Laing, E., Gubbens, J., Titgemeyer, F., Smith, C. P., et al. (2015). Genome-wide analysis of *in vivo* binding of the master regulator DasR in *Streptomyces coelicolor* identifies novel non-canonical targets. *PLoS One, 10*(4), e0122479. doi:10.1371/journal.pone.0122479

Swiercz, J. P., Nanji, T., Gloyd, M., Guarne, A., and Elliot, M. A. (2013). A novel nucleoid-associated protein specific to the Actinobacteria. *Nucleic Acids Res, 41*(7), 4171-4184. doi:10.1093/nar/gkt095

Swiercz, J. S., and Elliot, M. A. (2012). *Streptomyces Sporulation. Chapter 4 in: Bacterial spores : current research and applications* (E. Abel-Santos Ed.). Norfolk, UK: Caister Academic Press.

Szafran, M. J., Jakimowicz, D., and Elliot, M. A. (2020). Compaction and control-the role of chromosome-organizing proteins in *Streptomyces*. *FEMS Microbiol Rev, 44*(6), 725-739. doi:10.1093/femsre/fuaa028

Tendeng, C., Soutourina, O. A., Danchin, A., and Bertin, P. N. (2003). MvaT proteins in *Pseudomonas* spp.: a novel class of H-NS-like proteins. *Microbiology (Reading), 149*(Pt 11), 3047-3050. doi:10.1099/mic.0.C0125-0

Thanapipatsiri, A., Gomez-Escribano, J. P., Song, L., Bibb, M. J., Al-Bassam, M., Chandra, G., et al. (2016). Discovery of unusual biaryl polyketides by activation of a silent *Streptomyces venezuelae* biosynthetic gene cluster. *Chembiochem, 17*(22), 2189-2198. doi:10.1002/cbic.201600396

Thibessard, A., and Leblond, P. (2014). Subtelomere plasticity in the bacterium *Streptomyces*. In E. J. Louis & M. M. Becker (Eds.), *Subtelomeres* (pp. 243-258). Berlin, Heidelberg: Springer Berlin Heidelberg.

Tomono, A., Tsai, Y., Ohnishi, Y., and Horinouchi, S. (2005). Three chymotrypsin genes are members of the AdpA regulon in the A-factor regulatory cascade in *Streptomyces griseus*. *J Bacteriol, 187*(18), 6341-6353. doi:10.1128/JB.187.18.6341-6353.2005

Tschowri, N., Schumacher, M. A., Schlimpert, S., Chinnam, N. B., Findlay, K. C., Brennan, R. G., et al. (2014). Tetrameric c-di-GMP mediates effective transcription factor dimerization to control *Streptomyces* development. *Cell, 158*(5), 1136-1147. doi:10.1016/j.cell.2014.07.022

Vallet, I., Diggle, S. P., Stacey, R. E., Camara, M., Ventre, I., Lory, S., et al. (2004). Biofilm formation in *Pseudomonas aeruginosa*: fimbrial cup gene clusters are controlled by the transcriptional regulator MvaT. *J Bacteriol, 186*(9), 2880-2890. doi:10.1128/JB.186.9.2880-2890.2004

van der Valk, R. A., Vreede, J., Qin, L., Moolenaar, G. F., Hofmann, A., Goosen, N., et al. (2017). Mechanism of environmentally driven conformational changes that modulate H-NS DNA-bridging activity. *Elife, 6*. doi:10.7554/eLife.27369

Wade, J. T., Castro Roa, D., Grainger, D. C., Hurd, D., Busby, S. J., Struhl, K., et al. (2006). Extensive functional overlap between sigma factors in *Escherichia coli*. *Nat Struct Mol Biol, 13*(9), 806-814. doi:10.1038/nsmb1130

Wagemans, J., Delattre, A. S., Uytterhoeven, B., De Smet, J., Cenens, W., Aertsen, A., et al. (2015). Antibacterial phage ORFans of *Pseudomonas aeruginosa* phage LUZ24 reveal a novel MvaT inhibiting protein. *Front Microbiol, 6*, 1242. doi:10.3389/fmicb.2015.01242

Waksman, S. A. (1967). *The actinomycetes : a summary of current knowledge*.

Wang, R., Mast, Y., Wang, J., Zhang, W., Zhao, G., Wohlleben, W., et al. (2013). Identification of two-component system AfsQ1/Q2 regulon and its cross-regulation with GlnR in *Streptomyces coelicolor*. *Mol Microbiol, 87*(1), 30-48. doi:10.1111/mmi.12080

Weber, H., Polen, T., Heuveling, J., Wendisch, V. F., and Hengge, R. (2005). Genome-wide analysis of the general stress response network in *Escherichia coli*: sigmaS-dependent genes, promoters, and sigma factor selectivity. *J Bacteriol, 187*(5), 1591-1603. doi:10.1128/JB.187.5.1591-1603.2005

Wei, J., He, L., and Niu, G. (2018). Regulation of antibiotic biosynthesis in actinomycetes: Perspectives and challenges. *Synth Syst Biotechnol, 3*(4), 229-235. doi:10.1016/j.synbio.2018.10.005

Westfall, L. W., Carty, N. L., Layland, N., Kuan, P., Colmer-Hamood, J. A., and Hamood, A. N. (2006). *mvaT* mutation modifies the expression of the *Pseudomonas aeruginosa*

multidrug efflux operon *mexEF-oprN*. *FEMS Microbiol Lett, 255*(2), 247-254. doi:10.1111/j.1574-6968.2005.00075.x

Wiechert, J., Filipchyk, A., Hunnefeld, M., Gatgens, C., Brehm, J., Heermann, R., et al. (2020a). Deciphering the rules underlying xenogeneic silencing and counter-silencing of Lsr2-like proteins using CgpS of *Corynebacterium glutamicum* as a model. *mBio, 11*(1). doi:10.1128/mBio.02273-19

Wiechert, J., Gatgens, C., Wirtz, A., and Frunzke, J. (2020b). Inducible expression systems based on xenogeneic silencing and counter-silencing and design of a metabolic toggle switch. *ACS Synth Biol, 9*(8), 2023-2038. doi:10.1021/acssynbio.0c00111

Willems, A. R., Tahlan, K., Taguchi, T., Zhang, K., Lee, Z. Z., Ichinose, K., et al. (2008). Crystal structures of the *Streptomyces coelicolor* TetR-like protein ActR alone and in complex with actinorhodin or the actinorhodin biosynthetic precursor (S)-DNPA. *J Mol Biol, 376*(5), 1377-1387. doi:10.1016/j.jmb.2007.12.061

Willemse, J., Borst, J. W., de Waal, E., Bisseling, T., and van Wezel, G. P. (2011). Positive control of cell division: FtsZ is recruited by SsgB during sporulation of *Streptomyces*. *Genes Dev, 25*(1), 89-99. doi:10.1101/gad.600211

Winardhi, R. S., Yan, J., and Kenney, L. J. (2015). H-NS regulates gene expression and compacts the nucleoid: Insights from single-molecule experiments. *Biophys J, 109*(7), 1321-1329. doi:10.1016/j.bpj.2015.08.016

Xia, H., Li, X., Li, Z., Zhan, X., Mao, X., and Li, Y. (2020). The application of regulatory cascades in *Streptomyces*: yield enhancement and metabolite mining. *Front Microbiol, 11*, 406. doi:10.3389/fmicb.2020.00406

Xu, F., Nazari, B., Moon, K., Bushin, L. B., and Seyedsayamdost, M. R. (2017). Discovery of a cryptic antifungal compound from *Streptomyces albus* J1074 using high-throughput elicitor screens. *J Am Chem Soc, 139*(27), 9203-9212. doi:10.1021/jacs.7b02716

Xu, F., Wu, Y., Zhang, C., Davis, K. M., Moon, K., Bushin, L. B., et al. (2019). A genetics-free method for high-throughput discovery of cryptic microbial metabolites. *Nat Chem Biol, 15*(2), 161-168. doi:10.1038/s41589-018-0193-2

Xu, Y., Willems, A., Au-Yeung, C., Tahlan, K., and Nodwell, J. R. (2012). A two-step mechanism for the activation of actinorhodin export and resistance in *Streptomyces coelicolor*. *mBio, 3*(5), e00191-00112. doi:10.1128/mBio.00191-12

Yang, X. J., and Seto, E. (2007). HATs and HDACs: from structure, function and regulation to novel strategies for therapy and prevention. *Oncogene, 26*(37), 5310-5318. doi:10.1038/sj.onc.1210599

Yang, Y. H., Song, E., Willemse, J., Park, S. H., Kim, W. S., Kim, E. J., et al. (2012). A novel function of *Streptomyces* integration host factor (sIHF) in the control of antibiotic production and sporulation in *Streptomyces coelicolor*. *Antonie Van Leeuwenhoek, 101*(3), 479-492. doi:10.1007/s10482-011-9657-z

Yim, G., Wang, H. H., and Davies, J. (2007). Antibiotics as signalling molecules. *Philos Trans R Soc Lond B Biol Sci, 362*(1483), 1195-1200. doi:10.1098/rstb.2007.2044

Yoon, V., and Nodwell, J. R. (2014). Activating secondary metabolism with stress and chemicals. *J Ind Microbiol Biotechnol, 41*(2), 415-424. doi:10.1007/s10295-013-1387-y

Yu, Z., Reichheld, S. E., Savchenko, A., Parkinson, J., and Davidson, A. R. (2010). A comprehensive analysis of structural and sequence conservation in the TetR family transcriptional regulators. *J Mol Biol, 400*(4), 847-864. doi:10.1016/j.jmb.2010.05.062

Zambri, M. P., Williams, M. A. and Elliot, M. A. (2022) How *Streptomyces* thrive: Advancing our understanding of classical development and uncovering new behaviors. *Adv Microb Physiol.* 80:203-236. doi: 10.1016/bs.ampbs.2022.01.004. Epub 2022 Mar 18. PMID: 35489792.

Zeng, Z., Liu, X., Yao, J., Guo, Y., Li, B., Li, Y., et al. (2016). Cold adaptation regulated by cryptic prophage excision in *Shewanella oneidensis*. *ISME J, 10*(12), 2787-2800. doi:10.1038/ismej.2016.85

Zhang, J., Liang, Q., Xu, Z., Cui, M., Zhang, Q., Abreu, S., et al. (2020). The inhibition of antibiotic production in *Streptomyces coelicolor* over-expressing the TetR regulator SCO3201 is correlated with changes in the lipidome of the strain. *Front Microbiol, 11*, 1399. doi:10.3389/fmicb.2020.01399

Zhang, X., Andres, S. N., and Elliot, M. A. (2021). Interplay between nucleoid-associated proteins and transcription factors in controlling specialized metabolism in *Streptomyces*. *mBio, 12*(4), e0107721. doi:10.1128/mBio.01077-21

Zhang, X., Hindra, and Elliot, M. A. (2019). Unlocking the trove of metabolic treasures: activating silent biosynthetic gene clusters in bacteria and fungi. *Curr Opin Microbiol, 51*, 9-15. doi:10.1016/j.mib.2019.03.003

Zhu, B., Lee, S. J., Tan, M., Wang, E. D., and Richardson, C. C. (2012). Gene 5.5 protein of bacteriophage T7 in complex with *Escherichia coli* nucleoid protein H-NS and transfer

RNA masks transfer RNA priming in T7 DNA replication. *Proc Natl Acad Sci U S A, 109*(21), 8050-8055. doi:10.1073/pnas.1205990109

Zorro-Aranda, A., Escorcia-Rodriguez, J. M., Gonzalez-Kise, J. K., and Freyre-Gonzalez, J. A. (2022). Curation, inference, and assessment of a globally reconstructed gene regulatory network for *Streptomyces coelicolor*. *Sci Rep, 12*(1), 2840. doi:10.1038/s41598-022-06658-x